INFRARED SPECTROSCOPY AND DENSITY FUNCTIONAL THEORY OF TRANSITION METAL - NITROGEN COMPLEXES

by

EMMANUEL DINESH PILLAI

(Under the Direction of Dr. Michael A. Duncan)

ABSTRACT

Transition metal (TM) cation - nitrogen complexes of the form $TM^+(N_2)_n$ are investigated via infrared photodissociation spectroscopy (IRPD) and density functional theory (DFT). The bonding characteristics of a single nitrogen molecule to first row transition metal cations from Sc^+ to Zn^+ are explored with DFT. The computed geometries and energetics indicate nitrogen prefers to bond in the end-on configuration to the cations. All the complexes are predominantly bound by charge-quadrupole forces with some exhibiting partial covalent character. The degree of covalent character is determined by the extent of 3d-4s orbital hybridization of the metals. The early transition metals cause a greater perturbation of the N-N bond than the late row metal ions. However, the dissociation energies of the late row metal cations are larger than the early metal ions. The calculated energetics are compared to experimental data to test the accuracy of DFT methodologies.

Complexes of the form $V^+(N_2)_n$ and $Nb^+(N_2)_n$ are generated in a pulsed nozzle laser vaporization cluster source, size selected and studied by IRPD spectroscopy by probing the N-N stretch of nitrogen. In both systems, the IR forbidden N-N stretch of free nitrogen becomes active upon binding to the metal ions. Vibrational excitation of the complexes near 2200 - 2300

cm^{-1} leads to photodissociation. The complexes fragment by the loss of intact N_2 molecules and the IRPD spectra are obtained by monitoring the fragmentation yield as a function of the IR wavelength. The fragmentation mass spectra indicate that V^+ and Nb^+ have a coordination number of six. The IRPD spectra for both complexes have resonances red-shifted with respect to the N-N stretch in free nitrogen. The red-shifts are consistent with the Dewar-Chatt-Duncanson complexation model that is used to model such TM-ligand systems. DFT calculations are used to predict structures, energetics and ground electronic states of the small $TM^+(N_2)_n$ complexes. The IRPD spectra in conjunction with DFT calculations suggest that the metal ions undergo a spin-state change due to progressive ligand binding. The spectroscopy and theoretical predictions of these metal ion-ligand systems offers new insight into their chemistry.

INDEX WORDS: Ion Spectroscopy, Infrared Photodissociation, Metal-Nitrogen Complexes, Density Functional Theory, Spin-State Isomers, Metal Ion Solvation, Clusters, Mass Spectrometry, Molecular Beams

INFRARED SPECTROSCOPY AND DENSITY FUNCTIONAL THEORY OF TRANSITION METAL - NITROGEN COMPLEXES

by

EMMANUEL DINESH PILLAI

B.A., Berea College, U.S.A, 2002

A Dissertation Submitted to the Graduate Faculty of The University of Georgia in Partial Fulfillment of the Requirements for the Degree

DOCTOR OF PHILOSOPY

ATHENS, GEORGIA

2007

INFRARED SPECTROSCOPY AND DENSITY FUNCTIONAL THEORY OF TRANSITION METAL - NITROGEN COMPLEXES

by

EMMANUEL DINESH PILLAI

Major Professor:	Michael A. Duncan
Committee:	Steven P. Lewis
	Henning Meyer

Electronic Version Approved:

Maureen Grasso
Dean of the Graduate School
The University of Georgia
May 2007

DEDICATION

I thank Almighty God for giving me the strength to survive some of the darkest seasons of my life.

I dedicate my Ph.D to my father and mother, whose love, prayers and sacrifices have made me who I am today.

ACKNOWLEDGEMENTS

"For in much wisdom is much grief,

and he that increaseth knowledge increaseth sorrow."

- Ecclesiastes 1:18

"Education without character is a sin."

- Mahatma Gandhi

TABLE OF CONTENTS

Page

CHAPTER 1

INTRODUCTION

Gas phase ion chemistry studies have been studying metal ion containing compounds for nearly 50 years now. Metal ions have interested chemists because they are ubiquitous throughout all of the physical, chemical and biological disciplines and are crucial to modern industry and research. In surface science, the catalytic base for numerous synthetic reactions are pure metal and metal oxide surfaces.[1-5] For example, the synthesis of ammonia from nitrogen and hydrogen is carried out on iron and nickel oxide surfaces.[4,5] In biochemistry, the centers of enzymes contain different metals which largely determine their function and chemistry.[6-8] Terrestrial soil, water and the earth's atmosphere contain metal ions that influence the chemistry of these systems.[9-11] Metals ions come to be present in the earth's atmosphere from meteor ablation.[10,11] Neutral and ionic metal-ligand complexes form the very foundation of coordination chemistry and organometallic chemistry.[12-14] In nature, metals are predominantly present as ions in solution or ionic compounds rather than an isolated neutrals. This is because both main group and transition metals have very low ionization potentials and therefore donate their valence electrons readily to form bonds.[12-14] Hence, the chemistry of metal ions plays a significant role in metal-molecule interactions. Metal ion chemistry in the gas phase is particularly suited to study metal-ligand systems since the gas phase isolates these molecules from interactions that occur in the condensed phase. As a result, the validity of theoretical models of metal-ligand bonding can be directly tested with spectroscopic investigations in the gas phase. The work described in this dissertation involves the characterization of transition metal cation-nitrogen

complexes by gas phase infrared (IR) spectroscopy and density functional theory (DFT). This introduction will survey the work of various groups, including ours, in the area of gas phase metal ion chemistry. These studies have discovered fascinating new features of the bonding mechanism of these metal-molecular systems.

Gas phase metal ion complexes have been studied by various spectrometric and spectroscopic studies. Mass spectrometry techniques such as collision induced dissociation (CID)[15,16] and equilibrium mass spectrometry[17,18] can measure binding energies of metal-ligand complexes. Other mass spectrometry methods such as Fourier transform ion cyclotron resonance mass spectrometry have explored gas phase reactivities and thermodynamics.[19-24] These studies have probed the size-specific reactivity and chemical properties of metal clusters and complexes. Such mass spectrometric methods are particularly adept at separating ions with different masses and can track the changes in chemical characteristics as a function of their size. Most of these studies have focused on transition metals since they are highly reactive and can undergo insertion and elimination reactions. Mass spectrometry has focused on the ligation and solvation of single metallic ions. Interesting chemistry can occur when multiple ligands bind to a single metal ion and mass spectrometry has investigated such chemistry.[15-24] However, these studies have a fundamental drawback in that they cannot directly determine the structure of the metal complexes. The relative binding energies, thermodynamics and reactivities measured by these experiments can only provide clues to the structure, coordination numbers and electronic states of the complexes. Direct experimental elucidation of structure requires spectroscopic techniques to be applied to species produced and isolated by mass spectrometry.

The availability of lasers in the mid-1970's led to the development of laser vaporization sources that produce high densities of metal atoms and ions in the gas phase.[25] Subsequently, the

spectroscopic techniques such as laser resonance enhanced ionization spectroscopy and photodissociation spectroscopy emerged as methods to characterize gas phase metal clusters and complexes .[26-31] All these spectroscopic techniques are referred to as "action spectroscopy" where the molecular species initially absorbs radiation and then undergoes an "action" such as ionization or dissociation which can be monitored to obtain a spectrum. Gas phase spectroscopic techniques on metal complexes usually entail action spectroscopy because direct absorption or emission spectroscopy is not feasible. Even with laser vaporization sources, the metal densities that are produced in the gas phase are quite low and are not tractable for direct absorption spectroscopy. The resonance ionization and photodissociation experiments irradiate the metal complexes and monitor an event (ionization or fragmentation) to study them. Most of these spectroscopic experiments were done in the UV-visible regions of the spectrum because high energy pulsed lasers were available that operated in these regions. Laser resonance enhanced ionization spectroscopy has been applied to study neutral complexes while the photodissociation experiments have investigated ionic species.[26-31] Utilizing fixed-frequency UV-visible photodissociation our group studied numerous cationic metal clusters such as $Pb_nSb_m^+$, $Bi_nCr_m^+$, Te_n^+, Sn_n^+ and $M_nO_m^+$ and single metal cation-multiple ligand complexes such as $M^+(benzene)_n$, and $M^+(Coronene)_n$.[27] The fragmentation patterns from the photodissociation studies of these complexes provided insight into the bonding framework. The fundamental drawback of these single frequency photodissociation studies is that they too do not provide a direct determination of structure and bonding. Although the fragmentation schemes may identify stable cores of clusters or metal-ligand complexes, the structure of these systems can only be inferred.

Electronic and vibrational spectroscopy can provide more information on the structure of metal ion complexes than fixed-frequency photodissociation experiments. Several groups have

studied the electronic spectroscopy of metal ion systems to investigate structure.[28-35] The studies, however, focused on metals bound to only a single molecule or a noble gas. Our group focused on the bonding of main group metals such as Mg^+ and Ca^+ to small ligands such as CO_2, N_2, C_2H_2, CH_3OH and H_2O as well as to noble gases such as Ne and Ar. Other groups like Brucat and co-workers have studied complexes of transition metals with small molecules.[30] The transition metals studied have included V^+, Ni^+ and Co^+. Metz and co-workers have explored the chemistry Fe^+, Ni^+ and Co^+.[34] The binding of these metals to ligands is especially interesting since transition metals have low lying excited states that can form bonds. As a result, these excited states become the ground state in the metal-ligand complex and such phenomena can be identified by electronic spectroscopy. The electronic spectra of such metal ions bound to single ligands often contain vibrational bands. Analysis of the vibrational structure can be used to determine the binding energies of the complexes. Additionally, some of the spectra may also contain rotational structure, which can be analyzed to determine accurate structural parameters of the complexes. The bonding in metal-molecular complexes often involves interplay between ionic and covalent bonding forces and electronic spectroscopy provides the means to investigate these forces.

Although electronic spectroscopy is an effective technique to study metal ion chemistry, it is not without disadvantages. The most basic problem with electronic spectroscopy occurs when metal ions bound to more than one ligand are studied. Such complexes are prone to predissociate and their electronic spectra are essentially featureless. Upon irradiation by UV-visible light, the molecule possesses enough energy to overcome any reaction barriers and can undergo a metal-ligand reaction. Such an effect results in lifetime broadening that renders the electronic spectra with broad vibrational structure. Even though photochemistry of gas phase

metal-ligand systems is an exciting area of research, electronic spectroscopy is not convenient to study them. The low lying excited states of transition metals often participate in bonding which can convolute the electronic spectra. Additionally, transition metals ions are extremely reactive and initiate metal-ligand reactions, even in the absence of light. Such reactions too, are very interesting but not feasible to study by electronic spectroscopy because they lead to broad spectra.

Zero electron kinetic energy (ZEKE) photoelectron spectroscopy is an attractive alternative to traditional electronic spectroscopy to probe the ground electronic states of metal-ligand complexes. Such studies have been carried out by several groups.[36-40] ZEKE spectroscopy is utilized to characterize the ground state of the metal cation-ligand complex by ionizing the neutral, or characterize the neutral by ionizing its corresponding anion. The spectra are obtained by detecting the threshold photoelectrons (electrons with zero kinetic energy) that are produced as a tunable light source causes ionization of the neutral complex. Yang and co-workers have successfully used this technique to study numerous pure metal, metal oxide and metal-ligand systems such V_2, Nb_3N_2, Nb_3O, Zr_3O, $InNH_3$, AlN_3, $GaNH_3$, and $YO(CH3)_2$.[36] Sometimes a ZEKE spectrum provides rotationally resolved spectra and the geometric structure and electronic states of the clusters can be determined. However, ZEKE spectroscopy usually entails Frank-Condon factor calculations for complete analysis since there is a large change in structure between the neutral complex and its corresponding ion. ZEKE spectroscopy has its drawbacks, the biggest being that size selection of the complexes is not possible. This, however, is usually overcome by using mass dependent ionization thresholds as a way to mass select.

The other alternative to electronic spectroscopy in gas phase metal ion chemistry is IR spectroscopy. As mentioned above, direct absorption or emission spectroscopy is not possible

due to the low density of ions. A technique known as infrared photodissociation (IRPD) spectroscopy using line tunable CO_2 lasers initially showed that IR spectra of metal-ligand systems could be acquired.[41-43] However, because of the limited tuning range of CO_2 lasers, the IR spectra measured had poor resolution. The advent of free electron lasers and IR optical parametric oscillator/ amplifier (OPO/OPA) systems has changed all this by providing good resolution and tunability from the mid-IR to the far IR region of the spectrum. IRPD spectroscopy provides information on structure, coordination number, and electronic states of metal-multiple ligand systems that is impossible to acquire using other forms of spectroscopy. IRPD spectroscopy is useful for metallic systems as well as non-metal systems. Several groups have successfully applied this technique to investigate non-metallic neutral and ionic complexes.[44-51] IRPD studies of metal ion complexes were initially limited to alkali metal cations.[52] Since then, our group has applied IRPD spectroscopy to main group and transition metal cation-ligand complexes utilizing desktop OPO/OPA systems.[53-60] Our group has also studied metal oxides, metal carbides and metal-benzene systems using a free electron laser by collaborating with Meijer and co-workers.[61,62] Additionally, Meijer and co-workers and Maitre and co-workers have independently investigated metal oxide and metal-ligand systems using a free electron laser.[63,64]

Our IR studies of metal-ligand complexes performed at the University of Georgia uses an OPO/OPA system whose tunability is from 2000 to 4500 cm^{-1}. Using this laser system we have investigated various metal cation-ligand systems of the form $M^+(L)_n$ where L = CO_2,[53] C_2H_2,[54] C_6H_6,[55] H_2O,[56] and N_2.[58] After purchasing an $AgGaSe_2$ crystal for the IR source which provides a greater tuning range into the far IR region, we measured the IR spectrum of M^+(acetone) M^+= Mg, Ca, and Al near the carbonyl stretch of acetone at 1700 cm^{-1}. Our studies of these systems

have helped understand the coordination mechanism of metal ions as well as determine structure and ground electronic states. Our studies of $M^+(CO_2)_n$ complexes, where the ion was a transition metal, showed that CO_2 binds with its oxygen end to the metal ion. With two CO_2 ligands, transition metals such Fe^+ formed linear structures whereas Mg^+ formed bent structures.[53] The $M^+(CO_2)_n$ systems were excited near the asymmetric stretch of free CO_2 at 2349 cm^{-1}. This frequency is blue shifted upon complexation to the metal due to the nature of the interaction. Ion-quadrupole forces bind the $M^+(CO_2)_n$ complexes and the asymmetric vibration experiences an added repulsion as it vibrates against the metal. This added repulsion causes the asymmetric vibration to blue shift. Our IR studies of these complexes in conjunction with theoretical calculations have identified their bonding characteristics.

Our IRPD studies also focused on $M^+(H_2O)_n$ complexes by probing the asymmetric and symmetric O-H vibrations of H_2O.[56] The studies indicated that the O-H vibrations red-shift upon complexation. In $M^+(CO_2)_n$ systems, the blue shift of the ligand frequencies indicates the highly electrostatic nature of the bonding. In $M^+(H_2O)_n$ there is a large covalent factor in the bonding, which results in a red-shift of the ligand frequencies. The IR spectra of a few mono-ligated complexes were rotationally resolved allowing us to determine structural features such as bond lengths and angles.[56a,e] Analysis of the rotational structure led to the identification of the rotational temperature of the complexes. The progressive solvation of the Ni^+ by H_2O was systematically investigated up to nearly twenty H_2O molecules.[56d] This study showed the formation of hydrogen bonding networks beginning with $Ni^+(H_2O)_4$. IRPD studies of H_2O solvating of other metal ions are currently underway in our lab.

The IRPD studies were extended to study organometallic complexes such as $M^+(benzene)_n$[55] and $M^+(C_2H_2)$[54] in the gas phase. $M^+(benzene)_n$ complexes were studied using

IR OPO/OPA sources[55] and a free electron laser.[61] Using the bench top OPO/OPA system, the changes in the C-H stretching modes of free benzene near 3000 – 3100 cm^{-1} in $M^+(benzene)_n$ systems were investigated.[55] Using the free electron laser, benzene vibrational modes in the far IR region were examined. Periodic trends in main group and transition metal binding to benzene were studied and catalogued. In $M^+(C_2H_2)_n$ complexes, the asymmetric and symmetric CH frequencies near 3300 and 3400 cm^{-1} were excited to acquire the IRPD spectra. Unlike the $M^+(CO_2)_n$ complexes, where the ligand frequency blue shifted upon binding, the C-H vibrational frequencies red-shifted in the $M^+(C_2H_2)_n$ complexes. This was indicative of the bonding nature. The bonding in $M^+(CO_2)_n$ is dominated by electrostatic forces with little covalent bonding. The $M^+(C_2H_2)_n$ complexes possess large covalent character and this is exhibited by the frequency shifts of the ligands. We found the magnitude of the red-shifts for different metal cations such V^+, Fe^+, Co^+, and Ni^+ differed, which also indicated significant details of the bonding. The IRPD results also showed evidence for the possibility of intracluster reactions induced by photochemistry, ligand solvation, the reactive nature of the metal ions or a combination of these factors. The intracluster reaction was an extremely interesting result since C_2H_2 is known to react on metal surfaces in the condensed phase to form aromatic hydrocarbons.[65-69] Another surprising result from these experiments was the appearance of the symmetric C-H frequency in the IRPD spectrum. For a molecular vibrational frequency to be IR active, the vibration must produce a net change in the dipole moment of molecule. Since the symmetric C-H stretch does not produce this, it is not IR active in isolated C_2H_2. However, upon binding to the metal ion, the overall symmetry of the complex must be taken into account and the symmetric C-H does become IR active. The IRPD work on these organometallic systems such as $M^+(benzene)_n$ and

$M^+(C_2H_2)_n$ has provided considerable insight into how these metal cationic complexes interact and bond.

The IR activity of the symmetric C-H stretch of free acetylene being "switched on" in the $M^+(C_2H_2)$ complex was an important result as it eventually led to our IRPD studies of $M^+(N_2)_n$ where the free ligand has no IR active mode. As our recent studies on $M^+(N_2)_n$ have shown, the N_2 ligand "acquires" IR activity upon complexation to the metal ion.[58] The N-N stretch of free nitrogen occurs at 2330 cm^{-1} which has been measured by Raman spectroscopy.[70] The N_2 ligand can bind in either the "end-on" or "side-on" configuration to metal ions, preferring the former.[71-75] Our IRPD work on $M^+(N_2)_n$ complexes near the free N-N stretch provided evidence for the end-on bonding configuration of N_2, the red-shifting of the N-N frequency upon binding, coordination number of the metal ions and ground electronic states of the complexes. To our knowledge, these gas phase studies of isolated $M^+(N_2)_n$ complexes using IRPD spectroscopy are the first of its kind. This dissertation catalogues these studies where the metal cation is V^+ and Nb^+.

A review of gas phase metal ion chemistry would be incomplete without surveying the substantial contributions from theory. Experimental groups such as ours have usually complemented our IRPD studies with DFT calculations to elucidate structure and bonding. Theoretical groups have investigated metal ion-ligand species with high end computational techniques such coupled cluster singles and doubles method (CCSD), multiconfiguration interaction, modified pair coupled functional, Møller-Plesset (MP2) and hybrid density functional methods.[76-79] The chemical bonding theory that is most often applied to metal ion chemistry is ligand field theory.[77] The implementation of ligand field into *ab initio* quantum chemical methods requires extensive computational time even for modestly sized systems. As a

result, DFT has emerged as single most effective theoretical technique to study metal-ligand bonding since relatively large metal-molecular systems can be calculated with comparatively little computational time.[80]

The success of DFT methods in accurately calculating molecular properties such as structure, binding energies, vibrational frequencies, and other characteristics stems from the implementation of gradient-corrected functionals that are fit to experimental data to better describe reality. Metal ion-ligand bonding usually entails a synergistic mix of electrostatic and covalent bonding that ab initio methods find difficult to model. Since DFT contains functionals that are experimentally fit, it is well equipped to deal with complexes with competing bonding forces. In comparison to the Hartree-Fock (HF) method, which does not take full account of electron-electron correlation, DFT has proven to be more effective. DFT utilizes Kohn-Sham orbitals that include electron correlation in calculating bonding features. Several functionals have been proposed by numerous groups and of these the Becke-3-Lee-Yang-Parr is the most widely used.[81,82] The B3LYP functional provides accurate estimates for metal-ligand bond energies, IR frequencies and intensities. However, DFT does have its fundamental drawbacks. Transition metals often involve low lying excited states in their bonding and it is difficult solely with experiment to determine which states are involved in the bonding. DFT is notorious for miscalculating the energy differences between electronic states of metal ion complexes, often favoring the lower spin states. Even when the ordering of the states is calculated correctly, the absolute energy between the states can have huge errors. This can only be overcome by looking to other computational methods such as CCSD and MP2. DFT is also known to overestimate metal-ligand dissociation energies, but usually by no more than 6-10 kcal/mol. Finally, DFT is inept at modeling van der Waals molecules and purely electrostatic molecules. This is because

the functionals are not designed to treat dispersion forces, which dominate in such complexes. For such complexes, DFT usually does provide correct structural parameters, but inaccurate energetics and electronic states. Since electrostatic and covalent forces bind the $M^+(N_2)_n$ complexes, DFT has proved to be an ideal theoretical technique to use. Our IRPD spectroscopy on metal ion-nitrogen complexes is supplemented by theoretical calculations that have aided in our understanding of the bonding in these systems.

References

(1) Henrich, V. E.; Cox, P. A. *The Surface Science of Metal Oxides*, University Press, Cambridge, **1994**.

(2) Somorjai, G. A. *Introduction to Surface Chemistry and Catalysis*, John Wiley & Sons, New York, **1994**.

(3) Ozkan, U. S.; Watson, R. B. *Catalysis Today*. **2205**, *100*, 101.

(4) Rao, C. N. R.; Rao, G. R. *Surf. Sci. Rep.* **1991**, *13*, 221.

(5) a) Grunze, M.; Golze, M.; Hirschwald, W.; Freund, H. J.; Pulm, H; Seip, U; Tsai, M.C.; Ertl, G.; Kuppers, J. *Phys. Rev. Lett.* **1984**, *53*, 850. b) Tsai, M. C.; Seip, U.; Bassignana, C. I.; Kuppers, J.; Ertl, G.; *Surf. Sci*. **1985**, *155*, 387.

(6) a) Seigbahn, P. E. M.; Blomberg, M. R. A. *Annu. Rev. Phys. Chem.* **1999**, *50*, 221. b) Seigbahn, P. E. M.; Blomberg, M. R. A. *Chem. Rev*. **2000**, *100*, 421.

(7) I. Bertini, A. Sigel and H. Sigel, eds., *Handbook on Metalloproteins*, Marcel Dekker, New York, **2001**.

(8) Ma, J. C.; Dougherty, D. A. *Chem. Rev*. **1997**, *97*, 1303.

(9) Faure, G. *Principles and Practice of Inorganic Geochemistry*, MacMillan, New York, **1991**.

(10) Vierreck, R. A.; Murad, E.; Lai, S. T.; Knecht, D. J.; Pike, C. P.; Gardner, J. A.; Broadfoot, A. L.; Anderson, E. R.; McNeil, W. J. *Adv. Space. Res*. **1996**, *18*, 61.

(11) Cziczo, D. J.; Thomson, D. S.; Murphy, D. M. *Science*. **2001**, *291*, 1772.

(12) Cotton, F. A.; Wilkinson, G.; Murillo, C. A.; Bochmann, M. *Advanced Inorganic Chemistry*, 6th ed. John Wiley, New York, **1999**.

(13) Huheey, J. E.; Keiter, E. A.; Keiter, R. L. *Inorganic Chemistry*, 4th ed., HarperCollins, New York **1993**.

(14) Shriver, D.; Atkins, P. Inorganic Chemistry, 3rd ed., W. H. Freeman and Company, New York **1999**.

(15) a) Aristov, N.; Armentrout, P. B. *J. Am. Chem. Soc.* **1986**, *108*, 1806. b) Fisher, E. R.; Armentrout, P. B. *J. Phys. Chem.* **1990**, *94*, 1674. c) Fisher, E. R.; Armentrout, P. B. *J. Phys. Chem.* **1990**, *94*, 1674. d) Tjelta, B. L.; Walter, D.; Armentrout, P. B. *Intl. J. Mass. Spec.* **2001**, 204, 7. e) Dalleska, N. F.; Honma, K.; Sunderlin, L. S.; Armentrout, P. B. *J. Am. Chem. Soc.* **1994**, *116*, 3519. f) Armentrout, P.B.; Beauchamp, J. L. *Acc. Chem. Res.* **1989**, *22*, 315. g) Tan, L.; Liu, F.; Armentrout, P.B. *J. Chem. Phys*. **2006**, *124*, 1.

(16) Rodriguez-Cruz, S.; Jockusch, R. A.; Williams, E. R. *J. Am. Chem. Soc*. **1999**, *121*, 1986.

(17) a) Kabarle, P. *Ann. Rev. Phys. Chem.* **1977**, *28*, 445. b) Jayaweera, P.; Blades, A.T.; Ikonomou, M.G.; Kebarle, P. *J. Am. Chem. Soc.* **1990**, *112*, 2452. c) Nielsen, S.B.; Masella, M.; Kebarle, P. *J. Phys. Chem. A* **1999**, *103*, 9891. d) Peschke, M.; Blades, AT.; Kebarle, P. *Adv. Met. Semicond. Clusters.* **2001**, *5*, 77.

(18) a) Bushnell, J.E.; Kemper, P.R.; Bowers, M.T. *J. Phys. Chem.* **1995**, *99*, 15602. b) Weis, P.; Kemper, P.R.; Bowers, M.T., *J. Phys. Chem. A* **1997**, *101*, 8207. c) Kemper, P.R.; Bushnell, J.; Bowers, M.T.; Gellene, G.I. *J. Phys. Chem. A.* **1998**, *102*, 8590. d) Manard, M.J.; Kemper, P.R.; Bowers, M.T. *Int. J. Mass Spectrom.* **2005**, 241, 109.

(19) a) Schwarz, J.; Heinemann, C.; Schwarz, H. *J. Phys. Chem.* **1995**, *99*, 11405. b) Schalley, C.A.; Wesendrup, R.; Schroeder, D.; Schwarz, H. *Organometallics*. **1996**, *15*, 678. c) Schroeter, K.; Schalley, C.A.; Wesendrup, R.; Schroeder, D.; Schwarz, H. *Organometallics* **1997**, *16*, 986. d) Jackson, P.; Harvey, J.N.; Schroeder, D.; Schwarz,

H. *Int. J. Mass Spectrom.* **2001**, *204*, 233. e) Schwarz, H. *Ang. Chem., Int. Ed.* **2003**, *42*, 4442. f) Boehme, D. K.; Schwarz, H. *Ang. Chem., Int. Ed.* **2005**, *44(16)*, 2336.

(20) a) Heath, J. R.; Sheeks, R. A.; Cooksy, A. L.; Saykally, R. J. *Science* **1990**, *249*, 895. b) Casaes, Raphael; Provencal, Robert; Paul, Joshua; Saykally, Richard J. *J. Chem. Phys.* **2002**, 116, 6640.

(21) a) Cox, D. M.; Reichmann, K. C.; Trevor, D. J.; Kaldor, A. *J. Chem. Phys.* **1988**, *88*, 111-19. b) Eberhardt, W.; Fayet, P.; Cox, D. M.; Fu, Z.; Kaldor, A.; Sherwood, R.; Sondericker, D. *Phys. Rev. Lett.* **1990**, *64*, 780.

(22) a) Rufus, D.; Ranatunga, A.; Freiser, B.S. *Chem. Phys. Lett.* **1995**, *233*, 319. b) Freiser, B.S. *Organometallic Ion Chemistry*. Kluwer, Dordrecht, **1996**.

(23) a) Leuchtner, R. E.; Harms, A. C.; Castleman, A. W., Jr. *J. Chem. Phys.* **1990**, *92*, 6527. b) Kerns, K. P.; Guo, B. C.; Deng, H. T.; Castleman, A. W., Jr. *J. Am. Chem. Soc.* **1995**, *117*, 4026. c) Zemski, K. A.; Justes, D. R.; Castleman, A. W., Jr. *J. Phys. Chem. B* **2002**, *106*, 6136.

(24) a) Beyer, M.; Berg, C.; Görlitzer, H.W.; Schindler, T.; Achatz, U.; Albert, G.; Niedner-Schatteburg, G.; Bondybey, V.E. *J. Am. Chem. Soc.* **1996**, *118*, 7386. b) Bondybey, V.E.; Beyer, M.K. *Int. Rev. Phys. Chem.* **2002**, *21*, 277. c) Fox, B.S.; Balteanu, I.; Balaj, O.P.; Liu, H.; Beyer, M.K; Bondybey, V.E. *Phys. Chem. Chem. Phys.* **2002**, *4*, 2224.

(25) a) Dietz, T.G.; Duncan, M.A.; Powers, D.E.; Smalley, R.E. *J. Chem. Phys.* **1981**, *74*, 6511. b) Brucat, P.J.; Zheng, L.S.; Pattiette, C.L.; Yang, S.; Smalley, R.E. *J. Chem. Phys.* **1986**, *84*, 3078.

(26) Morse, M. D. *Chem. Rev*. **1986**, *86*, 1049.

(27) a) LaiHing, K.; Cheng, P. Y.; Taylor, T. G.; Willey, K. F.; Peschke, M.; Duncan, M. A. *Anal. Chem.* **1989**, *61*, 1458. b) Willey, K. F.; Cheng, P. Y.; Taylor, T. G.; Bishop, M. B.; Duncan, M. A. *J. Phys. Chem.* **1990**, *94*, 1544-9. c) Cornett, D. S.; Peschke, M.; LaiHing, K.; Cheng, P. Y.; Willey, K. F.; Duncan, M. A. *Rev. Sci. Instr.* **1992**, *63*, 2177. d) Pilgrim, J. S.; Duncan, M. A. *J. Am. Chem. Soc.* **1993**, *115*, 4395. e) Pilgrim, J. S.; Duncan, M. A. *J. Am. Chem. Soc.* **1993**, *115*, 6958. f) Pilgrim, J. S.; Duncan, M. A. *J. Am. Chem. Soc.* **1993**, *115*, 9724. g) France, M. R.; Buchanan, J. W.; Robinson, J. C.; Pullins, S. H.; Tucker, J. L.; King, R. B.; Duncan, M. A. *J. Phys. Chem. A.* **1997**, *101*, 6214. h) Buchanan, J. W.; Reddic, J. E.; Grieves, G. A.; Duncan, M. A. *J. Phys. Chem. A.* **1998**, *102*, 6390. i) Grieves, G. A.; Buchanan, J. W.; Reddic, J. E.; Duncan, M. A. *Int. J. Mass Spectrom.* **2001**, *204*, 223. j) Walker, N. R.; Grieves, G. A.; Jaeger, J. B.; Walters, R. S.; Duncan, M. A. *Int. J. Mass Spectrom.* **2003**, *228*, 285. k) Jaeger, T. D.; Duncan, M. A. *J. Phys. Chem. A* **2004**, *108*, 11296. l) Pillai, E. D.; Molek, K. S.; Duncan, M. A. *Chem. Phys. Lett.* **2005**, *405*, 247.

(28) a) Watanabe, H.; Iwata, S.; Hashimoto, K.; Misaizu, F.; Fuke, K. *J. Am. Chem. Soc.* **1995**, *117*, 755. b) Fuke, K.; Hashimoto, K.; Takasu, R. *Adv. Met. Semicond. Clusters* **2001**, *5*, 1.

(29) a) Liu, H.; Guo, W.; Yang, S. *J. Chem. Phys*. **2002**, *116*, 9690. b) Yang, X.; Hu. Y.; Yang, S. J. Phys. Chem. A. **2000**, *104*, 8496.

(30) Asher, R.L.; Bellert, D.; Buthelezi, T.; Lessen, D.; Brucat, P.J. *Chem. Phys. Lett.* **1995**, *234*, 119. b) Buthelezi, T.; Bellert, D.; Lewis, V.; Brucat, P.J. *Chem. Phys. Lett.* **1995**, *246*, 145. c) Buthelezi, T.; Bellert, D.; Lewis, V.; Brucat, P.J. *Chem. Phys. Lett.* **1995**, *242*, 627. d) Bellert, D.; Buthelezi, Dezfulian, K.; T.; Hayes, T.; Brucat, P.J. *Chem.*

Phys. Lett. **1996**, *260*, 458. e) Hayes, T.; Bellert, D.; Buthelezi, T.; Brucat, P.J. *Chem. Phys. Lett.* **1998**, *287*, 22. f) Bellert, D.; Buthelezi, T.; Brucat, P.J. *Chem. Phys. Lett.* **1998**, *290*, 316.

(31) a) Kleiber, P.D.; Chen, J. *Int. Rev. Phys. Chem.* **1998**, *17*, 1. b) Chen, J.; Wong, T.H.; Cheng, Y.C.; Montgomery, K.; Kleiber, P.D. *J. Chem. Phys.* **1998**, *108*, 2285. c) Chen, J.; Wong, T.H.; Kleiber, P.D.; Wang, K.H. *J. Chem. Phys.* **1999**, *110*, 11798. d) Cheng, Y.C.; Chen, J.; Ding, L.N.; Wong, T.H.; Kleiber, P.D.; Liu, D. K. *J. Chem. Phys.* **1996**, *104*, 6452.

(32) Shen, M.H.; Farrar, J.M. *J. Chem. Phys.* **1991,** *94*, 3322. b) Donnelly, S.G.; Farrar, J.M. *J. Chem. Phys.* **1993**, *98*, 5450. c) Qian, J.; Midey, A.J.; Donnelly, S.G.; Lee, J.I.; Farrar, J.M. *Chem. Phys. Lett.* **1995**, *244*, 414.

(33) a) Scurlock, C.T.; Pullins, S.H.; Reddic, J.E.; Duncan, M.A. *J. Chem. Phys.* **996**, *104*, 4591. b) Pullins, S.H.; Scurlock, C.T.; Reddic, J.E.; Duncan, M.A. *J. Chem. Phys.* **1996**, *104*, 7518. c) Velasquez, J.; Kirschner, K.N.; Reddic, J.E.; Duncan, M.A. *Chem. Phys. Lett.* **2001**, *343*, 613. d) Reddic, J.E.; Duncan, M.A. *J. Chem. Phys.* **2000**, *112*, 4974. e) Pullins, S.H.; Reddic, J.E.; France, M.R.; Duncan, M.A. *J. Chem. Phys.* **1998**, *108*, 2725. f) France, M. R.; Pullins, S. H.; Duncan, M. A. *J. Chem. Phys.* **1998**, *109*, 8842. g) France, M. R.; Pullins, S. H.; Duncan, M. A. *J. Chem. Phys.* **1998**, *108*, 7049. h) Kirschner, K.N.; Ma, B.; Bowen, J.P.; Duncan, M.A. *Chem. Phys. Lett.* **1998**, *295*, 204. i) Yeh, C. S.; Willey, K. F.; Robbins, D. L.; Pilgrim, J. S.; Duncan, M. A. *Chem. Phys. Lett.* **1992**, *196*, 233. j) Yeh, C. S.; Pilgrim, J. S.; Willey, K. F.; Robbins, D. L.; Duncan, M. A. *Int. Rev. Phys. Chem.* **1994**, *13*, 231. k) Pilgrim, J. S.; Yeh, C. S.; Berry, K. R.; Duncan, M. A. *J. Chem. Phys.* **1994**, *100*, 7945. l) Scurlock, C. T.; Pilgrim, J. S.;

Duncan, M. A. *J. Chem. Phys.* **1995**, *103*, 3293. m) Yeh, C.S.; Willey, K.F.; Robbins, D.L.; Duncan, M.A. *J. Chem. Phys.* **1993**, *98*, 1867. n) France, M.R.; Pullins, S. H.; Duncan, M.A. *Chem. Phys.* **1998**, *239*, 447. o) Reddic, J.E.; Duncan, M.A. *Chem. Phys. Lett.* **1999**, *312*, 96.

(34) a) Husband, J.; Aguirre, F.; Thompson, C.J.; Laperle, C.M.; Metz, R.B. *J. Phys. Chem. A*. **2000**, *104*, 2020. b) Thompson, C.J.; Husband, J.; Aguirre, F.; Metz, R.B. *J. Phys. Chem. A*. **2000**, *104*, 8155. c) Thompson, C.J.; Aguirre, F.; Husband, J.; Metz, R.B. *J. Phys. Chem. A*. **2000**, *104*, 9901. d) Faherty, K.P.; Thompson, C.J.; Aguirre, F.; Michen, J.; Metz, R.B. *J. Phys. Chem. A* **2001**, *105*, 10054.

(35) Lie, J.; Dagdigian, P. J. *Chem. Phys. Lett*. **1999**, *304*, 317.

(36) a) Rothschopf, G.K.; Perkins, J.S.; Li, S.; Yang, D.S. *J. Phys. Chem. A* **2000**, *104*, 8178. b) Li, S.; Rothschopf, G.K.; Pillai, E.D.; Sohnlein, B.R.; Wilson, B.M.; Yang, D.S. *J. Chem. Phys.* **2001**, *115*, 7968. c) Yang, D. S. *Adv. Met. Semicond. Clusters*. **2001**, *5*, 187. d) Rothschopf, G.K.; Li, S.; Yang, D.S. *J. Chem. Phys.* **2002**, *117*, 8800. e) Li, S.; Sohnlein, B.R.; Rothschopf, G.K.; Fuller, J.F.; Yang, D.S. *J. Chem. Phys.* **2003**, *119*, 5406. f) Sohnlein, B. R.; Fuller, J. F.; Yang, D. S. *J. Am. Chem. Soc*. **2006**, *128*, 10692. g) Yang, D. S. Coord. Chem. Rev. **2001**, *214*, 187.

(37) a) Wang, K.; Rodham, D.A.; McKoy, V.; Blake, G.A. *J. Chem. Phys.* **1998**, *108*, 4817. b) Rodham, D.A.; Blake, G.A. *Chem. Phys. Lett.* **1997**, *264*, 522.

(38) a) Wiley, K. F.; Yeh, C. S.; Duncan, M. A. *Chem. Phys. Lett*. **1993**, *211*, 156. b) Agreiter, J. K.; Knight, A. M.; Duncan, M. A. *Chem. Phys. Lett*. **1999**, *313*, 162.

(39) a) Robles, E.S.J.; Ellis, A.M.; Miller, T.A. *J. Phys. Chem.* **1992**, *96*, 3247. b) Robles, E.S.J.; Ellis, A.M.; Miller, T.A. *J. Phys. Chem.* **1992**, *96*, 8791. c) Panov, S.I.; Williamson, J.M.; Miller, T.A. *J. Chem. Phys.* **1995**, *102*, 7359.

(40) Cockett, M. C. R. *Chem. Soc. Rev*. **2005**, *34*, 935.

(41) a) Bloembergen, N.; Cantrell, C.D.; Larssen, D.M. *Springer Ser. Opt. Sci.* **1976**, *3*, 162. b) McDowell, R.S.; Galbraith, H.W.; Krohn, B.J.; Cantrell, C.D.; Hinkley, E. D. *Opt. Comm.* **1976**, *17*, 178. c) Marcus, R.A.; Noid, D.W.; Koszykowski, M.L. *Springer Ser. Chem. Phys.* **1978**, *3*, 298. d) Kung, A.H.; Dai, H.L.; Berman, M.R.; Moore, C.B. *Springer Ser. Opt. Sci.* **1979**, *21*, 309.

(42) Thorne, L.R.; Beauchamp, J.L. *Gas Phase Ion Chemistry,* **1984**, *3*, 41.

(43) a) Knickelbein, M.B.; Menezes, W.J.C. *Phys. Rev. Lett.* **1992**, *69*, 1046. b) Knickelbein, M.B. *J. Chem. Phys.* **1996**, *104*, 3217. c) Koretsky, G.M.; Knickelbein, M.B. *Chem. Phys. Lett.* **1997**, *267*, 485. d) Knickelbein, M.B. *J. Chem. Phys.* **1993**, *99*, 2377.

(44) a) Ayotte, P.; Weddle, G.H.; Kim, J.; Johnson, M.A. *J. Am. Chem. Soc.* **1998**, *120*, 12361. b) Ayotte, P.; Weddle, G.H.; Bailey, C.G.; Johnson, M.A.; Vila, F.; Jordan, K.D. *J. Chem. Phys.* **1999**, *110*, 6268. c) Ayotte, P.; Weddle, G.H.; Johnson, M.A. *J. Chem. Phys.* **1999**, *110*, 7129. d) Ayotte, P.; Kim, J.; Kelley, J.A.; Nielson, S.B.; Johnson, M.A. *J. Am. Chem. Soc.* **1999**, *121*, 6950. e) Ayotte, P.; Nielson, S.B.; Weddle, G.H.; Johnson, M.A.; Xantheas, S.S. *J. Phys. Chem. A.* **1999**, *103*, 10665. f) Nielson, S.B.; Ayotte, P.; Kelley, J.A.; Weddle, G.H.; Johnson, M.A. *J. Chem. Phys.* **1999**, *111*, 10464.

(45) a) Okumura, M.; Yeh, L.I.; Lee, Y.T. *J. Chem. Phys.* **1985**, *83*, 3705. b) Okumura, M.; Yeh, L.I.; Lee, Y.T. *J. Chem. Phys.* **1988**, *88*, 79. c) Yeh, L.I.;Okumura, M.; Meyers,

J.D.; Price, J.M.; Lee, Y.T. *J. Chem. Phys.* **1989**, *91*, 7319. d) Yeh, L.I.; Lee, Y.T.; Hougen, J.T. *J. Mol. Spectrosc.* **1994**, *164*, 473. e) Crofteon, M.W.; Price, J.M.; Lee, Y.T. *Springer Ser. Chem. Phys.* **1994**, *56*, 44. f) Boo, D.W.; Liu, Z.F.; Suits, A.G.; Tse, J.S.; Lee, Y.T. *Science* **1995**, *269*, 57. g) Wu, C.C.; Jiang, J.C.; Boo, D.W.; Lin, s.H.; Lee, Y.T. Chang, H.C.; *J. Chem. Phys.* **2000**, *112*, 176. h) Wu, C.C.; Jian, J.C.; Hahndorf, I.; Choudhuri, C.; Lee, Y.T.; Chang, H.C. *J. Phys.Chem. A* **2000**, *104*, 9556.

(46) a) Klapstein, Dieter; Leutwyler, Samuel; Maier, John P. *Chem. Phys. Lett.* **1981**, *84*, 534-8. b) King, M. A.; Klapstein, D.; Kroto, H. W.; Maier, J. P.; Nixon, J. F. *J. Mol. Struct.* **1982**, *80*, 23-8. c) Ruchti, T.; Rohrbacher, A.; Speck, T.; Connelly, J.P.; Bieske, E.J.; Maier J.P. *Chem. Phys.* **1996**, *209*, 169. d) Speck, Thomas; Linnartz, Harold; Maier, John P. *J. Chem. Phys.* **1997**, *107*, 8706-8708. e) Linnartz, Harold; Speck, Thomas; Maier, J. P. *Chem. Phys. Lett.* **1998**, *288*, 504-508.

(47) a) Johnson, M.S.; Kuwata, K.T.; Wong, C.K.; Okumura, M. *Chem. Phys. Lett.* **1996**, *260*, 551. b) Choi, J.H.; Kuwata, K.T.; Cao, Y.B.; Okumura, M. *J. Phys. Chem. A.* **1998**, *102*, 503. c) Choi, J.H.; Kuwata, K.T.; Hass, B. M.; Cao, Y.B.; Okumura, M. *J. Chem. Phys.* **1994**, *100*, 7153.

(48) a) Xu, C.; Burton, G.R.; Taylor, T.R.; Neumark, D.M. *J. Chem. Phys.* **1997**, *107*, 3428. b) Asmis, K.R.; Taylor, T.R.; Xu, C.; Neumark, D.M. *J. Chem. Phys.* **1998**, *109*, 4389. c) Lehr, L.; Zanni, M.T.; Frischkorn, C.; Weinkauf, R.; Neumark, D.M. *Science*. **1999**, *284*, 635. d) Lenzer, T.; Furlanetto, M.R.; Pivonka, N.L.; Neumark, D. *J. Chem. Phys.* **1999**, *110*, 6714. e) Greenblatt, B.J.; Zanni, M.T.; Neumark, D.M. *J. Chem. Phys.* **1999**, *111*, 10566. f) Greenblatt, B.J.; Zanni, M.T.; Neumark, D.M. *J. Chem. Phys.* **2000**, *112*,

601. g) Zanni, M.T.; Frischkorn, C.; Davis, A.V.; Neumark, D.M. *J. Phys. Chem. A* **2000**, *104*, 2527.

(49) a) Ebata, T.; Fujii, A.; Mikami, N. *Int. Rev. Phys. Chem.* **1998**, *17*, 331-361. b) Fujii, A.; Fujimaki, E.; Ebata, T.; Mikami, N. *J. Am. Chem. Soc.* **1998**, *120*, 13256-13257. c) Ebata, T.; Iwasaki, A.; Mikami, N. *J. Phys. Chem. A* **2000**, *104*, 7974-7979. d) Ebata, T.; Kayano, M.; Sato, S.; Mikami, N. *J. Phys. Chem. A* **2001**, *105*, 8623-8628. e) Fujii, A.; Ebata, T.; Mikami, N. *J. Phys. Chem. A* **2002**, *106*, 8554-8560. f) Miyazaki, M.; Fujii, A.; Ebata, T.; Mikami, N. *Science* **2004**, *304*, 1134-1137. g) Abou El-Nasr, E.; Fujii, A.; Yahagi, T.; Ebata, T.; Mikami, N. *J. Phys. Chem. A* **2005**, *109*, 2498-2504.

(50) a) Carney, J.R.; Hagemeister, F.C.; Zwier, T.S. *J. Chem. Phys.* **1998**, *108*, 3379. b) Gruenloh, C.J.; Carney, J.R.; Arrington, C.A.; Zwier, T.S.; Frederick, S.Y.; Jordan, K.D. *Science* **1997**, *276*,1678. c) Zwier, T.S. *Annu. Rev. Phys. Chem.* **1996**, *47*, 205. d) Frost, R.K.; Hagemeister, F.C.; Arrington, C.A.; Schleppenbach, D.; Zwier, T.S.; Jordan, K.D. *J. Chem. Phys.* **1996**, *105*, 2605. e) Pribble, R.N.; Garrett, A.W.; Haber, K.; Zwier, T.S. *J. Chem. Phys.* **1995**, *103*, 531. f) Pribble, R.N.; Zwier, T.S. *Science,* **1994**, *265*, 75.

(51) a) Brudermann, J.; Melzer, M.; Buck, U.; Kazimirski, J.K.; Sadlej, J.; Bush, V. *J. Chem. Phys.* **1999**, *110*, 10649. b) Buck, U.; Huisken, F. *Chem. Rev.* **2000**, *100*, 3863. c) Brudermann, J.; Buck, U.; Buch, V. *J. Phys. Chem. A* **2002**, *106*, 453. d) Steinbach, C.; Andersson, P.; Kazimirski, J.K.; Buck, U.; Buch, V.; Beu, T.A. *J. Phys. Chem. A* **2004**, *108*, 6165.

(52) a) Lisy, J.M. *Cluster Ions,* Ng. C; Baer, T.; Powis, I. (Eds.) Wiley, Chichester, **1993**. b) Weinheimer, C.J.; Lisy, J.M. *Int. J. Mass Spectrom Ion Process* **1996**, *159*, 197. c) Weinheimer, C.J.; Lisy, J.M. *J. Phys. Chem.* **1996**, *100*, 15303. d) Weinheimer, C.J.;

Lisy, J.M. *J. Chem. Phys.* **1996**, *105*, 2938. e) Lisy, J.M. *Int. Rev. Phys. Chem.* **1997**, *16*, 267. f) Cabarcos, O.M.; Weinheimer, C.J.; Lisy, J.M. *J. Chem. Phys.* **1998**, *108*, 5151. g) Cabarcos, O.M.; Weinheimer, C.J.; Lisy, J.M.; Xantheas, S.S. *J. Chem. Phys.* **1999**, *110*, 5. h) Cabarcos, O.M.; Weinheimer, C.J.; Lisy, J.M.; Xantheas, S.S. *J. Chem. Phys.* **1999**, *110*, 9516. i) Cabarcos; O.M.; Weinheimer, C.J.; Lisy, J.M., *J. Chem. Phys.* **1999**, *110*, 8429. j) Vaden, T.D.; Forinash, B.; Lisy, J.M. *J. Chem. Phys.* **2002** *117*, 4628. k) Kim, D.; Hu, S.; Tarakeshwar, P.; Kim, K. S.; Lisy, J. M. *J. Phys. Chem. A.* **2003**, *107*, 1228. l) Vaden, T. D.; Lisy, J. M. *J. Chem. Phys*. **2004**, *120*, 721. m) Vaden, T. D.; Weinheimer, C. J.; Lisy, J. M. *J. Chem. Phys*. **2004**, *121*, 3102. n) Vaden, T. D.; Lisy, J. M. *J. Chem. Phys*. **2005**, *123*, 743021. o) Vaden, T. D.; Lisy, J. M. *J. Chem. Phys*. **2006**, *124*, 21431. p)) Vaden, T. D.; Lisy, J. M. *J. Chem. Phys*. **2006**, 1*24*, 14315.

(53) a) Gregoire, G.; Velasquez, J.; Duncan, M. A. *Chem. Phys. Lett.* **2001**, *349*, 451. b) Gregoire, G.; Duncan, M. A. *J. Chem. Phys.* **2002**, *117*, 2120. c) Gregoire, G.; Brinkmann, N. R.; van Heijnsbergen, D.; Schaefer, H. F.; Duncan, M. A. *J. Phys. Chem. A* **2003**, *107*, 218. d) Walters, R. S.; Brinkmann, N. R.; Schaefer, H. F.; Duncan, M. A. *J. Phys. Chem. A* **2003**, *107*, 7396. e) Walker, N. R.; Grieves, G.A.; Walters, R. S.; Duncan, M. A. *Chem. Phys. Lett.* **2003**, *380*, 230. f) Walker, N. R.; Walters, R. S.; Grieves, G. A.; Duncan, M. A. *J. Chem. Phys.* **2004**, *121*, 10498. g) Walker, N. R.; Walters, R. S.; Duncan, M. A. *J. Chem. Phys.* **2004**, *120*, 10037-10045.

(54) a) Walters, R. S.; Jaeger, T. D.; Duncan, M. A. *J. Phys. Chem. A.* **2002**, *106*, 10482. b) Walters, R. S.; Corminboeuf, C.; Schleyer, P. v. R, Duncan, M. A. *J. Am. Chem. Soc.* **2005**, *127*, 1100. c) Walters, R. S.; Pillai, E. D.; Schleyer, P. v. R, Duncan, M. A. *J. Am. Chem. Soc*. **2005**, *127*, 17030.

(55) a) Jaeger, T. D.; Pillai, E. D.; Duncan, M. A. *J. Phys. Chem. A* **2004**, *108*, 6605. b) Jaeger, T. D.; Duncan, M. A. *J. Phys. Chem. A* **2005**, *109*, 3311. c) Jaeger, J. B.; Pillai, E. D.; Jaeger, T. D.; Duncan, M. A. *J. Phys. Chem. A* **2005**, *109*, 2801.

(56) a) Walker, N. R.; Walters, R. S.; Pillai, E. D.; Duncan, M. A. *J. Chem. Phys.* **2003**, *119*, 10471. b) Walters, R. S.; Duncan, M. A. *Austr. J. Chem.* **2004**, *57*, 1145. c) Tsai, B. M.; Jordan, K. D.; Walters, R. S.; Duncan, M. A. *J. Phys. Chem. A* d) Walters, R. S.; Pillai, E. D.; Duncan, M. A. *J. Am. Chem. Soc.* **2005**, *127*, 16599. e) Vaden, T. D.; Lisy, J. M. Carnegie, P. D.; Pillai, E. D.; Duncan, M. A. *Phys. Chem. Chem. Phys*. **2006**, *82*, 3078.

(57) Velasquez, J.; Pillai, E. D.; Carnegie, P. D.; Duncan, M. A. *J. Phys. Chem. A.* **2006**, *110*, 2325.

(58) a) Pillai, E. D.; Jaeger, T. D.; Duncan, M. A. *J. Phys. Chem. A* **2005**, *109*, 3521-3526. b) Pillai, E. D.; Jaeger, T. D.; Duncan, M. A. *J. Am. Chem. Soc.* **2007.** in press

(59) Duncan, M. A.; *Annu. Rev. Phys. Chem*. **1997**, *48*, 69.

(60) Duncan, M.A. *Intl. Rev. Phys. Chem.* **2003**, *22*, 407.

(61) a) van Heijnsbergen, D.; Jaeger, T.D.; von Helden, G.; Meijer, G.; Duncan, M.A. *Chem. Phys. Lett.* **2002**, *364*, 345. b) van Heijnsbergen, D.; von Helden, G.; Meijer, G.; Maitre, P.; Duncan, M.A. *J. Am. Chem. Soc.* **2002**, *124*, 1562. c) Jaeger, T.D.; Fielicke, A.; von Helden, G.; Meijer, G.; Duncan, M.A. *Chem. Phys. Lett.* **2004**, *392*, 409. d) Jaeger, T.D.; van Heijnsbergen, D.; Klippenstein, S.J.; von Helden, G.; Meijer, G.; Duncan, M.A. *J. Am. Chem. Soc.* **2004**, *126*, 10981.

(62) a) van Heijnsbergen, D.; von Helden, G.; Duncan, M.A.; van Roij, A. J. A.; Meijer, G. *Phys. Rev. Lett.* **1999**, *83*, 4983. b) von Helden, G.; van Heijnsbergen, D.; Duncan,

M.A.; Meijer, G. *Chem. Phys. Lett.* **2001**, *333*, 350. c) von Helden, G.; Kirilyuk, A.; van Heijnsbergen, D.; Sartakov, B.; Duncan, M.A.; Meijer, G. *Chem. Phys.* **2000**, *262*, 31. d) van Heijnsbergen, D.; Duncan, M.A.; Meijer, G.; von Helden, G. *Chem. Phys. Lett.* **2001**, *349*, 220. e) van Heijnsbergen, D.; Demyk, K.; Duncan, M.A.; Meijer, G.; von Helden, G. *Phys. Chem. Chem. Phys.* **2003**, *5*, 2515.

(63) a) Fielicke, A.; Meijer, G.; von Helden, G. *Eur. Phys. J. D.* **2003**, *24*, 69. b) Fielicke, A.; Meijer, G.; von Helden, G.; Simard, B.; Denommee, S.; Rayner, D. *J. Am. Chem. Soc.* **2003**, *125*, 11184. c) Fielicke, A.; Mitric, R.; Meijer, G.; Bonacic-Koutecky, V.; von Helden, G. *J. Am. Chem. Soc.* **2003**, *125*, 15716. d) Fielicke, A.; von Helden, G. ; Meijer, G. *J. Phys. Chem. B.* **2004**, *108*, 14591. e) Fielicke, A.; Kirilyuk, A.; Ratsch, C.; Behler, J.; Scheffler, M.; von Helden, G. ; Meijer, G. *Phys. Rev. Lett.* **2004**, *93*, 023401. f) Oomens, J.; Moore, D.T.; von Helden, G. ; Meijer, G.; Dunbar, R.C. *J. Am. Chem. Soc.* **2004**, *126*, 724.

(64) a) Lemaire, J.; Boissel, P.; Heninger, M.; Mestdagh, H.; Mauclaire, G.; Le Caer, S.; Ortega, J.M.; Maitre, P. *Spectra Anal.* **2003**, *32*, 28. b) Le Caer, S.; Heninger, M.; Lemaire, J.; Boissel, P.; Maitre, P.; Mestdagh, H. *Chem. Phys. Lett.* **2004**, *385*, 273. c) Simon, A.; Jones, W.; Ortega, J.M.; Boissel, P.; Lemaire, J.; Maitre, P. *J. Am. Chem. Soc.* **2004**, *126*, 11666

(65) Sheppard, N. J. *Elect. Spect. Rel. Phenom*. **1986**. *38*, 175.

(66) Van Hove, M. A.; Somorjai, G. A. *J. Mol. Catal. A*. **1998**, *131*, 243.

(67) Musaev, D.G.; Morokuma, K. *Adv. Chem. Phys*. **1996**, *95*, 61.

(68) Madix, R. *J. Appl. Surf. Sci*. **1982**, *14*, 41.

(69) Orr, B. J. *Intl. Rev. Phys. Chem.* **2006**, *25*, 655.

(70) Huber, K. P.; Herzberg, G. *Molecular Spectra and Molecular Structure IV. Constants of Diatomic Molecules*, Van Nostrand Reinhold Co. **1979**.

(71) a) Chatt, J.; Melville, D. P.; Richards, R. L. *J. Chem. Soc a)*. **1969**, *18*, 2841. b) Chatt, J.; Dilworth, J. R.; Richards, R. L. *Chem. Rev*. **1978**, 78, 589. c) Richards, R. L. *Coord. Chem. Rev*. **1996**, *153*, 83. d) Richared, R.L. *Coordination Chemistry Reviews*. **1996**, *154*, 83.

(72) a) Chatt, J.; Dilworth, J.R.; Leigh, G.J. *J. Organometal. Chem*. **1970**, *21*, P49. b) Chatt, J.; Leigh, G.J.; Thankarajan, N. *J. Organometal. Chem*. **1970**, *25*, C77. c) Leigh, G.J. *J. Mol. Cataly*. **1988**, *47*, 363. d) Leigh, G.J. *Can. J. Chem*. **2005**, *3*, 277.

(73) a) Tuczek, F.; Lehnert, N. *Angew. Chem. Int. Ed*. **1998**, *37*, 2636. b) Lehnert, N.; Tuczek, F. *Inorg. Chem*. **1999**, *38*, 1671. c) Studt, F.; Tuczek, F. J. *Computational Chemistry*. **2006**, *27*, 1278.

(74) a) Kovacs, J.; Speier, G.; Marko, L. *Inorg. Chimica*. **1970**, *4*, 3. b) Speier, G.; Marko, L. *J. Organometal. Chem*. **1970**, *21*, P46.

(75) a) Powell, C.B.; Hall, M.B. *Inorg. Chem*. **1984**, *23*, 4619. b) Zhenyang, L.; Hall, M.B. *Coord. Chem. Rev*. **1993**. *123*, 149.

(76) a) Bauschlicher, C.W., Jr.; Partridge, H.; Langhoff, S.R. *J. Phys. Chem.* **1992**, *96*, 3273. b) Sodupe, M.; Bauschlicher, C.W., Jr.; Langhoff, S.R. *J. Phys. Chem.* **1992**, *96*, 5350. c) Sodupe, M.; Bauschlicher, C.W.; Langhoff, S.R.; Partridge, H., *J. Phys. Chem.* **1992**, *96*, 2118. d) Partridge, H.; Bauschlicher, C.W., Jr.; Langhoff, S.R. *J. Phys. Chem.* **1992**, *96*, 5350. e) Bauschlicher, C.W., Jr.; Sodupe, M.; Partridge, H. *J. Chem. Phys.* **1992**, *96*, 4453. f) Partridge, H.; Bauschlicher, C.W., Jr. *Chem. Phys. Lett.* **1992**, *195*, 494. g) Sodupe, M.; Bauschlicher, C.W., Jr.; Partridge, H. *Chem. Phys. Lett.* **1992**, *192*, 185.

h) Bauschlicher, C.W., Jr. *Chem. Phys. Lett.* **1993**, *201*, 11. i) Sodupe, M.; Bauschlicher, *Chem. Phys.* **1994**, *185*, 163. j) Maitre, P.; Bauschlicher, C.W., Jr. *Chem. Phys.* **1994**, *225*, 467. k) Bauschlicher, C.W., Jr.; Partridge, H. *Chem. Phys. Lett.* **1995**, *239*, 241. l) Sodupe, M.; Branchadell, V.; Rosi, M.; Bauschlicher, C.W., Jr. *J. Phys. Chem. A.* **1997**, *101*, 7854. m) Bauschlicher, C. W., Jr.; Petterson, L. M.; Siegbahn, P. E. M. *J. Chem. Phys*. **1987**, 87, 2129. n) Zhou, M.; Andrews, L.; Bauschlicher, C. W. Jr. *Chem. Rev*. **2001**, 101, 1931.

(77) a) Lupinetti, A.J.; Fau, S.; Frenking, G.; Strauss, S.H. *J. Phys. Chem*. **1997**, *101*, 9951. b) Frenking, G.; Pidun, U. *J. Chem. Soc., Dalton Trans*. **1997**, 1653. c) Frenking, G.; Frohlich, N. *Chem. Rev*. **2000**, *100*, 717.

(78) a) Pandey, R.; Rao, B. K.; Jena, P.; Miguel, A. B. *J. Am. Chem. Soc*. **2001**, *123*, 7744. b) Gutsev, G. L.; Mochena, M. D.; Jena, P.; Bauschlicher, C. W. Jr. Partridge, H. *J. Chem. Phys*. **2004**, *121*, 6785.

(79) a) Yang, C.N.; Klippenstein, S.J. *J. Phys. Chem.* **1999**, *103*, 1094. b) Klippenstein, S.J.; Yang, C.N. *Int. J. Mass Spectrom.* **2000**, *201*, 253.

(80) Kock, W.; Holthausen, M. C. *A Chemist's Guide to Density Functional Theory*, 2nd ed. Wiley-Vch, Amsterdam, **2002**.

(81) Becke, A.D. *J. Chem. Phys*. **1993**, *98*, 5648.

(82) Lee, C.; Yang, W.; Parr, R.G. *Phys. Rev. B*. **1988**, *37*, 785.

CHAPTER 2

EXPERIMENTAL

Metal ion complexes are generated in our laboratory by laser ablation of rotating metal rods located in a pulsed nozzle source. An inert gas (usually He or Ar) carrying a small partial pressure of the molecular ligand of interest is used in a supersonic expansion to create the metal ion clusters. The metal-nitrogen complexes are produced in pure expansions of nitrogen gas with small amount of water added in. It has been empirically shown in our experiments that water enhances the cluster growth in the nozzle source. The pulsed-nozzle source and details of the molecular beam apparatus has been described in literature.[1-5] Figure 2.1 shows a schematic of our apparatus which includes the cluster formation chamber and a differentially pumped reflectron time-of-flight (RTOF) mass spectrometer. The cluster formation chamber is commonly referred to as the "source" chamber and is under a vacuum of approximately 10^{-7}- 10^{-6} torr. The mass spectrometer section of the instrument is under a vacuum of nearly 10^{-8} Torr. A General Valve (series 9) operating with a backing pressure of 60-80 psi is utilized to create a supersonic beam where cluster growth occurs. Light from the second or third harmonic of a Nd:YAG laser (532 nm, 355 nm) is employed to vaporize a rotating metal rod. The vaporization laser operates at a 10 Hz repetition rate and hence the entire pulsed experiment is run at 10 Hz. The normal pulse energies used range from 1-15 mJ/pulse. The rod is placed in a specially designed rod-holder known as the “cutaway” rod holder and the whole set-up is shown in Figure 2.2. The cationic metal complexes grow directly in the molecular beam or can be produced by photoionization of the neutrals with light at 193 nm from an ArF laser. The source can be

Figure 2.1 The molecular beam machine with the reflectron time-of-flight (RTOF) mass spectrometer.

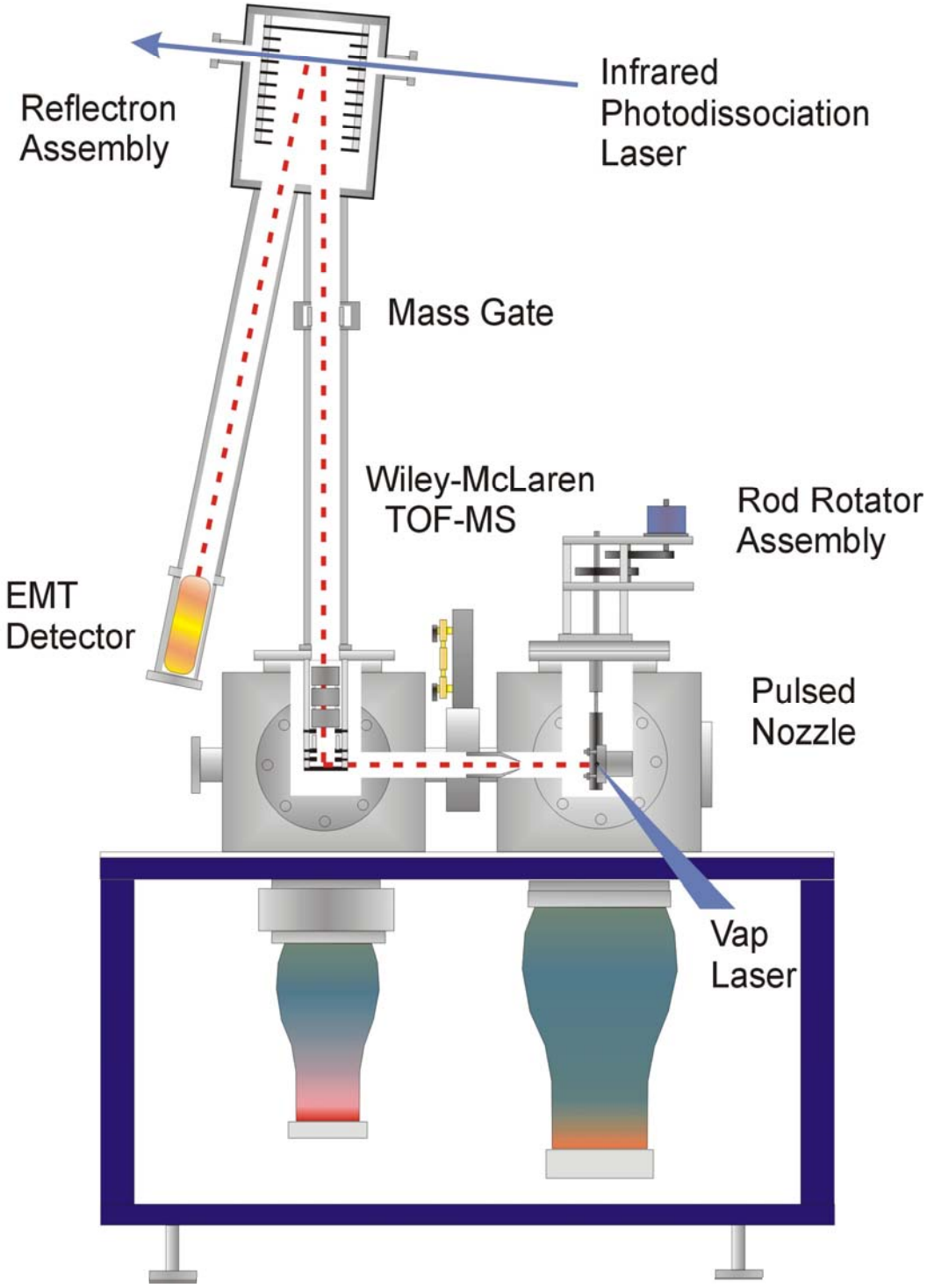
Reflectron
Assembly
Infrared
Photodissociation
Laser
Mass Gate
Wiley-McLaren
TOF-MS
Rod Rotator
Assembly
EMT
Detector
Pulsed
Nozzle
Vap
Laser

Figure 2.2 The laser vaporization cluster source showing the *General Valve* pulsed nozzle, the rotating rod, and the "cutaway" rod holder.

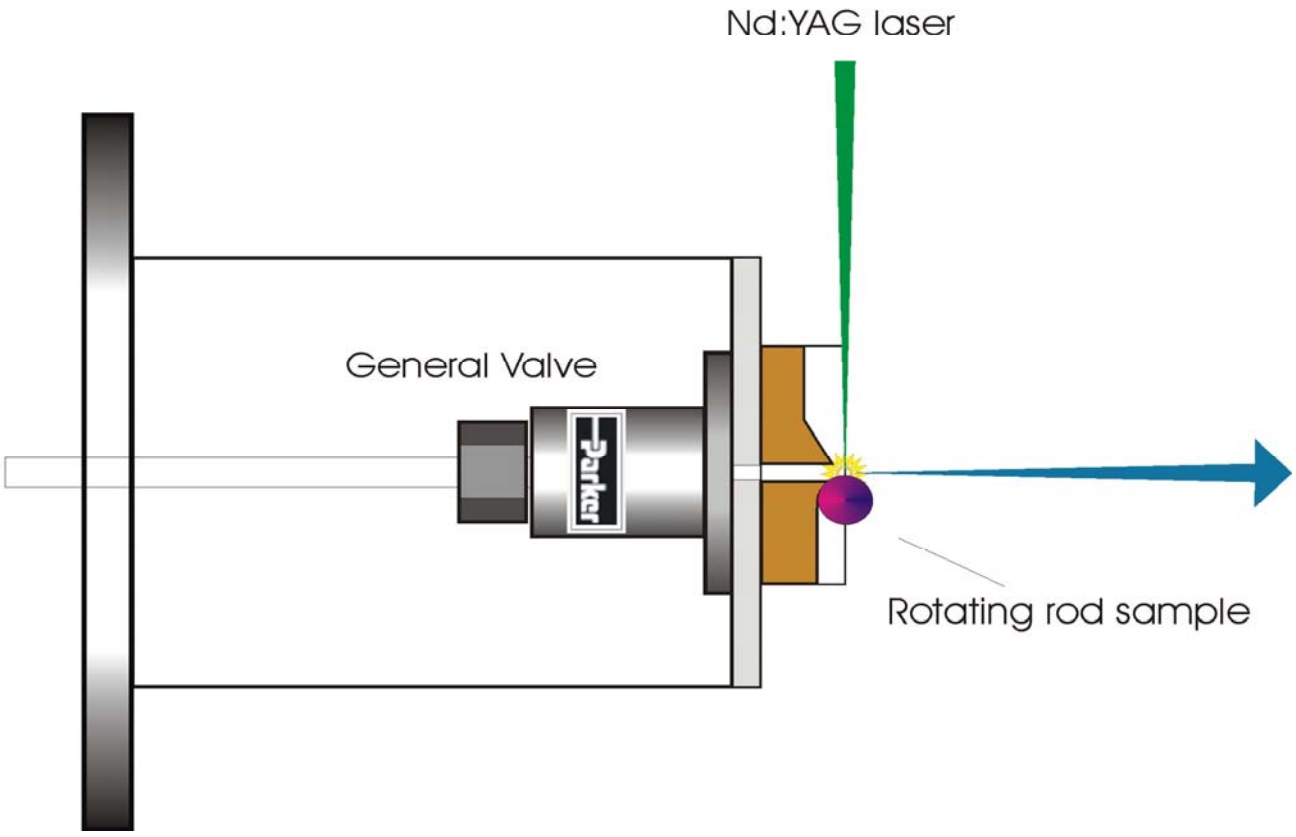
Nd:YAG laser
General Valve
Parker
Rotating rod sample

modified in various ways to produce different cluster sizes and compositions. For example, a cutaway source optimizes growth of single metal-multiple ligand (M^+-L_n) complexes whereas addition of a growth channel leads to clusters containing more than a single metal atom such as M_m^+ and M_m^+-L_n systems. The expansion produced is skimmed into the differentially pumped RTOF mass spectrometer chamber.

The RTOF mass spectrometer consists of acceleration plates that can be utilized in the pulsed mode to extract cationic clusters out of the beam or in the DC mode to study neutrals that are ionized by the ArF excimer laser. The extracted ions enter the first drift tube of the RTOF mass spectrometer where they may be size selected using a pair of pulsed deflection plates known as a "mass gate". These plates are pulsed to ground when ions of interest pass by it, allowing them to pass through to the reflectron area of the mass spectrometer. The mass selected ions then enter the reflectron or "turning" region, where a field gradient is applied to bring the ions to zero velocity before reaccelerating them into the second drift tube. The ions then strike an electron multiplier tube (EMT) where they are detected. The output of the EMT is first amplified by a pre-amplifier and fed into a digital oscilloscope (LeCroy WaveRunner 341). The signal of the ions emerges as voltage spikes as a function of the flight time through both arms of the MS. The oscilloscope is interfaced to a personal computer (PC) via an IEEE-488 digital card so that the signal can be read. Figure 2.3 shows a mass spectrum of $V^+(N_2)_n$ complexes obtained using our cluster source and RTOF mass spectrometer. The third harmonic of a Nd:YAG was used to ablate a ½" vanadium rod placed in the cutaway rod-holder. The complexes are produced in expansions of pure nitrogen. The intermediate masses in the mass spectrum correspond to $V^+(H_2O)(N_2)_y$ and are a by-product of the water that is added to the expansion gas to improve cluster growth.

Figure 2.3 The mass spectrum $V^+(N_2)_n$ and $V^+(H_2O)(N_2)_y$ complexes produced by laser vaporization in a pure nitrogen expansion.

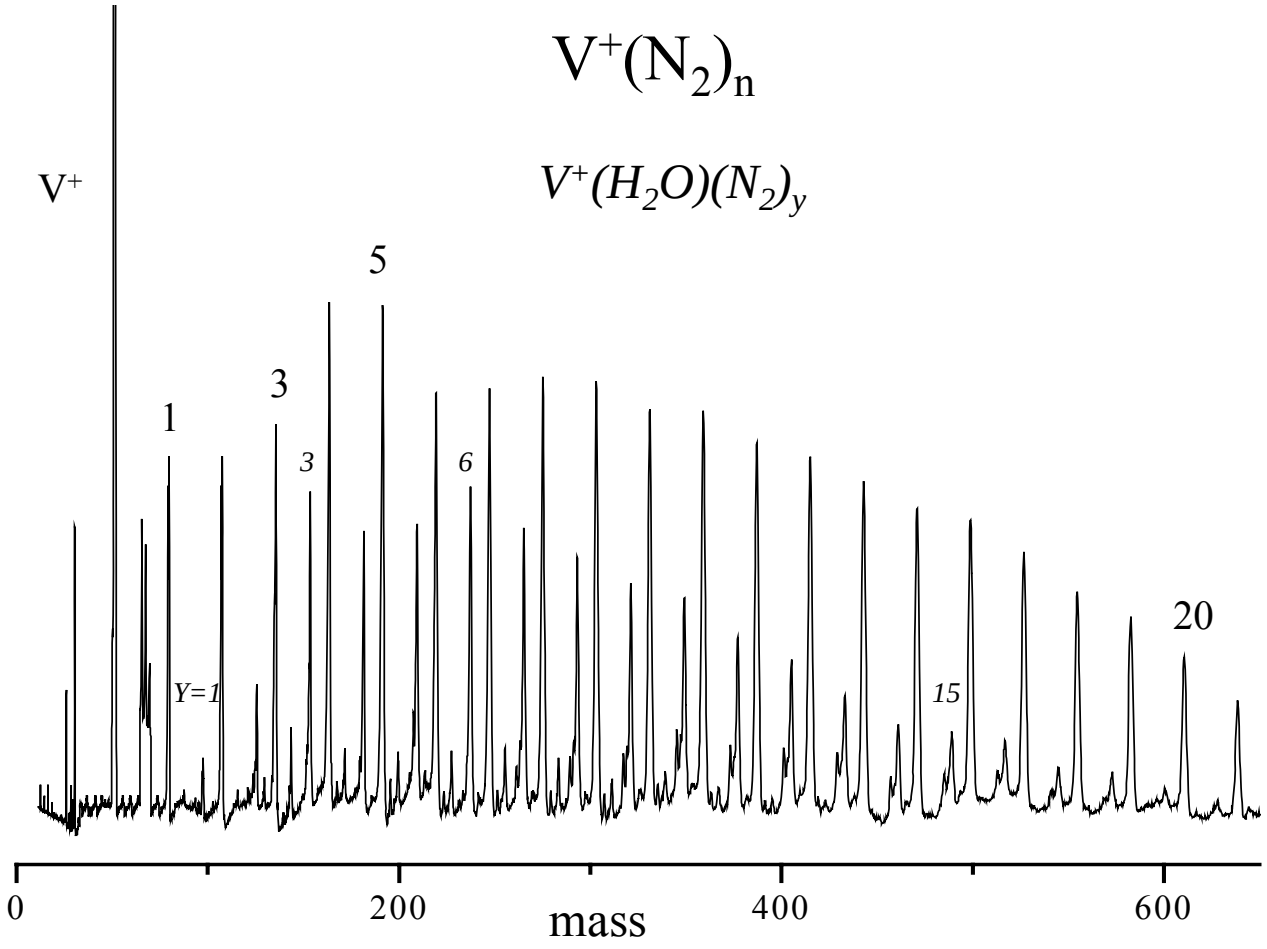
$V^+(N_2)_n$
V^+
$V^+(H_2O)(N_2)_y$
1
3
5
3
6
20
Y=1
15
0
200
400
600
mass

In preliminary runs, the mass gate is maintained at ground and all the ions that are generated in the cluster source or produced by photoionization by 193 nm are allowed to reach the detector. Analysis of the flight time is done in the following manner to deduce the masses of the ions. The ions from the source first enter the electric field produced by two plates known as the "repeller plate" and "draw-out-grid" (DOG), which are placed at the entrance of the mass spectrometer. Typical voltages on the repeller and DOG are 1000 V and 900 V respectively. The electric field produced by the plates is the difference between the voltages divided by their separation distance. The ions moving through this electric field experience an acceleration, which can be calculated from simple kinematics. After moving through the field, the kinetic energy (KE) of the ions is related to the ions' mass and velocity by the following equation:

$$KE = (½)mv^2$$

where m is the mass of the ion and v is its velocity. Since the velocity is given by v=d/t where d is the distance or length of the tube and t is the time taken to traverse it, the KE equation can be written as

$$m = 2\ (KE)\ (t/d)^2$$

Since the experiment is pulsed, the time when the voltages are applied to the repeller and the DOG are known which in effect is time zero. Then the time for the ions to reach the detector is measured using the oscilloscope. The ion masses are assigned by using a reference mass to calculate the masses of all the other ions. Since all the ions pass through the same electric field, they acquire the same kinetic energy. Therefore the kinetic energy of ion with mass m_1 is equal to the kinetic energy of ion with mass m_2:

$$KE_1 = KE_2$$

This can be written as:

$$m_1 v_1^2 = m_2 v_2^2$$

After some rearrangement, the equation now reads as:

$$m_1 = m_2 (t_1/t_2)^2$$

Since t_1 and t_2 are measured and if mass m_2 is known, then mass m_1 can be calculated. In such a manner, we first obtain a mass spectrum of all the ions present in the molecular beam. After assigning the peaks in the mass spectrum to specific ions, we identify species of interest. Since the mass flight time of all the ions are measured using the oscilloscope, we may turn on our mass gate at the appropriate time to deflect all other ions, allowing only the ion of interest to enter the reflectron.

To obtain an infrared spectrum, IR light is used to excite the mass selected complexes in the turning region in order to induce dissociation of the complexes. An IR OPO/OPA (optical parametric oscillator/amplifier) from Laser Vision pumped by a Continuum 8000 or 9010 seeded Nd:YAG provides the tunable infrared radiation used in our experiments. The pump energy from the Nd:YAG lasers ranges from 550 - 650 mJ/pulse of 1064 nm light. Figure 2.4 is generalized schematic of the operation of the OPO/OPA. The 1064 light is first split in a 30:70 ratio with the smaller portion passing through the OPO and the larger portion, through the OPA. Before passing to the OPO, the 1064 nm light passes through a frequency doubling crystal to convert the light to 532 nm. The OPO consists of two 532 nm pumped KTP crystals whereas the OPA consists of four 1064 nm pumped KTA crystals. The 532 nm light passing through the OPO is divided into a two beams known as the signal and idler beams. The signal and idler beams are related by the following equations :

$$\omega_{signal} > \omega_{idler}$$

Figure 2.4 The infrared optical parametric oscillator/amplifier (IR OPO/OPA) system from *LaserVision*.

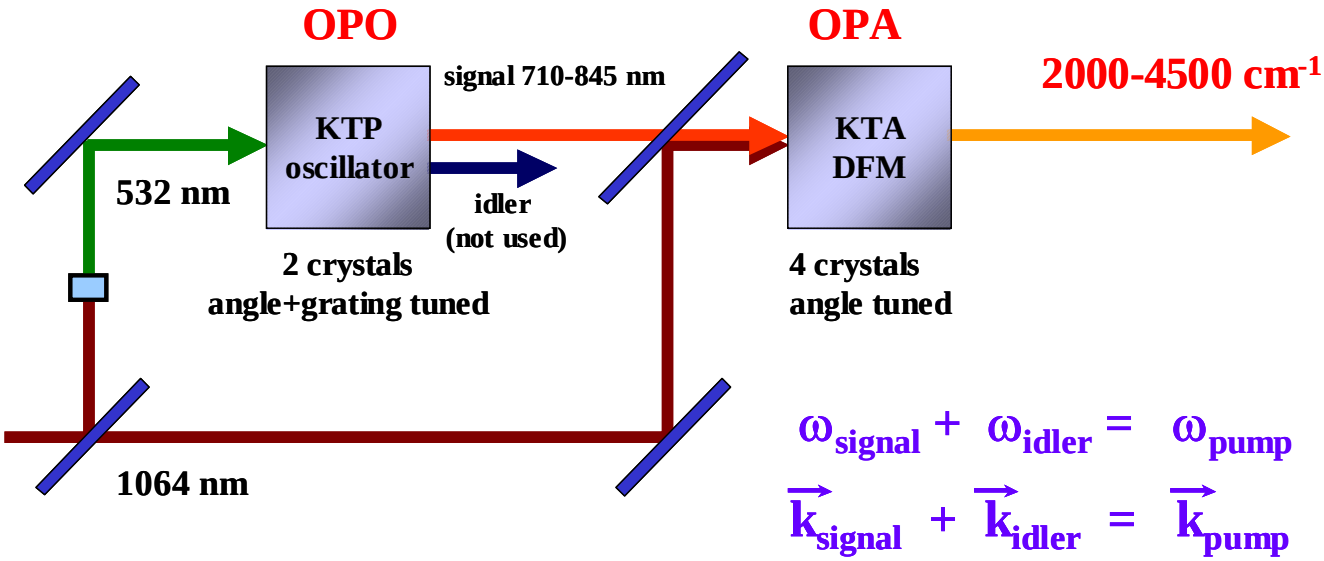
OPO
OPA
2000-4500 cm-1
signal 710-845 nm
KTP
oscillator
KTA
DFM
532 nm
idler
(not used)
2 crystals
angle+grating tuned
4 crystals
angle tuned
1064 nm
ωsignal + ωidler = ωpump
ksignal + kidler = kpump

$$\omega_{signal} \neq \omega_{idler}$$

$$\omega_{pump} = \omega_{signal} + \omega_{idler}$$

where ω is the frequency (cm^{-1}). The signal beam from the OPO is tunable light from 11,800 - 14,000 cm^{-1}, which passes into the OPA. Tunable IR light is produced from 2000 – 4500 cm^{-1} (2.2-4.9 μm) with difference frequency generation using the signal output from the oscillator and residual 1064 from the amplifier. The pulse energies range from 2 – 15 mJ/pulse with spectral linewidths on the order of 0.3 cm^{-1}. Typical scans are acquired over 250 laser shots at 0.5 cm^{-1} increments. Near 2200 cm^{-1} where most of the metal-nitrogen complexes were studied, the pulse energy ranged from 5 - 12 mJ/pulse. The metal-nitrogen spectra were obtained by usually taking 0.5 - 1.0 cm^{-1} steps. Using this experimental set-up, various metal-ligand systems have been studied by our group where the ligand has included CO_2,[6-9] C_2H_2,[10-12] C_6H_6,[13-15] H_2O,[16-18] and N_2.[19-20]

Our IR spectroscopy does not allow traditional absorption or emission spectroscopy because our ion densities are too low. In addition, the path length through the ion beam is small and so we cannot perform traditional absorption spectroscopy. Our form of spectroscopy is known as "action spectroscopy" where the sample of interest initially absorbs the radiation, following which a perturbation or "action" occurs which is then monitored to obtain a spectra. The "action" in our experiments is the dissociation of the complex that occurs upon irradiation. The IR light is tuned into a resonance with some vibrational frequency of the complex that results in dissociation. Usually the vibrational frequency excited is a particular fundamental mode of the ligand that is accessible by our IR source. This is schematically shown for the $Ni^+(C_2H_2)_7$ complex in Figure 2.5. The complex is first size selected and appears as a single peak in the mass spectrum A. The IR laser is then tuned into resonance with a C-H vibration of

Figure 2.5 The process of obtaining a fragmentation mass spectrum is shown for $Ni^{+}(C_2H_2)_7$. The complex is first size selected (A) and the IR laser is tuned into a vibrational resonance of the C-H stretching frequency that leads dissociation (B). The fragmentation mass spectrum (C) is obtained by subtracting the spectra with IR laser "On" - IR laser "Off".

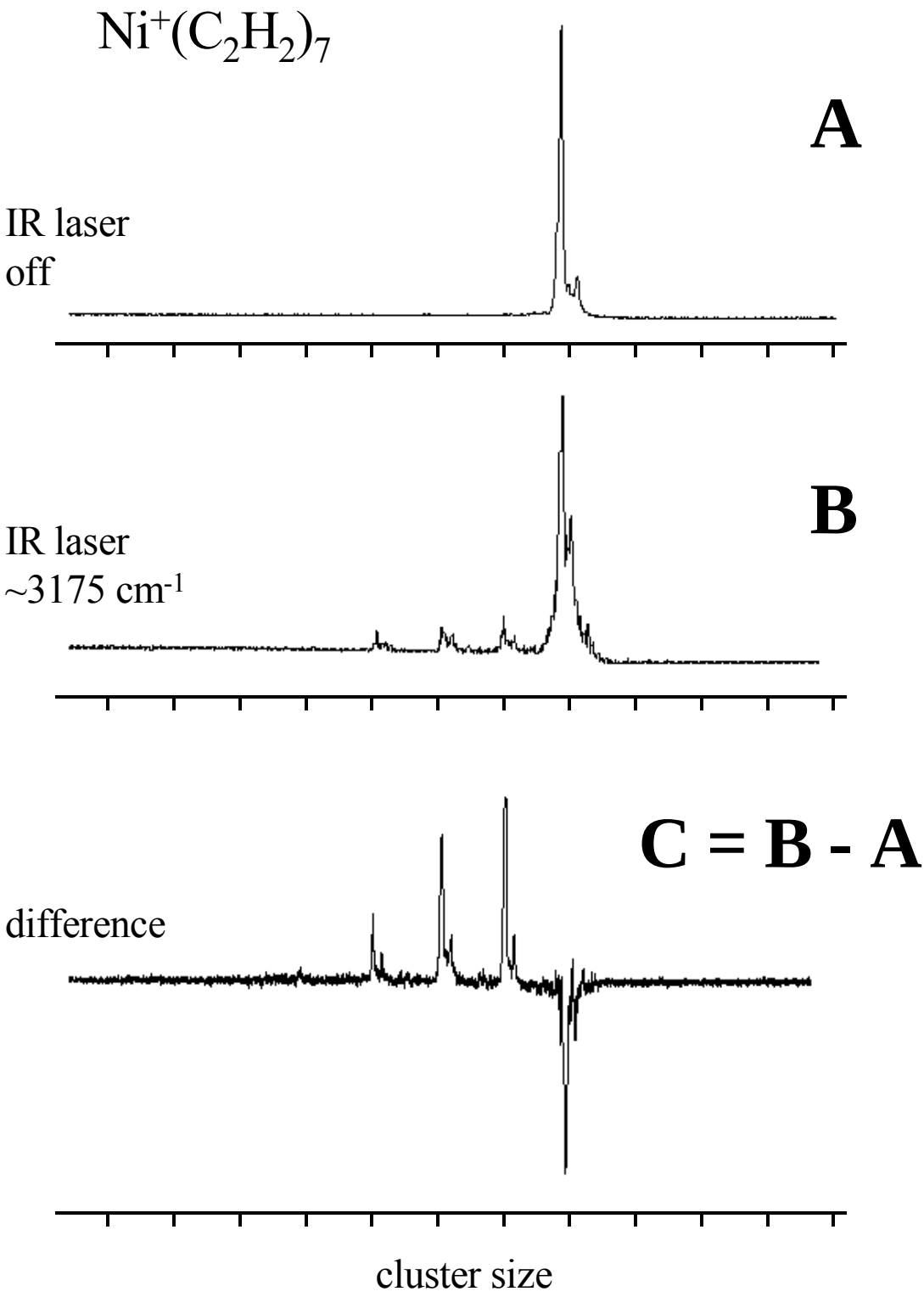
$Ni^+(C_2H_2)_7$
A
IR laser
off
B
IR laser
~3175 cm-1
C = B - A
difference
cluster size

C_2H_2 that leads to dissociation shown in mass spectrum B. The spectra are subtracted to produce the difference or fragmentation mass spectrum shown in C. Upon dissociation, the parent and daughter ions travel down the second drift tube where they are detected with the EMT. The infrared photodissociation (IRPD) spectra are acquired by monitoring the fragment yield as a function of the infrared wavelength.

To induce dissociation of the metal-ligand complexes by IR light, the IR photons corresponding to the vibrational frequencies must have enough energy to break the weakest bond in the complex, i.e. the metal cation-ligand bond. Table 2.1 lists characteristic binding energies of transition metal (TM) cations to various ligands and the vibrational frequency that is excited in our experiment. As can be seen, the bond energies are usually much greater than the energy of the incident IR photon and dissociation cannot take place unless a multi-photon occurs. But given our experimental pulse energies, multi-photon processes are very inefficient. However, as multiple ligands attach to the metal ion, the bonding capacity of the metal is distributed to the additional ligands and the per-ligand binding energy decreases.[21-25] Eventually, the binding energy is small enough for the IR photons to eliminate at least one ligand. This is seen in our work on metal-nitrogen complexes where the small complexes do not dissociate by IR excitation near 2300 cm^{-1}. The larger complexes do fragment by loss of N_2 molecules and we are able to acquire IRPD spectra of them.[19,20] In our studies of other metal cation-ligand complexes, we have employed a technique known as rare gas "tagging" to obtain IRPD spectra of the small complexes.[6-18] However, this technique was not applied to our study of metal cation-nitrogen complexes.

Table 2.1 Typical binding energies for transition metal (TM) cation-ligand complexes and IR frequencies that are excited in our experiments.

Complex	Binding Energy (cm^{-1})	Frequency Excited (cm^{-1})
$TM^+(N_2)$	4000 - 6000[a]	2330
$TM^+(CO_2)$	4000 - 6000[b]	2349
$TM^+(C_2H_2)$	10,500 - 15,700[c]	3289, 3374
$TM^+(C_6H_6)$	12,000 - 20,000[d]	~ 3000 - 3100
$TM^+(H_2O)$	10,500 - 15,700[e]	3657, 3756

[a]Reference 21

[b]Reference 22

[c]Reference 23

[d]Reference 24

[e]Reference 25

References

(1) LaiHing, K.; Cheng, P. Y.; Taylor, T. G.; Wiley, K. F.; Peschke, M.; Duncan, M. A. *Anal. Chem*. **1989**, *61*, 1458.

(2) Cornett, D. S.; Peschke, M.; LaiHing, K.; Cheng, P. Y.; Wiley, K. F.; Duncan, M.A. *Rev. Sci*. *Instrum.* **1992**, *63*, 2177.

(3) Yeh, C. S.; Pilgrim, J. S.; Robbins, D. L.; Wiley, K. F.; Duncan, M.A. *Int. Rev. Phys. Chem*. **1994**, *13*, 231.

(4) Duncan, M.A. *Ann. Rev. Phys. Chem*. **1997**, *48*, 69.

(5) Duncan, M.A. *Intl. Rev. Phys. Chem.* **2003**, *22(2)*, 407.

(6) Gregoire, G.; Duncan, M. A. *J. Chem. Phys.* **2002**, *117*, 2120.

(7) Walker, N. R.; Walters, R. S.; Grieves, G. A.; Duncan, M. A. *J. Chem. Phys*. **2004**, *121*, 10498.

(8) Walker, N. R.; Walters, R. S.; Duncan, M. A. *J. Chem. Phys*. **2004**, *120*, 10037.

(9) Jaeger, J.; Jaeger, T.; Duncan, M. A. *Intl. J. Mass. Spectrom.* **2003**, *228*, 285.

(10) Walters, R. S.; Jaeger, T. D.; Duncan, M. A. *J. Phys. Chem. A* **2002**, *106*, 10482.

(11) Walters, R. S.; Corminboeuf, C.; Schleyer, P. v. R, Duncan, M. A. *J. Am. Chem. Soc.* **2005**, *127*, 1100.

(12) Walters, R. S.; Pillai, E. D.; Schleyer, P. v. R, Duncan, M. A. *J. Am. Chem. Soc*. **2005**, *127*, 17030.

(13) Jaeger, T. D.; Pillai, E. D.; Duncan, M. A. *J. Phys. Chem. A*. **2004**, *108*, 6605.

(14) Jaeger, T. D.; Duncan, M. A. *J. Phys. Chem. A*. **2005**, *109*, 3311.

(15) Jaeger, J. B.; Pillai, E. D.; Jaeger, T. D.; Duncan, M. A. *J. Phys. Chem. A*. **2005**, *109*, 2801.

(16) Walker, N. R.; Walters, E. D.; Pillai, E. D.; Duncan, M. A. *J. Chem. Phys.* **2003**, *119*, 10471.

(17) Walters, R. S.; Duncan, M. A. *Austr. J. Chem.* **2004**, *57*, 1145.

(18) Walker, N. R.; Walters, R. S.; Jordan, K. D.; Duncan, M. A. *J. Phys. Chem. A.* **2005**, *109*, 7057.

(19) Pillai, E. D.; Jaeger, T. D.; Duncan, M. A. *J. Phys. Chem. A.* **2005**, *109*, 3521.

(20) Pillai, E. D.; Jaeger, T. D.; Duncan, M. A. *J. Am. Chem. Soc.* **2007.** in press.

(21) a) Khan, F. A.; Steele, D. L.; Armentrout, P. B. *J. Phys. Chem.* **1995**, 99,7819. b) Tjelta, B. L.; Armentrout, P. B. *J. Phys. Chem.* **1997**, 101, 2064. c) Tjelta, B. L.; Walter, D.; Armentrout, P. B. *Intl. J. Mass. Spec.* **2001**, 204, 7.

(22) a) Amity, A.; Muntean, F.; Walter, D.; Rue, C.; Armentrout, P. B. *J. Phys. Chem. A.* **2000**, *104*, 692. b) Griffen, J. B.; Armentrout, P. B. *J. Chem. Phys.* **1998**, *108*, 8075. c) Siever, M. R.; Armentrout, P. B. *J. Chem. Phys.* **1995**, *102*, 754.

(23) a) Sodupe, M.; Bauschlicher, C. W. J. Phys. Chem. 1991, 95, 8640. b) Klippenstein, S. J.; Yang, C. N. *Intl. J. Mass. Spect.* **2000**, *201*, 253. c) Frenking, G.; Frohlich, N. *Chem. Rev.* **2000**, *100*, 717.

(24) Meyer, F.; Khan, F. A.; Armentrout, P. B. *J. Am. Chem. Soc.* **1995**, *117*, 9740.

(25) a) Marinelli, P. J.; Squires, R. R. *J. Am. Chem. Soc.* **1989**, *111*, 4101. b) Magnera, T. M.; David, D. E.; Michl, J. *J. Am. Chem. Soc.* **1989**, *111*, 4100. c) Dalleska, N. F.; Honma, K.; Sunderlin, L. S.; Armentrout, P. B. *J. Am. Chem. Soc.* **1994**, *116*, 3519.

CHAPTER 3

THEORETICAL STUDY OF THE BONDING IN FIRST ROW TRANSITION METAL CATION - NITROGEN (N_2) COMPLEXES

The bonding of a single nitrogen molecule (N_2) to singly charged transition metal cations from Sc^+ to Zn^+ is investigated using density functional theory. The structural parameters, ground electronic states, bond dissociation energies, and vibrational frequencies for end-on and side-on bonded N_2 are computed using the B3LYP functional. The complexes are primarily bound by charge-quadrupole forces with some showing partial covalent character. The partial covalent nature of the bonding arises from the 3d-4s valence orbitals of the metal cations. For all the complexes, the linear, end-on bonded N_2, structure is found to be the lowest energy isomer because of the directional characteristics of the N_2 quadrupole moment. The ground electronic state of all the complexes except $Fe^+(N_2)$ is derived from the electronic ground state of the isolated metal cation. In $Fe^+(N_2)$, the first excited state ^4F of free Fe^+ forms the bond with N_2. In all the complexes, the N-N vibrational frequency is seen to red-shift from the value of free N_2. The early transition metal cations cause a greater red-shift than the late row metal ions. However, the late row metal cations bind N_2 stronger than the early metal ions. The calculated binding energies are compared to available experimental data to test the accuracy of density functional theory in treating such metal ion-ligand complexes.

Introduction

Molecular nitrogen (N_2) is extremely inert and although it is plentiful in the earth's atmosphere, only few organisms are capable of utilizing it. Nitrogen fixation is a process in which enzymes called nitrogenases convert N_2 to ammonia in biological systems.[1-10] The active sites of nitrogenases carry transition metals which precipitate the cleavage of the N-N triple bond.[2-10] However, the fundamental chemistry governing nitrogen fixation is not clearly understood.[3-8] The industrial production of ammonia from N_2 is carried out under extreme conditions on transition metal (TM) surfaces.[11-15] The Haber-Bosch process entails reacting N_2 with hydrogen on iron surfaces under high temperatures and pressures to produce ammonia. Here too, the cleavage or activation of the N-N triple bond, which is the rate determining state of the process, is poorly understood.[14,15] Therefore, understanding the characteristics of the bonding between N_2 and transition metals has been a longstanding goal of condensed phase and theoretical chemists. N_2 is isoelectronic to CO, a ligand which is highly reactive and binds strongly to various TM ions.[16-19] The binding of transition metals to CO forms the foundation of organometallic chemistry, coordination chemistry and molecular adsorption on metals in surface science.[16-19] Comparing the bonding nature of N_2 and CO has therefore interested inorganic, theoretical, and biochemical chemists.[20,21] In this article, the bonding of first row TM (Sc-Zn) cations to N_2 is investigated using density functional theory (DFT).

The synthesis of the first TM-N_2 complex $[Ru(NH_3)_5N_2]^{2+}$ in 1965 [22] led to a flurry of experimental and theoretical activity to learn how N_2 bonds in a TM-complex and predict reactivity trends.[2-4, 20-26] Initially, various inorganic chemists synthesized numerous TM-N_2 complexes and applied condensed phase spectroscopic techniques to decipher the bonding framework.[20-26] Darensbourg et al. studied the infrared (IR) spectra of TM-CO and TM-N_2

complexes and proposed that the frequency shift and IR intensity of the C-O and N-N vibration upon complexation indicated the strength of the metal-ligand bond.[20] However, these condensed phase TM-N_2 compounds could not be isolated from the counterions and bulky stabilizing ligands used to prepare them. Theoreticians in the early 1970's and 1980's lacked computational power and hence high accuracy ab initio calculations could not support these experimental observations and hypotheses. In spite of this, several groups were able to provide a rudimentary model of TM-N_2 bonding using fundamental molecular orbital theory.[4, 21-23] Together with observations from surface science, the models suggested that the N_2 activation in a TM-N_2 complex could be determined by the change in the N-N vibrational frequency and N-N bond distance.[4, 12-15] Only within the past 20 years, with the advent of high end theoretical techniques and data from gas phase isolated TM-N_2 complexes, have chemists been able to refine and improve these earlier models.[27-29,30-43]

Spectroscopic studies of gas-phase TM-N_2 eliminates many complications inherent to the condensed phase and are therefore tractable for theoretical analysis. Mass spectrometric studies have probed various first row TM^+-N_2 systems and proposed structures based on the bonding energetics.[27-29] Spectroscopic methods have determined structures, coordination numbers and ground electronic states of neutral and ionic TM-N_2 complexes.[30-36] Matrix isolation infrared spectroscopy[31-33] and matrix isolation electron spin resonance spectroscopy[34] of TM-N_2 have revealed structural features and electronic states involved in bonding. Infrared photodissociation (IRPD) spectroscopy of $V^+(N_2)_n$ and $Nb^+(N_2)_n$ was recently performed by our group and these experiments were the first to probe the N-N stretch of an isolated gas phase $TM^+(N_2)$.[35] All these gas phase studies were complemented by DFT calculations. Several groups have investigated geometries, bond energies and vibrational frequencies of TM-N_2 and TM^+-N_2 complexes using

ab initio and DFT calculations.[37-43] Neutral and ionic Fe(N_2) complexes have received significant attention due to their importance in surface science and biochemistry.[37-39a] $Co^+(N_2)$ has been investigated experimentally[28,30b] and theoretically.[39d,40] Kardahakis et al.[42] and Pilme et al.[43] have analyzed the bonding in neutral first row TM-N_2 systems using coupled-cluster multiconfigurational and DFT techniques respectively. However, to our knowledge no theoretical work has systematically studied first row TM cations from Sc^+ to Zn^+ with a single N_2 molecule.

DFT is an appealing theoretical technique for TM-ligand and multiply ligated complexes as it is computationally inexpensive compared to ab initio methods. It provides fairly accurate values for bond energies, IR frequencies and intensities.[44-46] TM cations interacting with small molecules involves a subtle play of covalent and electrostatic forces that is difficult to model with purely ab initio methods. However, since DFT contains exchange and correlations functions that are fitted to experimental results, it predicts energetics that are at least qualitatively correct.[44] Our group has complemented our IR work with DFT calculations on various metal cation-molecular complexes such $M^+(C_2H_2)_n$,[47] $M^+(H_2O)_n$,[48] $M^+(C_6H_6)_n$,[49] and $M^+(N_2)_n$.[35] In each case, the DFT predicted IR spectra were matched to experimental data allowing us to deduce structures and electronic configurations of the complexes. In this work, we apply this well proven DFT methodology to first row $TM^+(N_2)$ complexes to probe structure and bonding.

Theoretical Methods

The hybrid density functional B3LYP (Becke-3-Lee-Yang-Parr) was employed to determine structures, bond energies, vibrational frequencies and IR oscillator strengths. The B3LYP functional uses a hybrid Hatree-Fock method along with Becke's three parameter

exchange functional and the correlation functional of Lee, Yang, and Parr.[50] The Gaussian basis set in DGauss (DG), which is a double-zeta valence plus polarization (DZVP) and designated as DGDZVP was used to describe the TM^+. 6-311+G*, an all-electron triple zeta basis set employing polarization and diffuse functions was used for the N atoms. The B3LYP functional has been shown to work well for first row transition metals ions by various theoretical[44,45] and experimental[46-49] groups. The calculations explored all possible geometries without any symmetry constraints. Multiple spin states were explored for a given structure for each TM^+. The geometries were optimized for each complex and the stationary points verified as minima by computing vibrational frequencies. A systematic study of multiple functionals or basis sets was not performed since the methodology has been proven to accurately describe many TM^+-ligand systems.[42-47] The dissociation energies were not zero-point energy (ZPE) corrected since such corrections would result in only approximately ~1 kcal/mol difference to the final value. The calculated frequencies were scaled by a factor of 0.96 - the recommended value for the 6-311+G* basis set.[51] Such a scaling gave a value of 2359 cm^{-1} for the N_2 which is nearly identical to its experimental ω_e (ω_e=2358.6 cm^{-1}) and slightly larger than its measured fundamental frequency at 2330 cm^{-1}.[52] All calculations were performed using the Gaussian 03W package.[53]

Results and Discussion

General Description of the Bonding and Overall Trends

The electron configuration of N_2 is $(1\sigma_g)^2(1\sigma_u)^2(2\sigma_g)^2(2\sigma_u)^2(1\pi_u)^4(3\sigma_g)^2$ with the $3\sigma_g$ orbital higher in energy than the $1\pi_u$ orbital. The chemical inertness of N_2 emanates from its strong triple bond, closed shell electron configuration and large HOMO-LUMO gap.[1] Like CO, N_2 is a π-acceptor ligand although it is a much weaker π-acceptor. Unlike CO, nitrogen does not

have a permanent dipole moment but possesses a small negative quadrupole moment approximately half the magnitude of that for CO.[54]

The bonding scheme that is widely used to describe TM-ligand bonding is ligand field theory (LFT).[16,17] LFT essentially considers the TM-ligand bond as the spatial overlap of the metal d orbitals and ligand valence orbitals. The Dewar-Chatt-Ducanson (DCD)[55] model that is often used by inorganic chemists to explain TM compounds is a qualitative version of LFT and is very effective in elucidating periodic trends in geometries, bond energies, excitation energies, and other chemical properties. In the DCD model, the ligand valence orbitals, with σ-type symmetry, donate electron density to the empty metal d orbitals and the metals back-donate from filled orbitals, with π-type symmetry, to the empty orbitals of the ligand. This synergistic mix of σ-type donation and π-type back-donation is most often used to model TM-CO and TM-π-bonded ligands.[16-18]

The dissociation energies, electronic states, TM^+-N_2 bond length, N-N bond length and vibrational frequencies of the linear $TM^+(N_2)$ are tabulated in Table 3.1. Figure 3.1 is a plot of the computed dissociation energies of the first row TM^+-N_2 complexes having linear geometry. Unlike the majority of TM-carbonyl compounds that consist of a single isomer with only the C atom binding directly to the metal, N_2 may bind to a TM in the "end-on" or "side-on" configuration. Both geometries have been studied in this work. In Figure 3.1 we present the calculated binding energy (BE) for the linear structures to discuss overall bonding trends. Across the row from Sc^+ to Zn^+ the BE distribution has two maxima and one minimum. On the left side, $V^+(N_2)$ has the highest calculated BE of 22.0 kcal/mol. The minimum corresponds to $Mn^+(N_2)$ with a BE of 7.6 kcal/mol and on the right side the distribution peaks for $Co^+(N_2)$ and

Table 3.1 The ground electronic state, binding energy (BE), TM^+-N bond length, N-N bond length, vibrational frequencies and IR intensities for the linear $TM^+(N_2)$ complexes calculated using the B3LYP functional.

The binding energies (BE) are in kcal/mol, bond lengths in angstroms, frequencies in cm^{-1}, and IR intensities in km/mol.

TM^+	State	BE	TM^+-N	N-N	Frequencies (Intensities)
Sc	$^3\Sigma^-$	16.5	2.262	1.102	204(1), 223(5), 243(3), 2226(357)
Ti	$^4\Delta$	15.5	2.224	1.099	233(3), 233(3), 286(2), 2262(106)
V	$^5\Sigma^+$	22.0	2.104	1.099	207(4), 207(4), 288(0), 2285(49)
Cr	$^6\Sigma^+$	18.0	2.117	1.098	187(3), 187(3), 288(0), 2285(49)
Mn	$^7\Sigma^+$	7.6	2.565	1.095	116(0), 116(0), 128(39), 2351(46)
Fe	$^4\Sigma^-$	23.8	1.989	1.099	206(3), 207(4), 306(1), 2302(19)
Co	$^3\Sigma^+$	28.3	1.911	1.099	217(3), 217(3), 342(2), 2319(11)
Ni	$^2\Delta$	28.4	1.910	1.097	218(3), 218(3), 328(0), 2331(1)
Cu	$^1\Sigma^+$	27.3	1.927	1.096	222(2), 222(2), 305(0), 2344(1)
Zn	$^2\Sigma^+$	11.5	2.378	1.095	139(0), 139(0), 165(34), 2354(57)

Figure 3.1 Plot of dissociation energy (kcal/mol) of each $TM^+(N_2)$ complex from Sc^+ to Zn^+ versus the TM^+. The energies are calculated using the B3LYP functional.

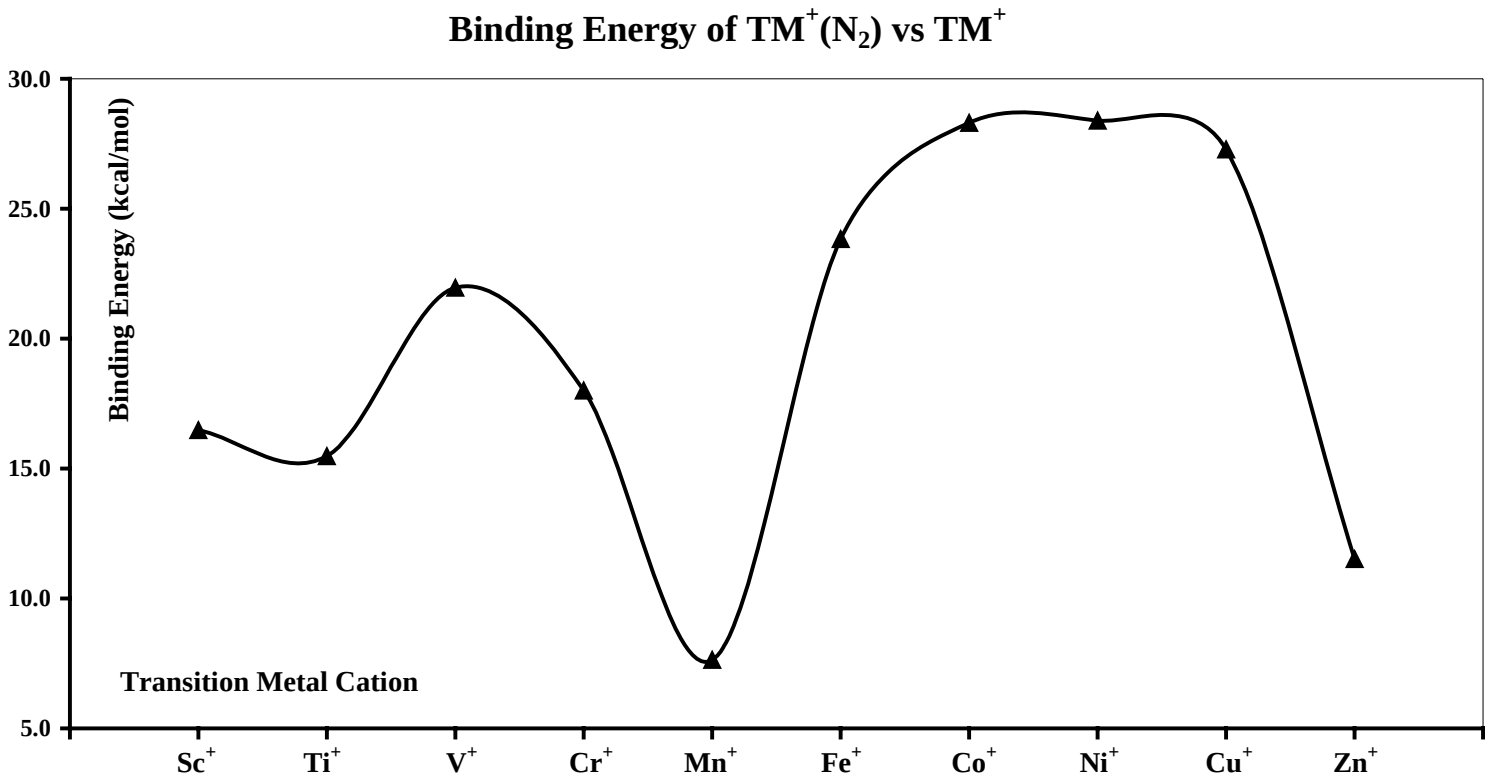
Binding Energy of TM+(N2) vs TM+
Binding Energy (kcal/mol)
30.0
25.0
20.0
15.0
10.0
5.0
Transition Metal Cation
Sc+
Ti+
V+
Cr+
Mn+
Fe+
Co+
Ni+
Cu+
Zn+

$Ni^+(N_2)$. Such a "double-hump" trend of physical properties for first and second row TM-compounds is well known to inorganic chemists and is indicative of the s-d orbital hybridization mechanism of TM ions.[16,17] A detailed analysis of TM bonding is beyond the scope of this work and only a brief outline will be given here. References 16 and 17 provide a more comprehensive description.

The bonding orbitals of the first row transition metals are the 3d orbitals, which sometimes form hybrid orbitals by overlapping with the diffuse 4s orbitals. TM cations have one of two possible electronic configurations : $d^n s$ or d^{n+1}. Beginning with Sc^+ and moving to Cr^+, the 3d orbital becomes more stable than the 4s. Hence, Sc^+ has a 3d4s electron configuration while Cr has a $3d^5$ configuration. The higher effective nuclear charge for Cr^+ also means that the d orbitals spatially contract and hence do not hybridize well with the 4s orbitals. With Mn^+, the sixth valence electron occupies an s orbital instead of doubly occupying a d orbital because the pairing energy for the d orbitals is large. However, beginning with Fe^+ the d orbitals do become doubly occupied because the increasing effective nuclear charge from Fe^+ to Zn^+ offsets any destabilization due to spin pairing. For Cu^+ and Zn^+ the d orbitals are completely filled, highly contracted and very stable and therefore do not participate in ligand bonding. This changing nature of the 3d orbitals across the first row means that the early transition metals form s-d hybrid orbitals more readily and consequently interact more strongly with ligands than the later metals. Sc, Ti and V are known to be the most reactive first row transition metals.[16,17] The availability of the d orbitals also means that most transition metals possess many low-lying excited states that may compete for bonding with the ground state.[16-18]

The strength of the TM-ligand interaction has often been evaluated by studying the frequency shifts of the ligand upon complexation. For example, TM-CO complexes are

classified as "classical" or "non-classical" by whether the free C-O vibration red-shifts or blue-shifts upon binding.[16-20] Numerous IR spectroscopic studies have determined the relative amount of σ-donation and π-back-donation in TM-CO compounds by measuring the magnitude of the blue shift or red shift of the C-O stretch as well as the IR intensity of the vibration.[16-20] Darensbourg and co-workers compared the relative σ-donation and π-acceptor capabilities of CO and N_2 by examining the IR spectra of TM-CO and TM-N_2 complexes.[20] In these studies and others, very little information could be gathered by studying the metal-ligand vibrations because of their low frequency and poor IR intensity. Rather, only the perturbation of the ligand frequencies upon bonding provided clues to the complexation mechanism. Therefore, we focus primarily on the changes in the N-N vibrational frequency in our discussion of the bonding. The N-N vibration is not IR active in free nitrogen, but as shown by Darensbourg et al.[20] and our experimental work,[35] the N-N stretch does become IR active upon binding to a TM.

As discussed above, N_2 can bind in the end-on or side-on configuration to a TM^+. Both geometries were studied by our calculations. Table 3.2 lists the dissociation energies, electronic states, TM^+-N_2 bond length, N-N bond length and vibrational frequencies of the T-shaped isomers and Table 3.3 compares the dissociation energies of the linear and T-shaped complexes. TM^+-N_2 complexes are bound primarily through charge-quadrupole forces and because N_2 has a negative quadrupole moment, the linear structures are favorable over the T-shaped geometries. Our results show that the most stable isomer for all first row TM^+-N_2 complexes is the linear configuration. The T-shaped structure is always more weakly bound than the linear isomer. This is also seen for all neutral TM(N_2) complexes.[42,44] The T-shaped structure is a first order saddle point for all the metal cations except for Sc^+, Ti^+, and Fe^+. This result is consistent with previous theoretical studies of neutral and ionic TM-N_2 complexes which all indicate that N_2 prefers to

Table 3.2 The ground electronic state, binding energy (BE), bond distance from TM^+ to center of N-N bond, N-N bond length, vibrational frequencies and IR intensities for the T-shaped $TM^+(N_2)$ complexes calculated using the B3LYP functional.

The binding energies (BE) are in kcal/mol, bond lengths in angstroms, frequencies in cm^{-1}, and IR intensities in km/mol.

TM^+	State	BE	TM^+-NN	N-N	Frequencies (Intensities)
Sc	$^3B_1$	7.4	2.166	1.139	261(15), 294(0), 1958(336)
Ti	$^4B_1$	9.6	2.257	1.117	174(2), 219(2), 2122(256)
V	$^5A_1$	6.7	2.362	1.105	-120(0), 173(0), 2243(45)
Cr	$^6A_1$	4.8	2.402	1.102	-167(0), 148(1), 2268(16)
Mn	$^7A_1$	0.5	3.321	1.097	-134(0), 44(16), 2334(4),
Fe	$^4B_2$	12.2	2.083	1.116	159(0), 247(2), 2149(72)
Co	$^3B_1$	10.9	2.095	1.112	-71(0), 224(1), 2190(28)
Ni	$^2A_2$	11.2	2.125	1.107	-412(23), 217(0), 2233(7)
Cu	$^1A_1$	10.8	2.147	1.105	-206(0), 185(0), 2253(1)
Zn	$^2A_1$	2.5	2.839	1.099	-172(0), 92(22), 2317(12)

Table 3.3 Binding energies (BE) in kcal/mol of the linear and T-shaped complexes of $TM^+(N_2)$ calculated using the B3LYP functional.

TM^+	BE (Linear)	BE (T-shaped)
Sc	16.5	7.4
Ti	15.5	9.6
V	22.0	6.7
Cr	18.0	4.8
Mn	7.6	0.53
Fe	23.8	12.2
Co	28.3	10.9
Ni	28.4	11.2
Cu	27.3	10.8
Zn	11.5	2.5

bind end-on in most complexes. However, a few metal compounds have been synthesized with side-on bonded N_2.[3f]

Early Transition Metal Cation - Nitrogen complexes.

The early TM cations from Sc^+ to Cr^+ are the most reactive and interact strongly with N_2. Neutral $Sc(N_2)$, $Ti(N_2)$, $V(N_2)$ and $Cr(N_2)$ have been studied by matrix isolation IR spectroscopy[31-33] and theoretical methods,[42,43] but very little work exists for the cations. The neutral complexes all form linear geometries. Likewise, the lowest energy isomers calculated for the cations are linear. The metal-ligand bond distances in angstroms for $Sc^+(N_2)$, $Ti^+(N_2)$, $V^+(N_2)$ and $Cr^+(N_2)$ are 2.262, 2.224, 2.104, and 2.117 respectively. The T-complex is a minimum for $Sc^+(N_2)$ and $Ti^+(N_2)$ but higher in energy than the linear isomer by approximately 10 and 5 kcal/mol respectively. For $V^+(N_2)$ and $Cr^+(N_2)$, the T-isomer is a first order saddle point. The electronic states of the complexes are listed in Table 3.1. All four metal cations bind to N_2 via the ground electronic state of the free cation. For example, the ground state electron configuration of Sc^+ is 3d4s giving rise to a ^3D state, which binds to N_2 resulting in an overall $^3\Sigma^-$ state for the complex. The corresponding electronic states of the isolated TM^+ in $Ti^+(N_2)$, $V^+(N_2)$ and $Cr^+(N_2)$ are $(3d^24s)$ ^4F, $(3d^4)$ ^5D, and $(3d^5)$ ^6S respectively. The metals all possess low lying excited states that could bind to the N_2 but only if the excitation energy is offset by the complexation energy. All excited states were studied and found to be much higher in energy.

The N-N stretch in all the first row $TM^+(N_2)$ complexes is computed to red-shift from the free nitrogen vibration at 2330 cm^{-1}. Figure 3.2 shows the magnitude of the red-shifts for all the linear complexes. The red-shifting of the N-N vibration upon binding is clearly predicted by the DCD model since the σ-donation and π-back-donation weakens the N-N triple bond

Figure 3.2 The magnitude of the red-shift in cm^{-1} of the N-N vibration (from free N_2) in $TM^+(N_2)$ complexes from Sc^+ to Zn^+.

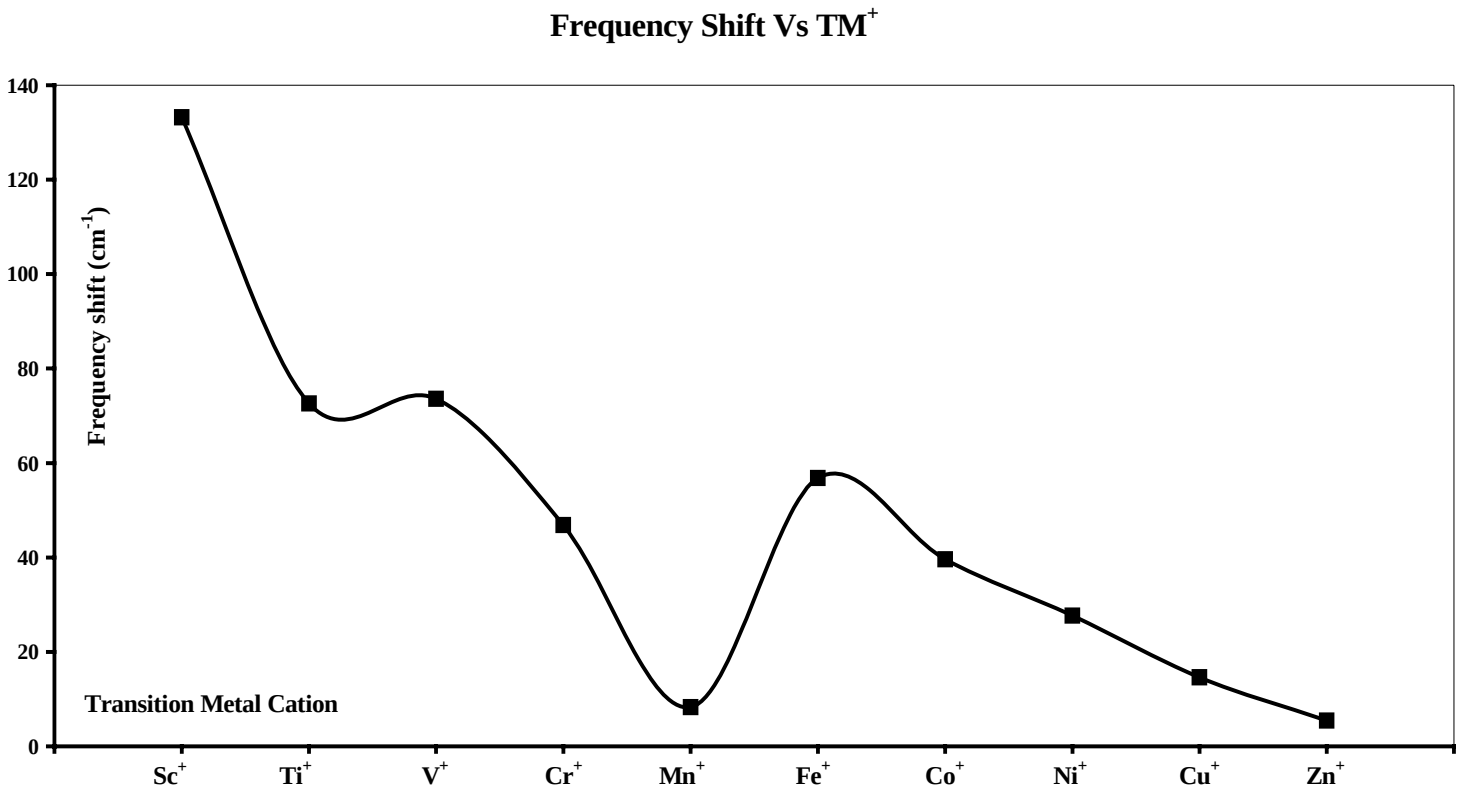
Frequency Shift Vs TM+
140
120
100
80
60
40
20
0
Frequency shift (cm-1)
Transition Metal Cation
Sc+
Ti+
V+
Cr+
Mn+
Fe+
Co+
Ni+
Cu+
Zn+

considerably.[17,55] Our IR spectroscopic study of $V^+(N_2)$ showed that this indeed occurs and also that complexation "turns on" the IR activity of the N_2.[35a] Sc^+ causes the largest perturbation of all the first row TM cations red-shifting the N-N stretch to 2226 cm^{-1} in the complex. The 3d-4s hybrid orbitals of Sc^+ have the largest radial distribution of the first row TM cations and can therefore hybridize easily and back-donate electron density very effectively. Since N_2 is a π-acceptor, all studies indicate that π-back-donation from the metal is more important than σ-donation from the ligand in the bonding.[16-18] The red-shifts caused by Ti^+ and V^+ are 73 cm^{-1} and 74 cm^{-1} respectively. The electron configuration of Ti^+ is $3d^24s$ while V^+ is $3d^4$. Since the 3d orbitals are more polarizable than the 4s, V^+ is able to interact just as strongly with N_2 as Ti^+. Cr^+ perturbs the ligand the least (red-shift of 47 cm^{-1}) among the four metal cations and this is due to its $3d^5$ electron configuration. The half-filled 3d-orbital is extremely stable and possesses large non-bonding character. An interesting effect is seen in the corresponding red-shifts of the T-complexes for all the metals. While the T-isomers are predicted to be higher in energy, the N-N vibration is red-shifted further in the complexes than in the corresponding linear complexes. For example, the red shift for linear $Sc^+(N_2)$ is 133 cm^{-1}, whereas in the T-shaped complex it is 401 cm^{-1}. A TM^+ binding directly to the N-N triple bond, therefore, causes a greater perturbation of the N-N vibrational frequency.

It is interesting to note that although these linear $TM^+(N_2)$ complexes cause the largest perturbation of the N-N bond, the complex dissociation energies are smaller than the late row TM cations. The binding energies for $Sc^+(N_2)$, $Ti^+(N_2)$, $V^+(N_2)$ and $Cr^+(N_2)$ are 16.5 kcal/mol, 15.5 kcal/mol, 22.0 kcal/mol and 18.0 kcal/mol respectively. The BE of $Cr^+(N_2)$ has been measured experimentally to be 14.1 kcal/mol[30a] and ab initio methods calculate it to be 12.2 kcal/mol.[39d] Our calculations overestimate the experimental value by 4 kcal/mol which is within

the error range for most DFT methods.[44] The later TM cations beginning with Fe^+ have dissociation energies higher than 22.0 kcal/mol. The magnitude of the N-N vibrational perturbation does not track with the binding energies. Such a trend was also seen in our combined experimental/theoretical study of $TM^+(C_2H_2)$ complexes.[47a] Although the early TM cations possess diffuse s-d hybrid orbitals, these orbitals are largely empty and cannot donate much electron density. The later TM cations have contracted valence orbitals but they are nearly filled and can contribute greater electron density. This is also why V^+ with its $3d^4$ configuration forms the strongest bond with N_2 of the early TM cations.

$Mn^+(N_2)$

$Mn^+(N_2)$ has a linear geometry and the T-complex is calculated to be a saddle point. The ground electronic state of the free cation $(3d^54s)\ ^7S$ forms the bond in the complex, leading to a $^7\Sigma^+$ state. The valence orbitals of Mn^+ are half-filled and are largely non-bonding. The complex is bonded by primarily charge-quadrupole forces with very little covalent character. Consequently, $Mn^+(N_2)$ has the weakest bond (BE=7.6 kcal/mol), the longest TM^+-N_2 bond distance (2.565 Å) and the N-N stretch red-shifts by only 8 cm^{-1}. The first excited state of Mn^+ is $(3d^54s)\ ^5S$, which lies about 9500 cm^{-1} higher in energy. It forms a stronger bond with N_2 (BE=24.9 kcal/mol) and lies only about 5 kcal/mol higher in energy than the septet linear complex. In $Mn^+(CO)$, the quintet state is found to be the lowest energy isomer[18,19] but TM^+-CO interactions are stronger than TM^+-N_2 interactions. The $^5S \leftarrow {}^7S$ excitation energy is large and it seems unlikely that any enhanced bonding with the inert N_2 molecule could compensate for this.

$Fe^+(N_2)$

$Fe^+(N_2)$ has received considerable attention from experimentalists[27c,d, 28a, 29] and theorists[37-39a] due to its relevance in biochemistry and catalysis. All studies indicate that the ground state of the complex is linear. Our calculations predict a linear ground state with a T-complex about 12 kcal/mol higher in energy. The ground state of the isolated Fe^+ is $(3d^64s)\ ^6D$ and the first excited state is $(3d^7)\ ^4F$ lying only about 1900 cm^{-1} higher in energy. Our results and previous calculations[38] confirm that it is the excited state of the Fe^+ that bonds to N_2 to form the lowest energy isomer. The $(^4F)\ Fe^+(N_2)$ is lower in energy by nearly 25 kcal/mol than the $(^6D)\ Fe^+(N_2)$. Beginning with Fe^+, the 3d orbitals become paired and as discussed above, the d orbital pairing energy is large. The d orbitals of Fe^+ are less diffuse than the earlier TM^+ and hybridize poorly with the 4s orbital. Since the $^4F \leftarrow {}^6D$ excitation energy is very low, the pairing energy is easily overcome and Fe^+ frequently bonds via its excited state.[16,17] The significant increase in bonding character by achieving the $3d^7$ electron configuration offsets the promotion energy. The BE of $(^4F)\ Fe^+(N_2)$ and $(^6D)\ Fe^+(N_2)$ is calculated to be 23.8 and 9.4 kcal/mol respectively. The metal-ligand bond in $(^4F)Fe^+(N_2)$ is 1.989 Å and is smaller than the early TM^+-N_2 distances because of the decreasing ionic radii that begins with Fe^+ and continues to Zn^+. For the T-shaped isomer, the binding energies for the quartet and sextet states are 12.2 and 0.9 kcal/mol respectively. The measured dissociation energy from collision induced dissociation (CID) experiments for the complex is 12.9 kcal/mol[27c,d] and our calculations overestimate this by nearly a factor of 2. Although the computed BE for the $(^4F)\ Fe^+(N_2)$ T-shaped isomer is close to the measured value, it is unlikely that DFT has miscalculated the relative stability of the linear and T-shaped isomers. What is likely, however, is that DFT has overestimated the energy separation of the two spin states. DFT is well known to misjudge the energy spacing between

different spins, often favoring low spin states.[44] The ^4F is known to become the bonding state of Fe^+, but typically with the addition of the second ligand.[16-18] Hence, it is probable that the experimental BE corresponds to a sextet linear complex which DFT calculates to be 9.4 kcal/mol. It is however, surprising that DFT overestimates the stability of the quartet state by such a large degree (25 kcal/mol).

$Co^+(N_2)$ and $Ni^+(N_2)$

$Co^+(N_2)$ and $Ni^+(N_2)$ are the most strongly bound complexes of the first row $TM^+(N_2)$ series. The BE for the linear complexes of $Co^+(N_2)$ and $Ni^+(N_2)$ are nearly identical at 28.3 kcal/mol and 28.4 kcal/mol respectively. The metal-ligand bond distances are 1.911 Å and 1.910 Å for $Co^+(N_2)$ and $Ni^+(N_2)$ respectively. $Co^+(N_2)$ has been studied experimentally[28c,30b] and theoretically.[39d,40] Brucat and co-workers[30b] initially proposed that the ground state is T-shaped. That has since been refuted by all the other experimental and theoretical work. Our calculations show that the linear isomer is lowest in energy with the T-complex a saddle point. The electronic state of $Co^+(N_2)$ is $^3\Sigma^+$ derived from the $(3d^8)$ ^3F ground state of the cation. The experimentally measured dissociation energy is 23.0 kcal/mol[28c] which is slightly overestimated by our calculations but within the error range for DFT techniques. $Ni^+(N_2)_n$ n=1-4 has been studied by CID experiments[27a] and the binding energy measured to be 26.5 ± 2.5 kcal/mol. Our calculated value of 28.4 kcal/mol for the linear complex is in excellent agreement with this. The most stable structure of $Ni^+(N_2)$ is linear and the T-complex is a saddle point. $Ni^+(N_2)$ is bound by the $(3d^9)$ ^2D state of Ni^+ resulting in a $^2\Delta$ state of the complex.

Although Co^+ and Ni^+ bind N_2 the strongest of the first row TM cation series, they red-shift the N-N frequency to a lesser extent than the earlier TM cations. As discussed above, the

dissociation energy and the magnitude of the red-shifts in $TM^+(N_2)$ complexes do not have a one to one correspondence. Even though the earlier TM cations possess diffuse valence orbitals, their 3d orbitals are mostly empty and therefore unable to donate significant electron density to the ligand. Co^+ and Ni^+ have electron configurations of $3d^8$ and $3d^9$ and though their d orbitals are spatially compacted, they possess considerable electronic density to form bonds. In addition to this, the ionic radius of Co^+ and Ni^+ is small compared with the early TM cations. This leads to greater charge density for these metal ions. Therefore, the electrostatic charge-quadrupole component of the bonding in $Co^+(N_2)$ and $Ni^+(N_2)$ is enhanced in these complexes.

$Cu^+(N_2)$ and $Zn^+(N_2)$

Cu^+ and Zn^+ have completely filled d-orbitals and hence their complexes with N_2 have very little covalent character. $Cu^+(N_2)$ has been studied by theoretical methods previously and the structure predicted to be linear.[41] Our calculations show that $Cu^+(N_2)$ and $Zn^+(N_2)$ are both linear with the T-complexes being higher energy saddle points. $Cu^+(N_2)$ is a $^1\Sigma^+$ complex formed by the $(3d^{10})$ ^1S ground state of the free cation. The $(3d^{10}4s)$ ^2S ground electronic state of Zn^+ forms the bond in $Zn^+(N_2)$ producing a $^2\Sigma^+$ complex. The binding energies for $Cu^+(N_2)$ and $Zn^+(N_2)$ are calculated to be 27.3 kcal/mol and 11.5 kcal/mol respectively. Previous DFT calculations for $Cu^+(N_2)$ estimate the value to 26.5 kcal/mol whereas MP2 predicts a value of 13.2.[41] It is surprising that $Cu^+(N_2)$ is predicted to have such a high BE in our calculations. Cu^+ is closed shell and there is very little covalent character in its bonding. DFT is well known to significantly overestimate purely electrostatic forces, which is probably the case for $Cu^+(N_2)$.[44] MP2 is far superior in predicting dissociation energies of purely electrostatic bonds and the value of 13.2 kcal/mol is more likely closer to the true value. The TM^+-N_2 bond distance for Cu^+ and

Zn^+ are 1.927 Å and 2.378 Å respectively. Cu^+ and Zn^+ red shift the N-N frequency by 15 cm^{-1} and 5 cm^{-1} respectively. These minor perturbations of the N-N bond and relative large metal-ligand bond lengths (especially for Zn^+) are indicative of the absence of substantial covalent bonding in these complexes.

Conclusion

DFT calculations have been applied to analyze the bonding mechanism of $TM^+(N_2)$ complexes where $TM^+ = Sc^+$ to Zn^+. Calculations using the B3LYP functional show that all the complexes are predominantly bound by charge-quadrupole interactions. The linear isomer is predicted to be the lowest energy structure for all the complexes because of the polarity of the quadrupole moment of N_2. The T-complex is found to be a saddle point for all the TM^+-N_2 systems except for $Sc^+(N_2)$, $Ti^+(N_2)$ and $Fe^+(N_2)$ where it is a higher energy minimum on the potential surface. The DFT calculated dissociation energies for the linear complexes range from 7.6 kcal/mol for $Mn^+(N_2)$ to 28.4 kcal/mol for $Ni^+(N_2)$. For all the complexes except $Fe^+(N_2)$, the bonding electronic state arises from the ground state of the free TM cation. Fe^+ binds to N_2 via its first excited electronic state. In all the complexes, the binding of N_2 causes the N-N vibrational frequency to red shift from its free N_2 value. The magnitude of the red-shift is larger for the T-isomers than the linear complexes, because direct bonding to the N-N triple bond causes a greater perturbation of the ligand. The red-shifts agree with the qualitative predictions of the Dewar-Chatt-Duncanson complexation model that is often used to describe such TM-ligand systems.

The first row TM cations may be divided into five broad categories in terms of their degree of interaction with the N_2 ligand in the linear complexes. The early TM cations Sc^+, Ti^+, V^+ and Cr^+ are the most reactive as they possess highly diffuse valence orbitals. As a result,

their interaction with the N_2 ligand causes the greatest shift of the N-N stretch. However, the dissociation energies for these complexes are smaller than the late row $TM^+(N_2)$ complexes because these metal ions lack electronic density in the 3d orbitals. Mn^+ interacts weakly with N_2 because its orbitals are half-filled precluding any covalent character to its bonding. $Fe^+(N_2)$ is extremely interesting in that the ground electronic state of the free metal cation bonds weakly to N_2. However, it possesses a low lying excited state with large bonding character and the complex is bound via this excited electronic state. There remains some discrepancy between the computed and experimentally measured dissociation energy for this complex and is most likely due to the inherent defects of DFT. $Co^+(N_2)$ and $Ni^+(N_2)$ form the strongest bond with N_2 although the perturbation of the N-N ligand in the complexes is smaller than for the early TM cations. The d orbitals of Co^+ and Ni^+ are nearly filled and they possess substantial electronic density to form strong bonds with ligands. The d orbitals of Cu^+ and Zn^+ are filled and extremely stable and they do not participate in bonding. $Cu^+(N_2)$ and $Zn^+(N_2)$ are bound by purely electrostatic forces and hence cause slight perturbations of the ligand. The dissociation energy of $Cu^+(N_2)$ is computed to be quite high for a purely electrostatic interaction. This is ascribed to the inadequacy of DFT methods in describing purely electrostatic interactions.

References

(1) Bazhenova, T.A.; Shilov, A.E. *Coordination Chemistry Reviews*. **1995**, *144*, 69.

(2) a) Tuczek, F.; Lehnert, N. *Angew. Chem. Int. Ed*. **1998**, *37*, 2636. b) Lehnert, N.; Tuczek, F. *Inorg. Chem*. **1999**, *38*, 1671. c) Studt, F.; Tuczek, F. J. *Computational Chemistry*. **2006**, *27*, 1278.

(3) a) Fryzuk, M.D.; Johnson, S.A. *Coordination Chemistry Reviews*. **2000**, *200-202*, 379. b) Fryzuk, M. D. *Chem. Record*. **2003**, *3***,** 2. c) Fryzuk, M. D.; Kozak, C. M.; Patrick, B. O. *Inorg. Chim. Acta*. **2003**, *345*, 53. d) Shaver, M.P.; Fryzuk, M.D. Adv. Synth. Catal. **2003**, *345*, 1061. e) MacKay, B.A.; Fryzuk, M.D. *Chem. Rev*. **2004**, *104*, 385. f) MacLachlan, E.A.; Fryzuk, M.D. *Organometallics*. **2006**, *25*, 1530.

(4) a) Chatt, J.; Melville, D. P.; Richards, R. L. *J. Chem. Soc (A)*. **1969**, *18*, 2841. b) Chatt, J.; Dilworth, J. R.; Richards, R. L. *Chem. Rev*. **1978**, 78, 589. c) Richards, R. L. *Coord. Chem. Rev*. **1996**, *153*, 83. d) Richared, R.L. *Coordination Chemistry Reviews*. **1996**, *154*, 83.

(5) Kuganathan, N.; Green, J.C.; Himmel, H.J. *New. J. Chem*. **2006**, *30*, 1253.

(6) Pelikan, P.; Boca, R. *Coordination Chemistry Reviews* **.1984**, *55*, 55.

(7) a) Christian, G.; Driver, J.; Stranger, R. *Faraday Discuss*. **2003**, *124*, 331. b) Christian, G.; Stranger, R. *Dalton Trans*. **2004**, *16*, 2492.

(8) Seigbahn, P. E. M.; Blomberg, M. R. A. *Chem. Rev*. **2000**, *100*, 421.

(9) Burgess, B. K.; Lowe, D. K. *Chem. Rev*. **1996**, *96*, 2983.

(10) Rincon, L.; Ruette, F.; Hernandez, A. *J. Mol. Spectrosc*. **1992**, *254*, 395.

(11) Somorjai, G.A. *Introduction to Surface Chemistry and Catalysis*, John Wiley & Sons, **1994**.

(12) Rao, C. N. R.; Rao, G. R. *Surf. Sci. Rep.* **1991**, *13*, 221.

(13) Arabczyk, W.; Jasinska, I.; Lubkowski, K. React. *Kinet. Catal. Lett*. **2004**, *83*, 385.

(14) a) Grunze, M.; Golze, M.; Hirschwald, W.; Freund, H. J.; Pulm, H; Seip, U; Tsai, M.C.; Ertl, G.; Kuppers, J. *Phys. Rev. Lett.* **1984**, *53*, 850. b) Tsai, M. C.; Seip, U.; Bassignana, C. I.; Kuppers, J.; Ertl, G.; *Surf. Sci*. **1985**, *155*, 387.

(15) Arabczyk, W.; Jasinska, I.; Lubkowski, K. *React. Kinet. Catal. Lett*. **2004**, *83*, 385.

(16) a) Cotton, F. A.; Wilkinson, G.; Murillo, C. A.; Bochmann, M. *Advanced Inorganic Chemistry*, 6th ed. John Wiley, New York, **1999**. b) Huheey, J. E.; Keiter, E. A.; Keiter, R. L. *Inorganic Chemistry*, 4th ed., HarperCollins, New York **1993**.

(17) a) Lupinetti, A.J.; Fau, S.; Frenking, G.; Strauss, S.H. *J. Phys. Chem*. **1997**, *101*, 9951. b) Frenking, G.; Pidun, U. *J. Chem. Soc., Dalton Trans*. **1997**, 1653. c) Frenking, G.; Frohlich, N. *Chem. Rev*. **2000**, *100*, 717.

(18) Zhou, M.; Andrews, L.; Bauschlicher, C. W. Jr. *Chem. Rev*. **2001**, 101, 1931.

(19) Ervin, K. M. *Int. Rev. Phys. Chem*. **2001**, *20*, 127.

(20) a) Hyde, C.L.; Darensbourg, D.J. *Inorg. Chem*. **1971**, *2*, 431. b) Darensbourg, D.J. *Inorg. Chem*. **1971**, *11*, 2399. c) Darensbourg, D.J. *Inorg. Chem*. **1972**, *11*, 1436. d) Hyde, C.L.; Darensbourg, D.J. *Inorg. Chem*. **1973**, *12*, 1075. e) Darensbourg, D.J.; Nelson, H. H.; Hyde, C.L. *Inorg. Chem*. **1974**, *13*, 2135.

(21) a) Chatt, J. *Pure and App. Chem*. **1970**, *24*, 425. b) Chatt, J. *J. Organomet. Chem*. **1975**, *100*, 17. c) Chatt, J.; Richards, R. L. *J. Organomet. Chem*. **1982**, *239*, 65.

(22) a) Allen, A.D.; Senoff, C.V *Chem. Commun*. **1965**, 621. b) Allen, A.D; Bottomley, F.; Harris, R.O.; Reinsalu, V.P.; Senoff, C.V. *J. Am. Chem. Soc*. **1967**, *89*, 5595. c) Allen,

A.D.; Harris, R.O.; Loescher, B.R.; Stevens. J.R.; Whiteley, R.N. *Chem. Rev*. **1973**, *73*, 11.

(23) a) Chatt, J.; Dilworth, J.R.; Leigh, G.J. *J. Organometal. Chem*. **1970**, *21*, P49. b) Chatt, J.; Leigh, G.J.; Thankarajan, N. *J. Organometal. Chem*. **1970**, *25*, C77. c) Leigh, G.J. *J. Mol. Cataly*. **1988**, *47*, 363. d) Leigh, G.J. *Can. J. Chem*. **2005**, *3*, 277.

(24) a) Moskovits, M.; Ozin, G.A. J. Chem. Phys. 1973, 58, 1251. b) Huber, H.; Kundig, E.P.; Moskovits, M.; Ozin, G.A. *J. Am. Chem. Soc*. **1973**, *95*, 332. c) Klotzbucher, W.; Ozin, G.A. *J. Am. Chem. Soc.* **1975**, *97*, 2672. d) Lever, A. B. P.; Ozin, G. A. *Inorg. Chem.* **1997**, *16*, 2012.

(25) a) Kovacs, J.; Speier, G.; Marko, L. *Inorg. Chimica*. **1970**, *4*, 3. b) Speier, G.; Marko, L. *J. Organometal. Chem*. **1970**, *21*, P46.

(26) a) Powell, C.B.; Hall, M.B. *Inorg. Chem*. **1984**, *23*, 4619. b) Zhenyang, L.; Hall, M.B. *Coord. Chem. Rev*. **1993**. *123*, 149.

(27) a) Khan, F. A.; Steele, D. L.; Armentrout, P. B. *J. Phys. Chem*. **1995**, 99,7819. b) Tjelta, B. L.; Armentrout, P. B. *J. Phys. Chem*. **1997**, 101, 2064. c) Tjelta, B. L.; Walter, D.; Armentrout, P. B. *Intl. J. Mass. Spec.* **2001**, 204, 7. d) Tan, L.; Liu, F.; Armentrout, P.B. *J. Chem. Phys*. **2006**, *124*, 1.

(28) a) Schwarz, J.; Heinemann, C.; Schwarz, H. *J. Phys. Chem*. **1995**, *99*, 11405. b) Dieterle, M.; Harvey, J.N.; Heinemann, C.; Schwarz, J.; Schroeder, D.; Schwarz, H. *Chem. Phys. Lett*. **1997**, *277(5,6)*, 399. c) Heinemann, C.; Schwarz, J.; Schwarz, H. *J. Phys. Chem*. **1996**, *100*, 6088.

(29) Rollason, R.J.; Plane, J.M.C. *J. Chem. Soc., Faraday Trans*. **1998**, *94*, 3067**.**

(30) a) Lessen, D.E.; Asher, R.L.; Brucat, P.J. *Chem. Phys. Lett*. **1991**, *177*, 380. b) Asher, R. L.; Buthelezi, B.; Brucat, P. J. *J. Phys. Chem*. **1995**, *99*, 1068.

(31) a) Chertihin, G.V.; Andrews, L. *J. Phys. Chem*. **1994**, *98*, 5891. b) Andrews, L.; Bare, W. D.; Chertihin, G. V. *J. Phys. Chem. A*. **1997**, *101*, 8417. c) Zhou, M.; Andrews. L. *J. Phys. Chem. A*. **1998**, *102*, 9061. d) Andrews, L. *J. Electron. Spec. Rel. Pheno*. **1998**, *97*, 63. e) Andrews, L.; Citra, A.; Chertihin, G.V.; Bare, W.D.; Neurock, M. *J. Phys. Chem. A*. **1998**, *102*, 2561. f) Chertihin, G.V.; Andrews, L.; Bauschlicher, C.W. Jr. *J. Am. Chem. Soc*. **1998**, *120*, 3205.

(32) Green, D. W.; Hodges, R. V.; Gruen, D. M. *Inorg. Chem*. **1976**, *15*, 970.

(33) a) Manceron, L.; Alikhani, M.E.; Joly, H.A. *Chem. Phys*. **1998**, *228*, 73. b) Krim, L.; Manceron, L.; Alikhani, M.E. *J. Phys. Chem. A*. **1999**, *103*, 2592. c) Himmel, H.J.; Manceron, L. *Dalton Trans*. **2005**, *15*, 2615

(34) Parrish, S. H.; Van Zee, R. J.; Weltner, W., Jr. *J. Phys. Chem. A*. **1999**, *103*, 1025.

(35) a) Pillai, E.D.; Jaeger, T.D; Duncan, M.A. *J. Phys. Chem. A*. **2005**, 109, 3521. b) Pillai, E.D.; Jaeger, T.D; Duncan, M.A. *J. Am. Chem. Soc*. **2007**, in press.

(36) Grills, D.C.; Huang, K.W.; Muckerman, J.T.; Fujita, E. *Coordination Chemistry Reviews*. **2006**, *250*, 1681.

(37) Duarte, A. D.; Salahub, D. R.; Haslett, T.; Moskovits, M. *Inorganic Chemistry*. **1999**, *38*, 3895.

(38) Zacarias, A.; Torrens, H.; Castro, M.; *Intl. J. Quant. Chem*. **1997**, *61*, 467.

(39) a) Bauschlicher, C. W. Jr.; Petterson, L. M.; Siegbahn, P. E. M. *J. Chem. Phys*. **1987**, *87*, 2129. b) Bauschlicher, C. W. Jr. *Chem. Phys. Lett*. **1985**, *115*, 387. c) Bauschlicher, C.

W. Jr.; Langhoff, S.R.; Barnes, L.A. *Chem. Phys*. **1989**, *129*, 431. d) Bauschlicher, C. W., Jr.; Partridge, H.; Langhoff, S.R. *J. Phys. Chem.* **1992**, *96*, 2475.

(40) Adamo, C.; Telesca, R.; Lelj, F. *Chem. Phys. Lett*. **1996**, *254*, 314.

(41) Ducere, J.M.; Goursot, A.; Berthomieu, D. *J. Phys. Chem. A*. **2005**, *109*, 400.

(42) Kardahakis, S.; Koukounas, C.; Mavridis, A. *J. Chem. Phys*. **2006**, *124*, 104306.

(43) Pilme, J.; Silvi, B.; Alikhani, M.E. *J. Phys. Chem. A*. **2000**, *109*, 10028.

(44) a) Yang, C.N.; Klippenstein, S. J. *J. Phys. Chem. A*. **1999**, *103*, 1094. b) Ryzhov, V.; Yang, C.N.; Klippenstein, S. Dunbar, R.C. Int. *J. Mass. Spectrom. Ion. Process*. **1999**, *185*, 912. c) Gapeev, A.; Yang, C.N.; Klippenstein, S. Dunbar, R.C. *J. Phys. Chem*. **2000**, *104*, 3246. d) Klippenstein, S. J.; Yang, C. N. *Intl. J. Mass. Spectrom*. **2000**, *201*, 253.

(45) a) Ricca, A.; Bauschlicher, C. W. Jr. *Theor. Chim. Acta*. **1995**, *92*, 123. b) Bauschlicher, C. W. Jr.; Maitre, P. *J. Phys. Chem.* **1995**, *99*, 344. c) Bauschlicher, C. W. Jr.; Maitre, P. *J. Phys. Chem.* **1995**, *99*, 6836.

(46) Bushnell, J.E.; Maitre, P.; Kemper, P.R.; Bowers, M.T. *J. Chem. Phys*. **1997**, *106*, 10153.

(47) a) Walters, R. S.; Corminboeuf, C.; Schleyer, P. v. R.; Duncan, M. A. *J. Am. Chem. Soc.* **2005**, *127*, 1100. b) Walters, R. S.; Pillai, E. D.; Schleyer, P. v. R, Duncan, M. A. *J. Am. Chem. Soc*. **2005**, *127*, 17030.

(48) a) Walker, N. R.; Walters, E. D.; Pillai, E. D.; Duncan, M. A. *J. Chem. Phys.* **2003**, *119*, 10471. b) Walters, R.S.; Pillai, E.D.; Duncan, M.A. *J. Am. Chem. Soc*. **2005**, *127*, 16599.

(49) Jaeger, T. D.; Pillai, E. D.; Duncan, M. A. *J. Phys. Chem. A*. **2004**, *108*, 6605.

(50) a) Becke, A.D. *J. Chem. Phys*. **1993**, *98*, 5648. b) Lee, C.; Yang, W.; Parr, R.G. *Phys. Rev. B*. **1988**, *37*, 785.

(51) a) Anderson, M. P.; Uvdal, P. *J. Phys. Chem. A.* **2005**, *109*, 2937. b) Scott, A. P.; Radom, L. *J. Phys. Chem*. **1996**, *100*, 16502.

(52) Huber, K. P.; Herzberg, G. *Molecular Spectra and Molecular Structure IV. Constants of Diatomic Molecules*, Van Nostrand Reinhold Co. **1979**.

(53) Frisch, M. J.; Trucks, G. W.; . Schlegel, H. B.; Scuseria, G. E.; Robb, M. A.; Cheeseman, J. R.; Montgomery, J. A., Jr.; Vreven, T.; Kudin, K. N.; Burant, J. C.; Millam, J. M.; Iyengar, S. S.; Tomasi, J.; Barone, V.; Mennucci, B.; Cossi, M.; Scalmani, G.; Rega, N.; Petersson, G. A.; Nakatsuji, H.' Hada, M.; Ehara, M.; Toyata, K.; Fukuda, R.; Hasegawa, J.; Ishida, M.; Nakajima, T.; Honda, Y.; Kitao, O.; Nakai, H.; Klene, M.; Li, X.; Knox, J. E.; Hratchian, H. P.; Cross, J. B.; Adamo, C.; Jaramillo, J.; Gomperts, R.; Stratmann, R. E.; Yazyev, O.; Austin, A. J.; Cammi, R.; Pomelli, C.; Ochterski, J. W.; Ayala, P. Y.; Morokuma, K.; Voth, G. A.; Salvador, P.; Dannenberg, J. J.; Zakrzewski, V. G.; Dapprich, S.; Daniels, A. D.; Strain, M. C.; Farkas, O.; Malick, D. K.; Rabuck, A. D.; Raghavachari, K.; Foresman, J. B.; Ortiz, J. V.; Cui, Q.; Baboul, A. G.; Clifford, S.; Cioslowski, J.; Stefanov, B. B.; Liu, G.; Liashenko, A.; Piskorz, P.; Komaromi, I.; Martin, R. L.; Fox, D. J.; Keith, T.; Al-Laham, M. A.; Peng, C. Y.; Nanayakkara, A.; Challacombe, M.; Gill, P. M. W.; Johnson, B.; Chen. W.; Wong, M. W.; Gonzalez, C.; Pople, J. A. *Gaussian 03 (Revision B.02)*; Gaussian, Inc.: Pittsburgh, PA, 2003.

(54) Rigby, M.; Smith, E.B.; Wakeham, W.A.; Maitland, G.C. *The Forces Between Molecules*, Oxford Science Publications, **1986**.

(55) a) Chatt, J.; Rowe, G. A.; Williams, A. A. *Proc. Chem. Soc*. **1957**, 208. b) Chatt, J.; Duncanson, L.,A.; Guy, R. G. *J. Chem. Soc*. **1961**, 827.

CHAPTER 4

INFRARED SPECTROSCOPY OF $V^+(N_2)_n$ COMPLEXES : STRUCTURES, COORDINATION AND SPIN STATES

$V^+(N_2)_n$ complexes are generated in a pulsed nozzle laser vaporization source. Complexes of the size n=3-14 are mass selected and investigated via infrared photodissociation spectroscopy in the N-N stretch region of nitrogen. The infrared forbidden N-N stretch of free nitrogen becomes IR active once the molecule is bound to the metal ion. Photodissociation proceeds solely through the elimination of intact N_2 molecules for all cluster sizes and the fragmentation spectra reveal the coordination number of V^+ to be six. The dissociation process is enhanced on vibrational resonances and the IR spectrum is obtained by monitoring the fragmentation yield as a function of wavelength. The smaller complexes have resonances that are red-shifted with respect to free nitrogen consistent with the Dewar-Chatt-Duncanson complexation model. At cluster sizes of $n \geq 9$ new bands are measured, assigned to spin-state isomers. Density functional theory calculations are used to predict structures, electronic states, relative energies of isomers and IR spectra of $V^+(N_2)_n$ n=1-4 complexes.Comparisons between the measured IR spectra and theoretical predictions offer new understanding into the bonding mechanisms of these metal ion complexes. To our knowledge, this is the first gas phase IR spectroscopic study of an isolated transition metal cation – nitrogen complex.

Introduction

Studies of metal and metal ion complexes in the gas phase are important as they provide simple models to understand complex solvent-solute interactions, metal-ligand bonding and molecule adsorption on metal surfaces.[1-3] Transition metal (TM) ion – nitrogen complexes are interesting because of their relationship to various biological and catalytic systems. For example, nitrogenases are naturally occurring enzymes that contain transition metal centers and catalyze the reduction of N_2 to ammonia.[4] The study of metal complexes has greatly facilitated the understanding of the mechanism of these enzymes.[5,6] Transition metal – nitrogen interactions also play an essential role in the industrial synthesis of ammonia from N_2 on iron surfaces.[7] The reduction of N_2 in biological environments and in surface science takes place by the "activation" of the N-N triple bond and the degree of activation is gauged by the change in the N-N bond distance vis-à-vis the N-N vibrational frequency.[7,8] In this study we investigate the perturbation on the N-N stretch in $V^+(N_2)_n$ using infrared photodissociation spectroscopy.

Metal-nitrogen complexes, including vanadium nitrogen, have been investigated in the condensed phase and in gas phase ion chemistry. In the latter area, ligand exchange studies and collision induced dissociation have been utilized to investigate bonding energetics of various TM cation-nitrogen complexes.[9] The binding of N_2 to a TM cation can occur in either the "end-on" or "side-on" configurations. Electronic spectroscopic studies carried out by Brucat and co-workers[10] on $Co^+(N_2)$ presented evidence for a side-on bonded ground state, but a combined experimental (FT-ICR mass spectrometry) and theoretical (ab initio calculations using coupled cluster and multireference configuration interaction wave functions) study carried out by Schwarz[11] and co-workers disputed this conclusion. Detailed investigations of the structures, energies and vibrational frequencies of the neutral and ionic $Fe(N_2)$ cluster using ab initio and

DFT methods have been carried out by various groups[12-14] and reveal that N_2 will bind primarily end-on. In the condensed phase, experimental studies have been carried out to measure changes in the N-N frequency on metal surfaces.[8,15] In reference to vanadium nitrogen, Andrews and co-workers[16] have acquired infrared spectra of neutral $V(N_2)_n$ complexes for n= 4 and 6, as well as metal-nitride insertion products in an argon matrix environment. Finally, Weltner and co-workers[17] have obtained ESR spectra of $V(N_2)_6$ in a nitrogen matrix and proposed structures. In our present work, we present infrared photodissociation spectra for $V^+(N_2)_n$ complexes in the N-N stretch region.[40a]

Although conventional infrared spectroscopy has been applied to study the metal surface-adsorbate interactions,[7] these measurements are difficult in the gas phase. However, gas phase experiments isolate the species of interest from complex interactions with solvent and solid environments and hence provide ideal models for theoretical studies. Recently, our group has been successful in employing infrared photodissociation spectroscopy to study various metal cation-molecule complexes such as $M^+(CO_2)_n$,[18-21] $M^+(C_2H_2)n$,[22,23] $M^+(H_2O)_n$,[24,25] and $M^+(C_6H_6)_n$[26,27]. In the present work, we apply this technique to study the N-N stretch in $V^+(N_2)_n$ ions where n = 3-12. Unlike previously studied ligands such as CO_2 or H_2O that already possess an IR active chromophore, the N_2 molecule has no IR activity in the isolated gas phase. However, in our previous work with metal-acetylene complexes[22,23] the IR-forbidden modes of free acetylene did become active. In addition, density functional (DFT) calculations predict that the N-N moiety becomes strongly IR active once it is bound to TM cations.

Experimental

The $V^+(N_2)_n$ complexes are generated by laser ablation of a rotating vanadium rod placed in a pulsed nozzle source. The source and the molecular beam apparatus have been described elsewhere.[28,29] A General Valve (series 9) operating with a backing pressure of 70-80 psi of pure nitrogen gas is utilized to create a supersonic beam where cluster growth occurs. Light from the third harmonic of a Spectra Physics Nd:YAG (Quanta Ray INDI 10) is employed to vaporize the rotating vanadium rod. The expansion produced is skimmed into a differentially pumped mass spectrometer chamber where the cationic complexes are extracted from the molecular beam with pulsed acceleration voltages. The ions enter the first drift tube of the reflectron time-of-flight (RTOF) mass spectrometer where they are size selected using pulsed deflection plates. The mass selected ions then enter the reflectron or turning region where a voltage gradient is applied to bring the ions to zero velocity before accelerating them into the second drift tube. Infrared light acquired through an Nd:YAG pumped optical parametric oscillator /amplifier (OPO/OPA, LaserVision) is used to excite the mass selected ions in the turning region in order to induce dissociation. Parent and fragment ions are detected by an electron multiplier tube located at the end of the second drift tube whose output is recorded with a digital oscilloscope (LeCroy WaveRunner LT-342) connected to a PC via an IEEE-488 interface. The infrared spectra are acquired by monitoring the fragment yield as a function of the laser wavelength.

Theoretical Methods

The structure, energetics, vibrational frequencies and IR oscillators strengths for $V^+(N_2)_n$ n=1-4 were calculated using density functional theory (DFT). The B3LYP (Becke-3-Lee-Yang-Parr) functional available on the Gaussian 03W package[30] was utilized in the calculations along

with an all-electron triple zeta basis set with diffuse and polarization functions (6-311+G*). The nitrogen molecules were presumed to bind in the end-on or side-on configurations, but the calculations allowed for symmetry breaking from $C_{\infty v}$ and C_{2v} symmetry in order to obtain true minima. The primary interaction between the TM cation and nitrogen was believed to be electrostatic in nature and hence the electronic states considered were those of the isolated vanadium cation. The vibrational frequencies were scaled by 0.96 and this brought the calculated value of N_2 to 2359 cm^{-1}. The experimental ω_e is 2358.6 and the fundamental frequency of N_2 occurs at 2330 cm^{-1}.[44]

Results and Discussion

The mass spectrum for $V^+(N_2)_n$ complexes produced by laser vaporization of a vanadium rod in a pure N_2 gas expansion is shown in Figure 4.1. A less intense set of peaks corresponding to $V^+(H_2O)(N_2)_y$ complexes are also present in the mass spectrum and are a by-product of the water present in the gas lines. Water is intentionally added because we have found empirically that it improves the singly charged ion yield in our expansion, especially for weakly bound systems such TM^+-Ar_n and TM^+-$(N_2)_n$.[26] As shown, complexes of $V^+(N_2)_n$ for n=1-21 are produced in our instrument. It is unlikely that all the nitrogen molecules are bounded directly to the metal ion. IR spectroscopy is used determine the perturbation, if any, that occurs in the N_2 molecule when it binds to the metal cation and when the second or subsequent layers of N_2 molecules form, i.e. the coordination number for the vanadium cation.

Figure 4.2 shows an example of IR photodissociation of selected $V^+(N_2)_n$ complexes at wavelengths near 2290 cm^{-1} which is 40 cm^{-1} red of the free N-N stretch. The negative going peaks correspond to the depletion of the mass-selected parent ions and the positive peaks

Figure 4.1 The mass distribution of $V^+(N_2)_n$ and $V^+(H_2O)(N_2)_y$ produced by laser vaporization in a pure N_2 gas expansion.

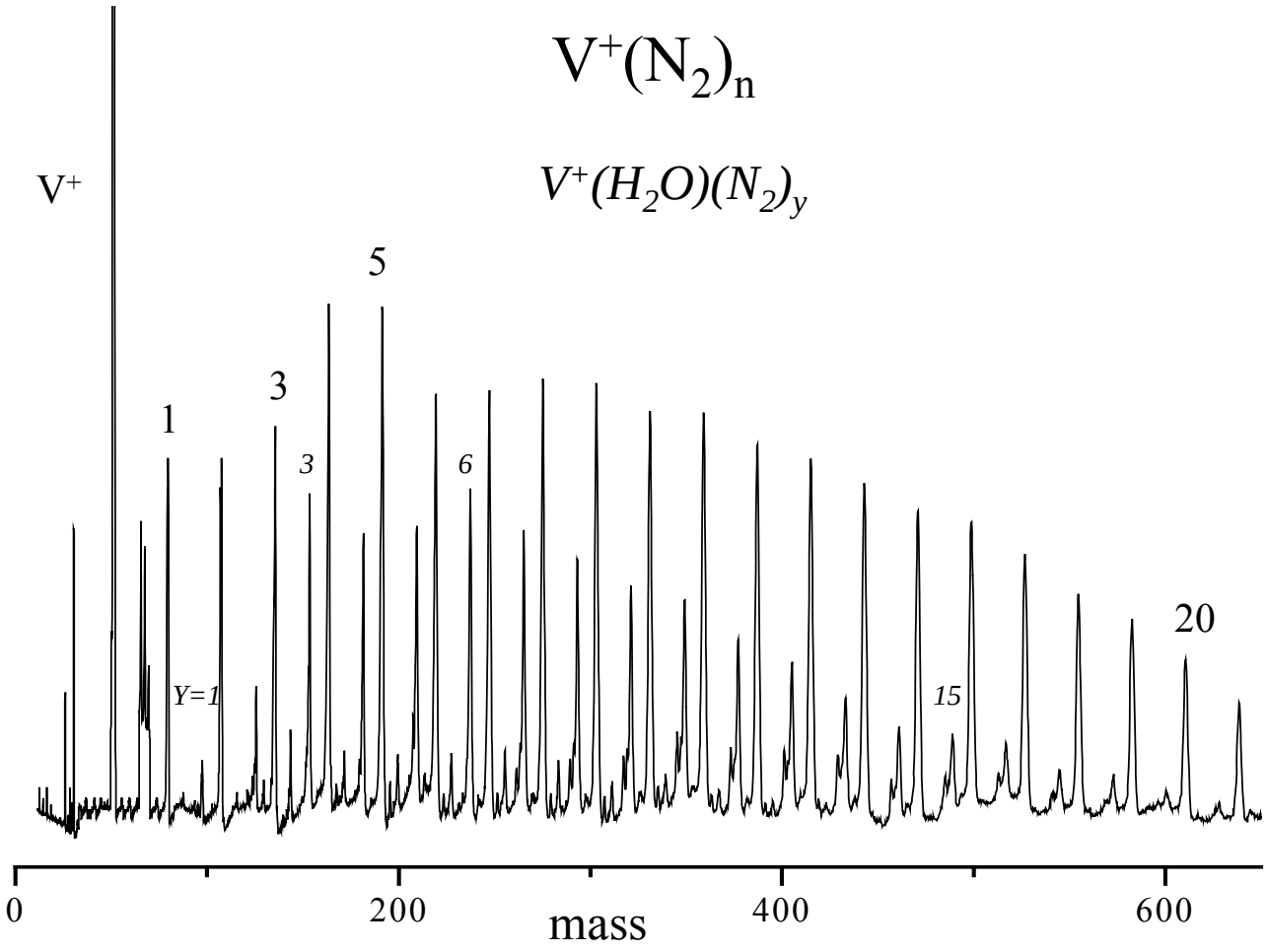
V+(N2)n
V+
V+(H2O)(N2)y
5
3
1
3
6
20
Y=1
15
0
200
400
600
mass

Figure 4.2 The mass fragmentation spectra for selected $V^+(N_2)_n$ complexes with n=5,7,8,9, and 10. The complexes fragment by loss of N_2 and the loss process for the large clusters terminates at n=6.

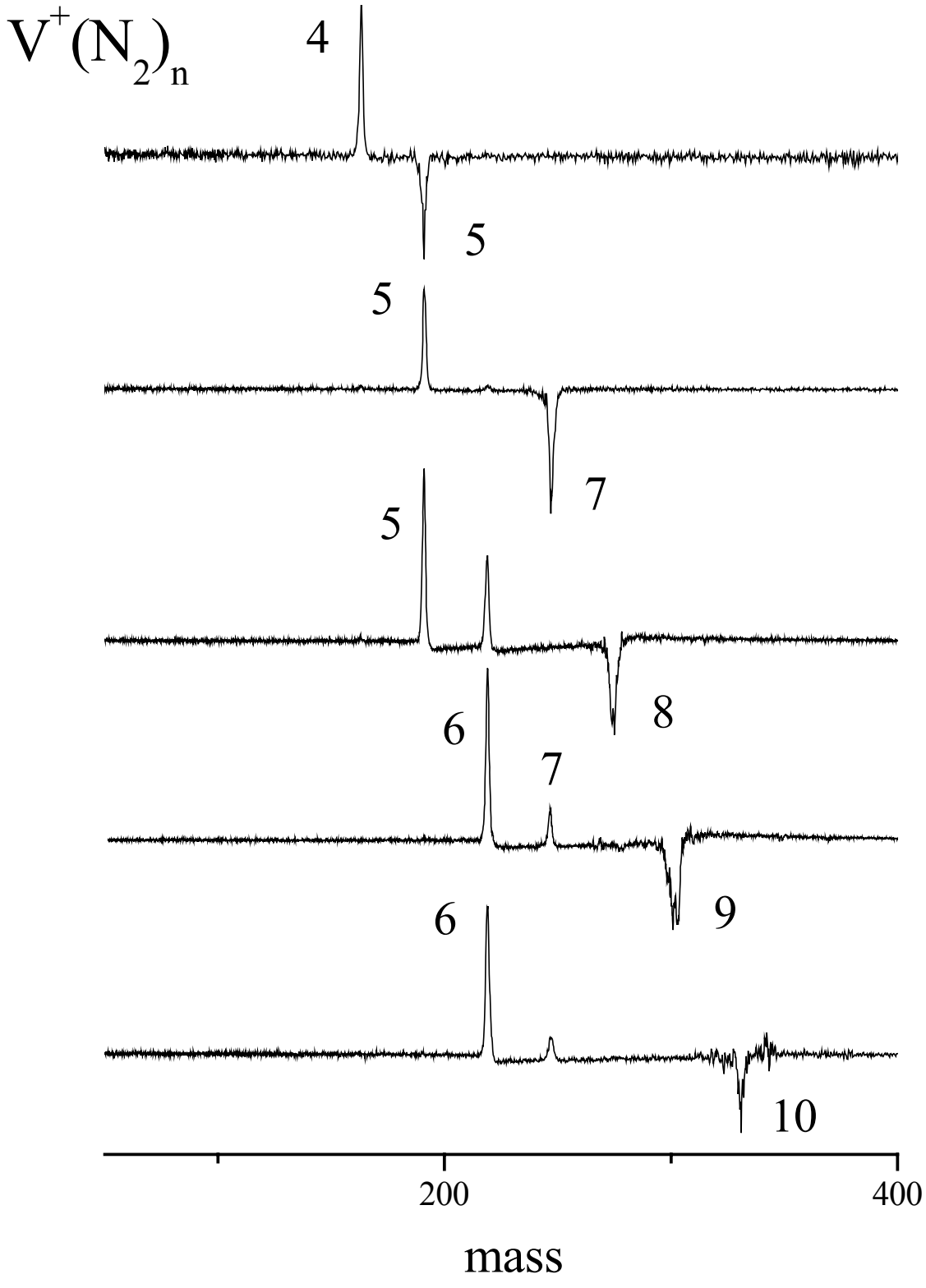
V+(N2)n
4
5
5
7
5
8
6
7
9
6
10
200
400
mass

represent the photofragments formed. The fragment masses show that the complexes dissociate by the successive elimination of whole N_2 molecules. There is no evidence for nitride fragments that might appear if the nitrogen molecules were dissociated due to metal bonding or by photochemistry. Insertion reactions are not expected since these complexes are expected to bind primarily due to electrostatic interactions (charge-quadrupole for metal cation-N_2 and quadrupole-quadrupole for N_2-N_2).[12-14, 31-33] Another salient feature in the fragmentation spectra is the termination at $V^+(N_2)_6$ in the sequential elimination of N_2 molecules from larger complexes. The simplest explanation for this trend is that in the n = 6 and smaller complexes the nitrogen molecules must attach themselves directly to the metal cation. The binding energy of nitrogen to vanadium cation is not known experimentally, however Armentrout and co-workers have measured the energetics for the isoelectronic species $V^+(CO)_n$.[34] The binding energies of CO to vanadium cation for up to seven ligands range from about 6000 cm^{-1} to 9500 cm^{-1} and the values for the N_2 ligand should be slightly smaller. Conversely the $(N_2)_2$ dimer bond energy is predicted to be about 50-100 cm^{-1}.[32,33] In the larger complexes, it is likely that some of the N_2 molecules are not bonded directly to the metal, consequently these complexes must have lower dissociation energies for the removal of outer ligands. It could be argued that $V^+(N_2)_7$ should be an unusually stable system because it is an 18-electron system. However seven nitrogen ligands may create steric hindrance, thus offsetting any benefit acquired by an 18-electron scheme. A similar argument has been put forth by Armentrout and co-workers for the relatively greater stability of $V^+(CO)_6$ as compared to $V^+(CO)_7$.[34]

Figures 4.3 and 4.4 show the IR spectrum acquired for $V^+(N_2)_n$ for n=3-14 which are recorded in all mass channels corresponding to loss of whole N_2 molecules. The dashed line indicates the frequency of free nitrogen at 2330 cm^{-1}. It is clearly evident from the spectrum that

Figure 4.3 The IR photodissociation spectra for $V^+(N_2)_n$ with n=3-8 obtained by monitoring the loss of N_2 as a function of wavelength. The vertical dashed line indicates the N-N vibrational frequency of free N_2.

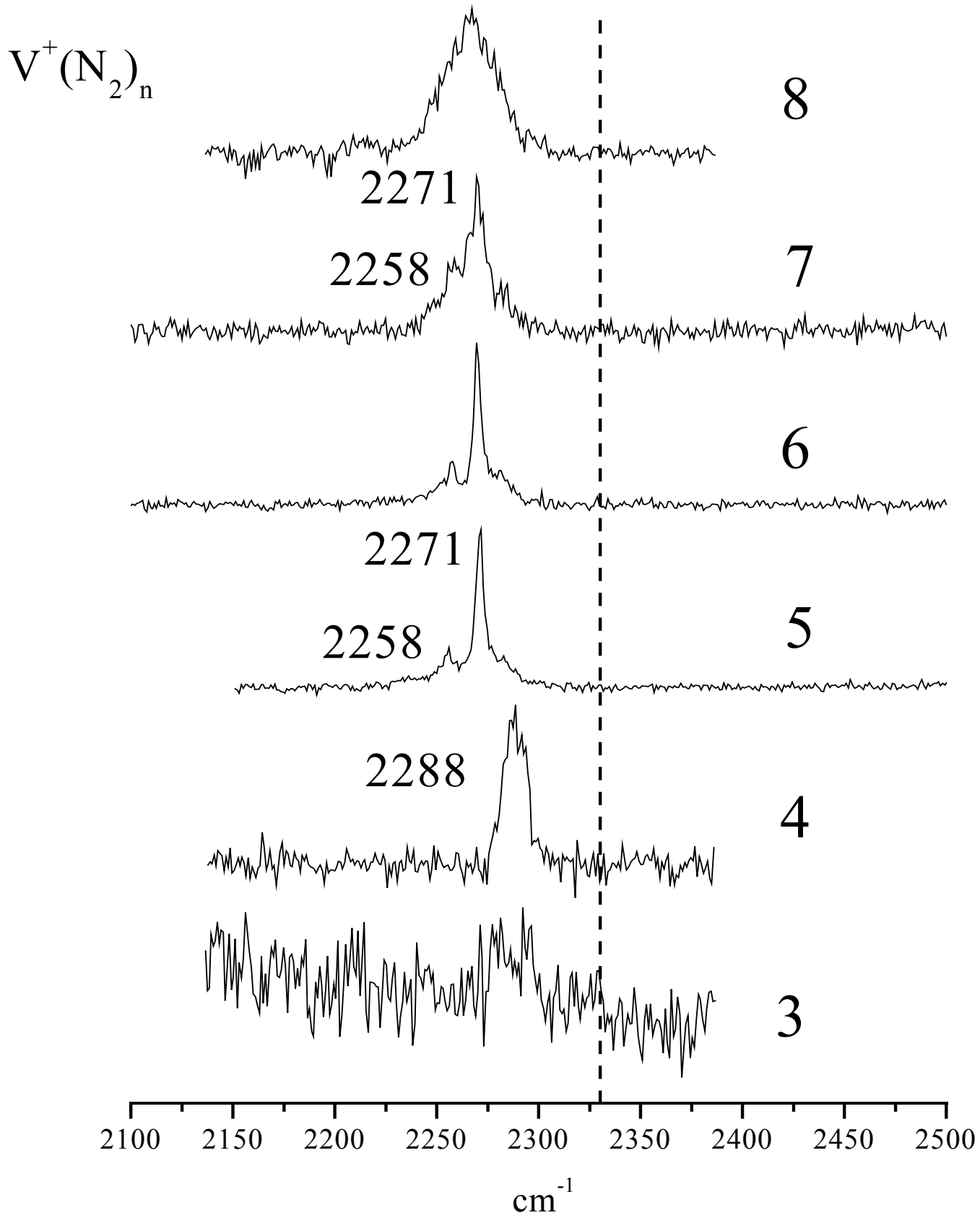
V+(N2)n
8
2271
2258
7
6
2271
2258
5
2288
4
3
2100
2150
2200
2250
2300
2350
2400
2450
2500
cm-1

Figure 4.4 The IR photodissociation spectra for $V^+(N_2)_n$ with n=9-14. The vertical dashed line indicates the frequency of free nitrogen.

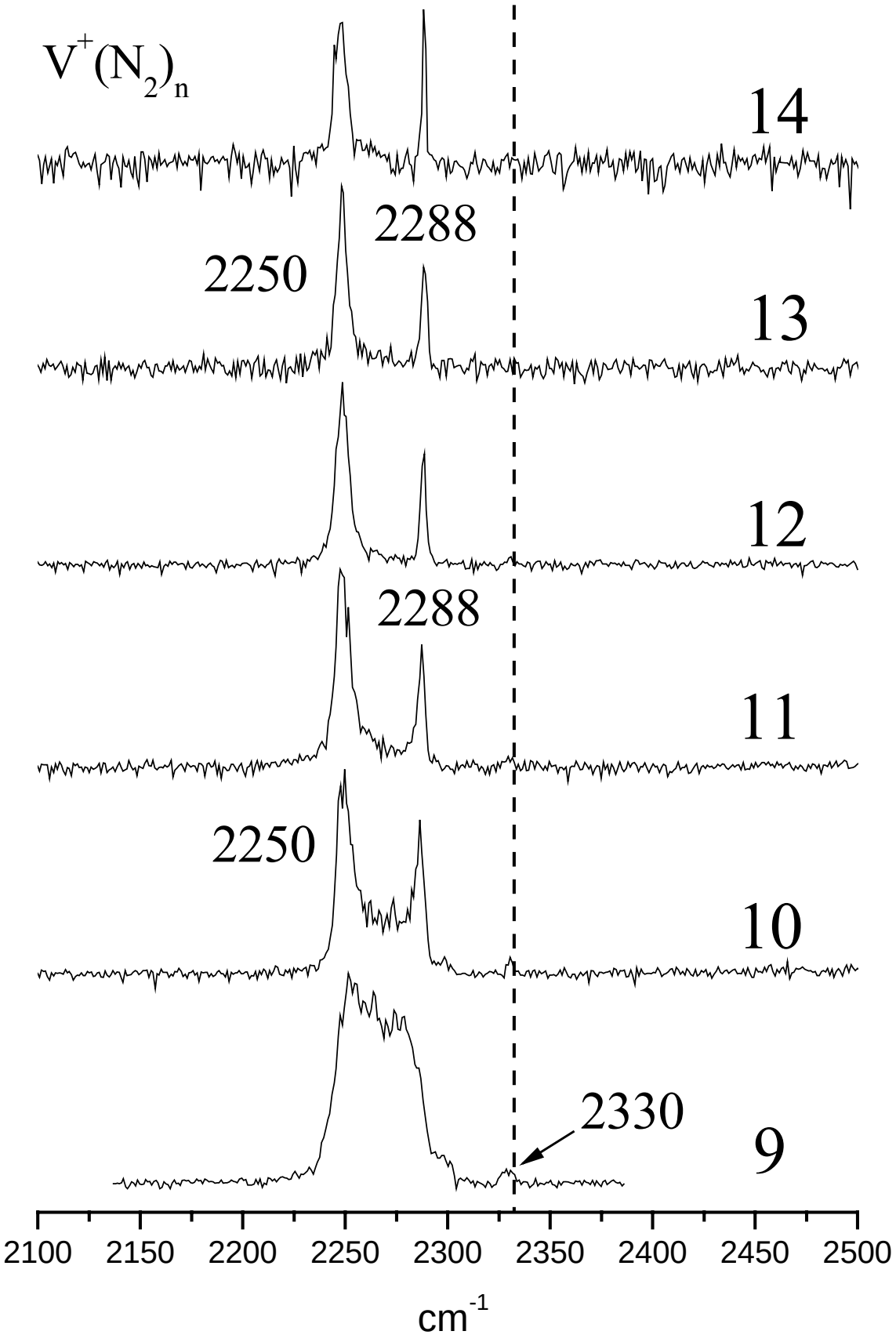
V+(N2)n
14
2288
2250
13
12
2288
11
2250
10
2330
9
2100
2150
2200
2250
2300
2350
2400
2450
2500
cm-1

the IR forbidden N-N vibration of free nitrogen is "switched on" by the vanadium cation. The small complexes have a one main peak that is red shifted from free nitrogen by about 40 cm^{-1}. Some of the small complexes (n=5-7) also have a second peak that is further red shifted than the main peak and lesser in intensity. The large complexes have two red shifted peaks of comparable intensity. The red-shifts of the principal peaks seen so far can be understood qualitatively using the so-called Dewar-Chatt-Duncanson complexation model, which is often applied to TM-carbonyl complexes.[35,36] In this picture, the bonding includes σ-type donation of electron density from the ligand into the d-orbitals of the metal and π-type back-donation of metal electron density into the π* orbitals of the ligand.[37,38] Both factors help to weaken the N-N bond and drive the vibrational frequency to lower values. Complexes of size $n \leq 3$ gave broad, featureless spectra with low signal/noise ratio and reasons for this are discussed below.

$V^+(N_2)_4$ is the smallest cluster for which an IR spectrum with a reasonable signal to noise ratio can be acquired. The spectrum for the n=3 complex exhibits a single broad feature centered at 2285 cm^{-1}. It is not surprising for small complexes to display spectra with low signal/noise ratio. Large complexes tend to have lower binding energies compared to smaller ones since the electrostatic charge of the metal ion is shared by additional ligands. Due to the larger binding energies, photofragmentation in the smaller complexes probably proceeds by multiphoton processes, which are in general, inefficient. This may lead to the poor signal/noise ratio. The complexes in our experiment are cooled via supersonic expansion, but some complexes may still retain excess internal energy causing them to dissociate effortlessly and hence producing broad spectra. The broad spectra may also arise because a small percentage of the complexes may be weakly bound isomeric forms of the more strongly bound complexes and as a result fragment readily. The spectrum of $V^+(N_2)_3$ therefore has a low signal/noise ratio and shows no distinct

peaks. The spectrum of $V^+(N_2)_4$ is more intense than that for the n=3 cluster, with a single peak centered at 2288 cm^{-1} that is 42 cm^{-1} red-shifted from the free N_2 vibration.

The spectrum of $V^+(N_2)_5$ is somewhat different from the spectra of the smaller complexes. Firstly, it has a higher signal/noise ratio with the principal peak now appearing at 2271 cm^{-1}. This is now a 17 cm^{-1} red-shift from the principal peak in the n=4 spectrum and an 59 cm^{-1} red-shift from free nitrogen. A minor, yet reproducible, peak is also evident in the spectrum, emerging slightly to the red of the primary peak. This secondary feature positioned at 2258 cm^{-1} is also present in the spectra for the n=6 and 7 cluster sizes, although it is slightly less prominent for the n=7 complex. The spectra of the $V^+(N_2)_5$ and $V^+(N_2)_6$ are identical with apparently no change in the peak positions or the signal/noise ratio. The spectrum of $V^+(N_2)_7$ is similar to the n=5 and 6 spectra with a prominent peak centered at 2271 $cm^{-1}$and a smaller feature at 2258 cm^{-1}, but the linewidth is broader. The linewidth of the peak in the spectra of the n=5 and 6 complex is roughly 8 cm^{-1} at FWHM, whereas the linewidth in n=7 spectra is about 15 cm^{-1}. This apparent broadening of the red-shifted peak is also noticeable in the spectra for the n=8 complex, where yet again only one principal feature centered at 2271 cm^{-1} is observed but whose linewidth now at FWHM is roughly 29 cm^{-1}. In the $V^+(N_2)_9$ spectrum, we detect the continuing trend of increasing linewidth with little or no shift of the center of the principal peak. The main feature now has a peak width of about 42 cm^{-1} but there is also a small reproducible peak at 2330 cm^{-1}. Based on our results above, only the first six N_2 molecules are bound to the metal ion. Thus, beginning with the n=7 cluster we suspect the onset of the second solvation sphere, but given that the N_2-N_2 complex is bound by only 100 cm^{-1}, it is doubtful the N-N vibration is strongly IR active within such a van der Waals dimer. In fact, from spectroscopic studies available for $(N_2)_2$, the proposed geometry is T-shaped with an IR mode at 2329 cm^{-1}.[31]

This basically falls right on the vibration of free nitrogen at 2330 cm^{-1}.[44] Thus, we ascribe this feature to the presence of one or more N_2 molecules in the second solvation sphere.

The spectrum of $V^+(N_2)_{10}$ is noticeable different from the spectra of the smaller complexes. The broad feature of the n=9 spectrum has now split into two distinct peaks separated by 38 cm^{-1}. The larger peak is centered at 2250 cm^{-1} with a linewidth at FWHM of 9 cm^{-1}, whereas the smaller peak falls at 2288 cm^{-1} and corresponds closely to the single peak in the n=4 spectrum. It must be noted that these two primary peaks are not separated completely by baseline but are conjoined. The feature at 2330 cm^{-1} present in the n=9 spectrum, corresponding to external nitrogens, is also present in the n=10 spectrum. The spectra of the complexes greater than $V^+(N_2)_{10}$ reveal no significant changes with regard to peak positions or intensities. However, the spectra gradually become smoother and the two peaks become more separated. The 2330 cm^{-1} band gradually becomes too weak to detect.

In order to further investigate these infrared photodissociation spectra, we performed comprehensive DFT calculations on the n=1-4 cluster sizes. Figure 4.5 shows the optimized geometric structures for the n=1-4 complexes sizes calculated using the methods mentioned in the theoretical section. The predicted IR active frequencies along with the oscillator strengths, and dissociation energy (D_e) for the addition of the last ligand are listed in Table 4.1. Further details of the structures are listed in Appendix A. Studies were only done for the n=1-4 complexes because calculations for the larger complexes failed due to convergence difficulties. For each complex, the ground state (^5D) and first excited state associated with a spin change (^3F) for the isolated V^+ were studied. For all complexes, the quintet was more stable than the triplet by 15-30 kcal/mol. The results of all the calculations are listed in Appendix A. For the n=1 cluster, two minima corresponding to the end-on and side-on configurations were found with the

Figure 4.5 Calculated structures for $V^+(N_2)_n$ n=1-4 using B3LYP/6-311+G*. Bond distances are in angstroms and bond angles in degrees.

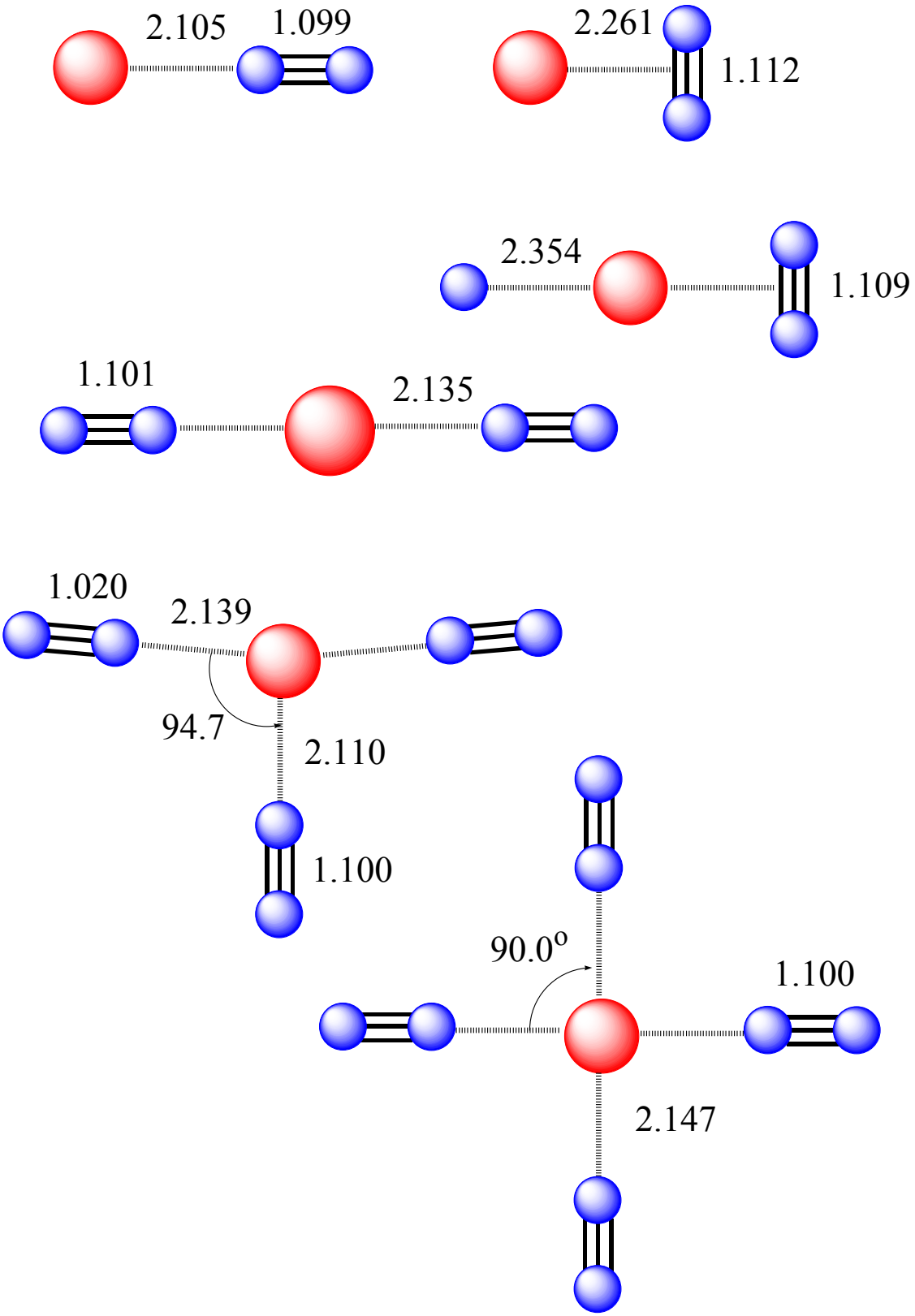
2.105
1.099
2.261
1.112
2.354
1.109
1.101
2.135
1.020
2.139
94.7
2.110
1.100
90.0°
1.100
2.147

Table 4.1 The results of theory for the quintet electronic states of $V^+(N_2)_n$ complexes. Binding energies (relative to separated V^+ and nN_2), dissociation energies (D_e) for the process $V^+(N_2)_n \rightarrow V^+(N_2)_{n-1}$, predicted frequencies and IR oscillator strengths for calculated structures shown in Figure 4.5 (using B3LYP/6-311+G*). Frequencies were scaled by 0.96.

	Structure	B.E (kcal/mol)	D_e (kcal/mol)	IR Freq. (cm^{-1})	IR Oscillator Strength (km/mol)
n=1	Linear	33.8	33.8	2291	55
	T-shaped	18.6	18.6	2160	169
2	Linear	53.1	19.7	2262	354
	Mixed	40.3	6.7*	2182, 2292	311, 67
	T-shaped	27.0	8.5	2181	544
3	Linear	71.7	18.9	2267, 2275	129, 263
4	Linear	88.3	33.8	2279	246

*for removal of the more weakly bound T-configured ligand.

end-on structure more strongly bound by about 15 kcal/mol. For both structures, the N-N frequency predicted is significantly red shifted compared to free nitrogen. For the linear complex, this shift is about 40 cm^{-1}, whereas for the T-shaped complex it is approximately 171 cm^{-1}. Also of significance to this work are the non-zero values for the infrared oscillator strengths predicted by theory and observed experimentally. A greater red-shift is expected for the T-shaped complexes given that the metal ion is directly bonded to the π electron framework and hence can perturb the N-N bond to a larger extent as compared to the linear complex. For the n=2 complex, minima were found for both linear (2L), both T-shaped (2T) and one L, one T (L-T) configurations. The all linear complex was found to be a minimum whereas the 2T complex is higher in energy. The L-T complex is a minimum but higher in energy than the 2L complex but lower in energy than the 2T complex. The 2-T has D_{2d} symmetry where the nitrogens are staggered. Again red shifts are predicted that are greater for the 2T complex as opposed to the 2L complex. The all linear complex is calculated to have a frequency near 2262 cm^{-1} with a dissociation energy (D_e) of 19.7 kcal/mol, whereas the T-complex has a frequency of 2209 cm^{-1} with a D_e of 8.5 kcal/mol. The L-T complex has two vibrations, one corresponding to the L isomer and the other to the T isomer. For complexes larger than n=2 it is possible to envision additional isomers where one N_2 binds end-on while the others bind side-on. For such systems we have not performed an exhaustive search of the potential surface for all possible isomers. We have not explored these possibilities because such complexes would have two distinct IR bands whereas in the spectra for the small complexes we observe only a single band. Hence the spectra suggest that at least in the smaller complexes, the structures are highly symmetric and that all the N_2 molecules bind in equivalent orientations.

As can be seen from the trend so far, the linear complexes appear to bind more strongly and their predicted frequencies fall within the range where we observe our IR bands. This trend continues for the n=3 cluster, where no minima could be found for all three N_2 molecules binding in the side-on orientation. For end-on bonded nitrogen, a minimum energy structure is found that is distorted from a trigonal planar structure. Attempts to constrain the molecule to a trigonal planar arrangement did not lead to a stationary point. The stable structure found has a D_e of 18.9 kcal/mol with two IR active modes, one at 2267 cm^{-1} and the other at 2275 cm^{-1} (with the latter twice as intense as the former). Changing the orientation of the axial N_2 to side-on bonded resulted in a second order saddle point with a D_e of 3.80 kcal/mol. Unfortunately the n=3 spectrum with its low signal/noise ratio does not lend itself to any vibrational analysis. However, the spectrum has structure in the 2270-2300 cm^{-1} region consistent with the predictions of theory.

For $V^+(N_2)_4$, the only structure with equivalent nitrogens resulting in a stationary point has square planar symmetry, as shown in Fig 4.5 Such a structure is understandable because the vanadium ion is well known to form octahedral and square pyramidal structures in condensed phase inorganic chemistry,[39] and a square planar structure is a precursor to such geometries. This structure is predicted to have a doubly degenerate vibration resulting in a single IR band that is only 9 cm^{-1} off from the peak in the spectrum. We can therefore conclude that the spectroscopic data and theoretical predictions support the presence of end-on bonded nitrogen molecules in a square planar arrangement for the n=4 complex.

The primary band in the n=5 and 6 spectra falls at 2271 cm^{-1} which is 17 cm^{-1} further to the red of the n=4 band. Such a shift in the principal peak between the n=4 and the n=5,6 complexes was also observed in our work with $Nb^+(N_2)_n$.[40b] However, in that system there is

only one band for all complexes sizes. The small shift (in comparison to n=4) seen for the n=5,6 complexes suggest similar structures to the n=4 complex. Therefore, square pyramidal symmetry for $V^+(N_2)_5$ and octahedral for $V^+(N_2)_6$ are likely candidates for these complexes. Moreover, the vanadium ion favors these symmetries in the condensed phase.[39] The n=5 and 6 spectra do have an additional peak at 2258 cm^{-1} with much lower intensity. This band may be the precursor to the intense, further red-shifted peak (appearing at 2250 cm^{-1}) that appears in the larger complexes beginning with $V^+(N_2)_{10}$. It is also possible that the complexes are comprised of geometries that are distorted from square pyramidal and octahedral geometries. Weltner and co-workers[17] interpreted the electron-spin-resonance spectrum of neutral vanadium hexanitrogen as evidence of tetragonal axial elongation of the octahedral crystal field due to Jahn-Teller effects, thus reducing the symmetry to D_{4h}. In such a situation, one N_2 (for n=5) and two N_2 (for n=6) molecules are in slightly distorted positions compared to the other nitrogen molecules and hence will have slightly different IR absorptions. This could well describe the presence of the secondary peak in the IR spectra of n=5 and 6.

Beginning with $V^+(N_2)_7$ a general increase in the linewidth of the principal peak is seen and this splits eventually into a doublet at $V^+(N_2)_{10}$. It can be surmised that the general broadening seen for the n=7,8 and 9 complexes is the naissance of the doublet that is ultimately seen for the larger complexes. The further red-shifted and more intense peak at 2250 cm^{-1} appears to be the result of a new interaction that is absent in the smaller complexes, since the smaller band at 2288 cm^{-1} corresponds well to the single peak in the n=4,5,6 and 7 spectrum. In order to understand the presence of the doublet we consider three possibilities. Firstly, it is possible that some of the N_2 molecules bind in the side-on configuration to the metal ion. However, such a situation is hard to envision given that DFT calculations consistently favor end-

on binding over side-on bonded N_2 molecules. Moreover, the predicted vibrational frequencies for any side-on bonded N_2 falls between 2100 – 2210 cm^{-1} – a region in the IR spectra where on bands are observed. The second possible explanation for the doublet is an *intracluster* reaction brought about by solvation effects and/or photochemistry. An intracluster reaction induced by solvation is an intriguing possibility. Such reactions have been detected in our lab previously with $Ni^+(CO_2)_n$,[19] $V^+(CO_2)_n$,[20] $Si^+(CO_2)_n$,[21] and $Ni^+(C_2H_2)_n$[22] complexes. Here, an intracluster reaction would lead to metal-nitride complexes, which seems unlikely. There is no evidence in the mass spectrum for the formation of vanadium-nitride complexes. Furthermore, the fragmentation spectra (Figure 4.2) all show the elimination of only intact nitrogen molecules. However, these arguments alone cannot rule out the possibility of a reaction. If any reaction did take place, it would lead to a N-V-N product that might form a core around which further N_2 molecules will agglomerate. If such a complex does form, it could not be distinguished by mass spectrometry. Therefore, we performed DFT calculations using the B3LYP/6-311+G* method to consider the energetics of the N-V-N product. This product is a third order saddle point lying about 160 kcal/mol higher in energy than linear V-N-N complex. Although the absolute value of the energetics and the nature of the stationary point may be an artifact of the method used, it is reasonable to conclude that N-V-N is an unstable product. We can therefore rule out such a reaction as the source of the 2250 cm^{-1} band.

The final alternative to consider is the possibility of a spin change induced on the vanadium cation by the presence of secondary solvation ligands. Transition metals frequently possess low lying excited states that compete with the ground state for the lowest energy conformation.[41,42] The vanadium cation is a quintet in its isolated form (d^4, ^5D) and the first excited electronic state associated with a spin change is a triplet (d^3s, ^3F), which lies 25.2

kcal/mol cm^{-1} higher in energy. These two electronic configurations were calculated as contenders for the ground state of $V^+(N_2)_4$. The $^3A_{1g}$ state in $V^+(N_2)_4$ is predicted to lie higher in energy by approximately 20.7 kcal/mol than the $^5B_{2g}$ state. The binding of nitrogen at least in the n=4 cluster is not expected to change the spin multiplicity of V^+. However, we anticipate such a spin change only with the larger complexes where the 2250 cm^{-1} band is seen clearly. The triplet is also predicted to have only one IR frequency vibration that falls near 2225 cm^{-1} with twice the intensity of the IR band as for the quintet state. Figure 4.6 shows the spectra of the n=4 and 12 cluster along with the predicted frequency position for the quintet and triplet states. The predicted frequency for the $^5B_{2g}$ state agrees well with n=4 spectrum, whereas there is no observed band that corresponds to the $^3A_{1g}$ state complex. However, the triplet frequency band matches very well to the 2250 cm^{-1} band in the n=12 spectra and the quintet frequency corresponds to the minor peak in the spectra. Based on these results, it is reasonable to conclude that the doublet seen in the IR spectra of the larger complexes is due to the presence of vanadium-nitrogen complexes that possess two different electronic states and that the lower multiplicity state is generated principally due to solvation effects.

Various groups, including ours, have invoked such a ligand induced spin change in the vanadium cation. Bowers and co-workers[43] investigating the binding energies of $V^+(H_2)_n$ n=1-7 ascribe the anomalously high binding energy of the n=6 cluster to a change in the spin state from a quintet to a triplet. In our previous work with $V^+(benzene)_n$ complexes[26] the possibility of a spin change needed to be considered to interpret the IR spectra, but discrepancies between the experimental results and theoretical predictions prevented a conclusive argument. These examples along with the present work describe the propensity of the vanadium ion to alter its electronic state.

Figure 4.6 Calculated spectra for $V^+(N_2)_4$ for ^5D and ^3F electronic states of V^+ compared to the experimental spectra of $V^+(N_2)_4$ and $V^+(N_2)_{12}$. Predicted intensities have been normalized for direct comparison.

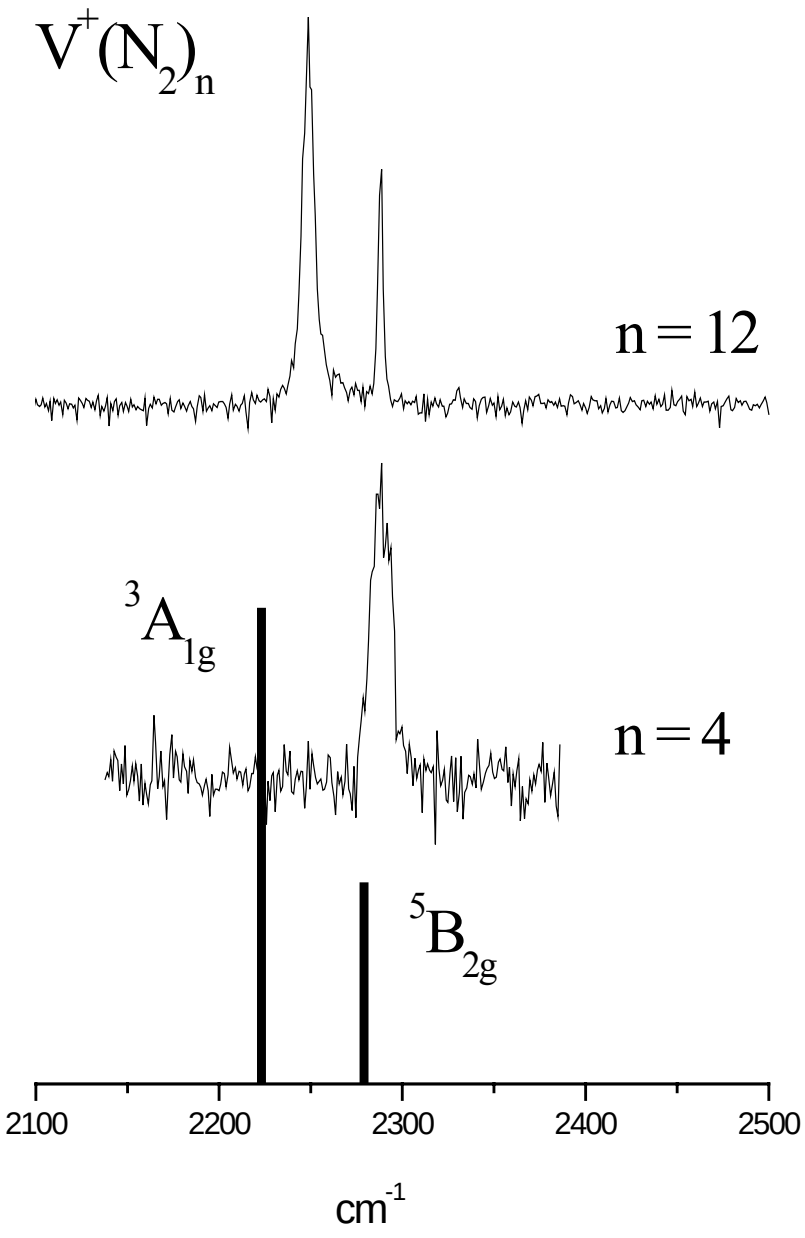
V+(N2)n
n = 12
3A1g
n = 4
5B2g
2100
2200
2300
2400
2500
cm-1

Although, the IR spectra of the larger complexes indicate a possible spin state change in the vanadium cation, it is surprising that both spin states co-exist in our molecular beam. This is only possible if the energy difference between the two spin states is extremely small (~50 cm^{-1}). Our recent work on $Nb^+(N_2)_n$ complexes revealed a spin state change as well but only one band was present in the IRPD spectra.[40b] For the $Nb^+(N_2)_n$ system we were able to perform DFT calculations up to the n=6 complex size and thereby obtain the energetics between the different spin states. Since DFT calculations are usually more difficult for first row transition metals,[35] we are unable to calculate energetics for $V^+(N_2)_n$ complexes larger than n=4. Future theoretical work would have to compute the energetics and IR spectra for quintet and triplet spin states of the larger complexes.

Conclusion

This work reports the first gas phase infrared spectra of $V^+(N_2)_n$ complexes, which is also apparently the first IR data for metal ion – nitrogen complexes in the N-N stretching region. Photodissociation for all cluster sizes occurs exclusively by the loss of whole N_2 molecules. The fragmentation mass spectra show the termination at n=6 for the elimination of N_2 for the larger complexes signifying that the initial six N_2 molecules comprise the first solvation sphere for V^+. The IR spectra of the small complexes show a single peak that is red-shifted with respect to free nitrogen and is consistent with the qualitative predictions of the DCD model. This single band eventually splits into a doublet separated by 38 cm^{-1} at the n=10 cluster size and with minimal changes after that for the bigger complexes. Structural and spin-state isomers are considered as possible explanations for the doublet. Coupled with DFT calculations, the IR spectra present strong evidence for only end-on bonded N_2 molecules and no side-on bonded nitrogens. The

possibility of an intracluster reaction brought on by progressive solvation is considered and ruled out based on experimental and theoretical evidence.

A possible spin change in the vanadium cation is the best explanation for the doublet in the larger complexes. Predictions from DFT for the two different electronic states of V^+ match well with the IR spectra and lead to this conclusion. However, further theoretical studies for the larger complexes needs to be undertaken in order to completely verify the hypothesis. These new IR studies can be extended to suitable metal ion – nitrogen complexes. Further studies to examine the trends in the vibrational shifts for different metal – nitrogen complexes and the correspondence between experiment and theory are currently underway in our lab.

References

(1) Eller, K.; Schwarz, *H. Chem. Rev*. **1991**, *91*, 1121.

(2) Freiser, B.S. ed., *Organometallic Ion Chemistry*; Kluwer: Dordrecht, **1996**.

(3) Duncan, M.A., ed. Adv. *Metal and Semiconductor Clusters*, Elsevier: Amsterdam, **2001**, Vol 5.

(4) Seigbahn, P.E.M.; Blomberg, M.R.A. *Chem. Rev*. **2000**, *100*, 421.

(5) Burgess, B. K.; Lowe, D. K. *Chem. Rev*. **1996**, *96*, 2983.

(6) Rincon, L.; Ruette, F.; Hernandez, A. *J. Mol. Spectrosc*. **1992**, *254*, 395.

(7) Somorjai, G.A. *Introduction to Surface Chemistry and Catalysis.* John Wiley & Sons, Inc.: New York, **1994**.

(8) Rao, C. N. R.; Rao, G. R. *Surf. Sci. Rep.* **1991**, *13*, 221.

(9) a) Khan, F.A.; Steele, D.L.; Armentrout, P.B. *J. Phys. Chem*. **1995**, *99*, 7819. b) Tjelta, B.L.; Armentrout, P.B. *J. Phys. Chem*. **1997**, *101*, 2064. c) Tjelta, B.L.; Walter, D.; Armentrout, P.B. *Intl. J. Mass. Spec.* **2001**, *204*, 7.

(10) Asher, R. L.; Buthelezi, B.; Brucat, P. J. *J. Phys. Chem*. **1995**, *99*, 1068.

(11) Heinemann, C.; Schwarz, J.; Schwarz, H. *J. Phys. Chem*. **1996**, *100*, 6088.

(12) Zacarias, A.; Torrens, H.; Castro, M.; *Intl. J. Quant.Chem.* **1997**, *61*, 467.

(13) Bauschlicher, C. W. Jr.; Petterson, L. M.; Siegbahn, P. E. M. *J. Chem. Phys*. **1987**, *87*, 2129.

(14) Duarte, A. D.; Salahub, D. R.; Haslett, T.; Moskovits, M. *Inorganic Chemistry*. **1999**, *38*, 3895.

(15) a) Grunze, M.; Golze, M.; Hirschwald, W.; Freund, H.J.; Pulm, H; Seip, U; Tsai, M.C.; Ertl, G.; Kuppers,J. Phys. Rev. Lett. **1984**, 53, 850. b) Tsai, M. C.; Seip, U.; Bassignana, C. I.; Kuppers, J.; Ertl, G.; *Surf. Sci*. **1985**, *155*, 387.

(16) Andrews, L.; Bare, W. D.; Chertihin, G. V. *J. Phys. Chem. A.* **1997**, *101*, 8417.

(17) Parrish, S. H.; Van Zee, R. J.; Weltner, W. Jr. *J. Phys. Chem. A.* **1999**, *103*, 1025.

(18) Gregoire, G.; Duncan, M. A. *J. Chem. Phys.* **2002**, *117*, 2120.

(19) Walker, N. R.; Walters, R. S.; Grieves, G. A.; Duncan, M. A. *J. Chem. Phys*. **2004**, *121*, 10498.

(20) Walker, N. R.; Walters, R. S.; Duncan, M. A. *J. Chem. Phys*. **2004**, *120*, 10037.

(21) Jaeger, J.; Jaeger, T.; Duncan, M. A. *Intl. J. Mass. Spect.* **2003**, *228*, 285.

(22) Walters, R. S.; Jaeger, T. D.; Duncan, M. A. *J. Phys. Chem. A.* **2002**, *106*, 10482.

(23) a) Walters, R. S.; Corminboeuf, C.; Schleyer, P. v. R.; Duncan, M. A. *J. Am. Chem. Soc.* **2005**, *127*, 1100. b) Walters, R. S.; Pillai, E. D.; Schleyer, P. v. R, Duncan, M. A. *J. Am. Chem. Soc*. **2005**, *127*, 17030.

(24) Walker, N. R.; Walters, E. D.; Pillai, E. D.; Duncan, M. A. *J. Chem. Phys.* **2003**, *119*, 10471.

(25) Walters, R.S.; Pillai, E.D.; Duncan, M.A. *J. Am. Chem. Soc*. **2005**, *127*, 16599.

(26) Jaeger, T. D.; Pillai, E. D.; Duncan, M. A. *J. Phys. Chem. A.* **2004**, *108*, 6605.

(27) Jaeger, T. D.; Duncan, M. A. *J. Phys. Chem. A.* **2005**, *109*, 3311.

(28) Duncan, M. A.; *Annu. Rev. Phys. Chem.***1997**, *48*, 69.

(29) Duncan, M.A. *Intl. Rev. Phys. Chem.* **2003**, *22*, 407.

(30) Frisch, M. J.; Trucks, G. W.; . Schlegel, H. B.; Scuseria, G. E.; Robb, M. A.; Cheeseman, J. R.; Montgomery, J. A. Jr.; Vreven, T.; Kudin, K. N.; Burant, J. C.;

Millam, J. M.; Iyengar, S. S.; Tomasi, J.; Barone, V.; Mennucci, B.; Cossi, M.; Scalmani, G.; Rega, N.; Petersson, G. A.; Nakatsuji, H.' Hada, M.; Ehara, M.; Toyata, K.; Fukuda, R.; Hasegawa, J.; Ishida, M.; Nakajima, T.; Honda, Y.; Kitao, O.; Nakai, H.; Klene, M.; Li, N.; Knon, J. E.; Hratchian, H. P.; Cross, J. B.; Adamo, C.; Jaramillo, J.; Gomperts, R.; Stratmann, R. E.; Yazyev, O.; Austin, A. J.; Cammi, R.; Pomelli, C.; Ochterski, J. W.; Ayala, P. Y.; Morokuma, K.; Voth, G. A.; Salvador, P.; Dannenberg, J. J.; Zakrzewski, V. G.; Dapprich, S.; Daniels, A. D.; Strain, M. C.; Farkas, O.; Malick, D. K.; Rabuck, A. D.; Raghavachari, K.; Foresman, J. B.; Ortiz, J. V.; Cui, Q.; Baboul, A. G.; Clifford, S.; Cioslowski, J.; Stefanov, B. B.; Liu, G.; Liashenko, A.; Piskorz, P.; Komaromi, I.; Martin, R. L.; Fon, D. J.; Keith, T.; Al-Laham, M. A.; Peng, C. Y.; Nanayakkara, A.; Challacombe, M.; Gill, P. M. W.; Johnson, B.; Chen. W.; Wong, M. W.; Gonzalez, C.; Pople, J. A. *Gaussian 03 (Revision B.02)*; Gaussian, Inc.: Pittsburgh, PA, 2003.

(31) Long, C. A.; Henderson, G.; Ewing, G. E. *Chem. Phys*. **1973**, *2*, 485.

(32) Couronne, O.; Ellinger, Y. *Chem. Phys. Lett*. **2000**, *306*, 71.

(33) Aquilanti, V.; Bartolomei, M.; Cappelletti, D.; Carmona-Novillo, E.; Pirani, F. *J. Chem. Phys*. **2002**, *117*, 615.

(34) Sievers, M. R.; Armentrout, P. B. *J. Phys. Chem*. **1995**, *99*, 8135.

(35) Frenking, G.; Frohlich, N. *Chem. Rev*. **2000**, *100*, 717.

(36) Zhou, M.; Andrews, L.; Bauschlicher, C. W. Jr. *Chem. Rev*. **2001**, *101*, 1931

(37) Chatt, J.; Rowe, G. A.; Williams, A. A. *Proc. Chem. Soc*. **1957**, 208.

(38) Chatt, J.; Duncanson, L.A.; Guy, R. G. *J. Chem. Soc*. **1961**, 827.

(39) Cotton, F. A.; Wilkinson, G.; Murillo, C. A.; Bochmann, M. *Advanced Inorganic Chemistry*, 6th ed. John Wiley: New York, **1999**.

(40) a) Pillai, E. D.; Jaeger, T. D.; Duncan, M. A. *J. Phys. Chem. A.* **2005**, *109*, 3521. b) Pillai, E. D.; Jaeger, T. D.; Duncan. *J. Am. Chem. Soc.* **2007**. in press.

(41) Bauschlicher, C. W. Jr.; Langhoff, S. R. *Intl. Rev. Phys. Chem*. **1990**, *9*, 149.

(42) Bauschlicher, C. W. Jr.; Langhoff, S. R.; Partridge, H. *Adv. Ser. Phys. Chem*. **1995**, *2*, 1280.

(43) Bushnell, J. E.; Kemper, P. R.; Bowers, M. T. *J. Phys. Chem.* **1993**, *97*, 11627.

(44) Huber, K. P.; Herzberg, G. *Molecular Spectra and Molecular Structure IV. Constants of Diatomic Molecules*, Van Nostrand Reinhold Co. **1979**.

CHAPTER 5

IR SPECTROSCOPY AND DENSITY FUNCTIONAL THEORY OF $Nb^+(N_2)_n$ COMPLEXES : EVIDENCE FOR A SPIN-STATE CHANGE

Infrared photodissociation spectroscopy is reported for $Nb^+(N_2)_n$ complexes in the size range n=3-16 in the N-N stretch region. As seen for $V^+(N_2)_n$, binding to a transition metal cation causes the IR forbidden N-N stretch of free N_2 to become active. The complexes fragment by the loss of intact N_2 molecules when excited in the N-N stretch region and monitoring the fragmentation yield as a function of laser wavelength produces an IR spectrum. The fragmentation mass spectra for $Nb^+(N_2)_{6-9}$ indicate that Nb^+ has a coordination of six ligands. The IR spectra for $Nb^+(N_2)_{4-7}$ contain bands red-shifted from the N-N stretch in free nitrogen consistent with the qualitative guidelines of inorganic chemistry. Using the predictions of density functional theory, structures and ground electronic states for each cluster size are proposed. The IR spectra indicates that at the cluster size of n=5, the Nb^+ undergoes a spin change due to ligand effects. The red shifts seen for $Nb^+(N_2)_n$ are greater than those for $V^+(N_2)_n$ for the corresponding complex sizes.

Introduction

Biological and catalytic systems contain numerous examples of molecular and atomic nitrogen interacting with a transition metal (TM).[1-8] The natural catalyst of nitrogen fixation is an enzyme that carries Fe, Mo, and V at its active sites.[1-5] Studies of gas phase metal clusters have greatly improved our understanding of the chemistry at these sites.[2,3] TM-nitrogen interactions are also important in the synthesis of ammonia.[6-8] The dissociation of N_2 by catalytic iron surfaces is the rate-determining step in ammonia production, although the mechanism has not yet been fully understood.[7,8] TM-nitrogen complexes are isoelectronic to TM-carbonyl complexes which are considered prototypical systems in coordination chemistry and inorganic and organometallic chemistry.[9-11] Hence there has been a longstanding theoretical and experimental interest in metal containing nitrogen compounds to draw comparisons between N_2 and CO as ligands.[12] In this paper, we investigate the bonding interactions between the Nb^+ and multiple N_2 ligands by probing the N-N vibrational stretch using infrared photodissociation spectroscopy (IRPD).

There has been substantial interest in first row TM-nitrogen interactions and these complexes have been studied by theoretical,[13-15] mass spectrometric,[16] and optical spectroscopic methods.[17-21] Initial theoretical efforts have focused on the Fe-N_2 complex due to its relevance in biochemistry and surface catalysis and probed its structures and bonding energetics.[13-15] Mass spectroscopic methods have been used to measure bond energies for various first row TM^+-nitrogen complexes[16] whereas electronic spectroscopy has probed their structures.[17-19] Second row TM-ligand chemistry is appealing because these metals are usually more reactive than their first-row counterparts and hence can trigger ligand activation and dissociation.[9,22-24] Consequently, the reactivity of second row transition metals towards various ligands has been

examined by theoretical methods[25] and gas phase kinetic measurements.[26,27] Motivated by this, a number of studies have been undertaken to investigate the reactivity of neutral and ionic Nb clusters with several ligands.[28-36] Armentrout and co-workers have studied the activation of small hydrocarbons by Nb^+.[28] Matrix isolation infrared spectroscopy has been applied to neutral $Nb(N_2)_n$ complexes in order to determine structures.[29,30] Electron-spin resonance spectroscopy coupled with matrix isolation has been applied to neutral $Nb(N_2)_6$ and $Nb(CO)_6$ complexes and structures were established.[21] Various groups have investigated the reactivity of size specific neutral and ionic Nb clusters towards small molecules such as N_2,[31-33] CO,[32] D_2,[33] NO and NO_2.[34] These studies show that the chemical reactivity of the Nb clusters is dependent on the cluster size and its overall charge. To supplement the experimental work on Nb clusters, theory has probed the underlying structures and bonding in these systems.[35,36] Ab initio and density functional theory (DFT) have investigated the geometries and electronic states of Nb_m clusters and their adducts with nitrogen.[35,36] In this work, investigate the structure and bonding patterns in $Nb^+(N_2)_{1-16}$ complexes with IRPD spectroscopy and DFT calculations.

Our recent report on the IRPD spectroscopy of $V^+(N_2)_n$ was the first study that probed the N-N stretch of an isolated $TM^+(N_2)$ complex and thereby confirmed its structure and ground electronic state.[37a] $Nb^+(N_2)_n$ is our second study of a $TM^+(N_2)_n$ system.[37b] Until recently such studies were not possible due to the unavailability of suitable laser sources. However, utilizing new optical parametric oscillator/amplifier (OPO/OPA) laser sources, we have been able to apply IRPD spectroscopy to $TM^+(N_2)_n$ and additional metal cation-ligand complexes such as $M^+(CO_2)_n$[38], $M^+(C_2H_2)$[39], $M^+(H_2O)$[40], and $M^+(C_6H_6)$[41]. These studies have confirmed the structure and other bonding parameters of these gas phase metal ion complexes. However, all these studies have involved either a main group metal or a first row transition metal and aided in

the discussion of relative trends in bonding across a period. This paper represents our first attempt to apply IRPD spectroscopy to a second row TM^+-ligand complex, namely $Nb^+(N_2)$, and thereby observe periodicity down a group. Unlike ligands such as C_2H_2 and H_2O, N_2 does not have an IR active mode in the gas phase. However, as evidenced by our work with $V^+(N_2)_n$, nitrogen binding to a TM^+ does "switch-on" the IR activity of the N-N stretch (due to the reduced symmetry of the TM^+-N_2 complex) and its intensity is easily detectable by IRPD.

Experimental

A detailed description of the experimental apparatus has been published elsewhere.[42] Briefly, the $Nb^+(N_2)_n$ complexes are produced in a pulsed nozzle cluster source by ablating a ½" Nb rod with the third harmonic of a Nd:YAG laser. A General Valve (Series 9) operating with a backing pressure of 70-80 psi and pulse durations of 260-280 μs is employed to generate pure nitrogen expansions that lead to cluster growth. The expansion is skimmed into a differentially pumped reflectron time-of-flight mass spectrometer where positively charged acceleration plates inject the cationic complexes into the first drift tube. The parent ions of interest are then size selected with a pulsed deflection plate known as a "mass gate". The size selected ions enter the reflectron region where a series of voltage plates apply a voltage gradient causing them to decelerate, turn and then accelerate into the second drift tube. At the "turning point" the ions are excited with tunable IR light acquired through a Nd:YAG pumped optical parametric oscillator/amplifier (OPO/OPA, LaserVision) to induce dissociation. The parent and fragment ions accelerate into the second drift region where an electron multiplier tube in conjunction with a LeCroy WaveRunner LT-342 digital oscilloscope detects them. The signal is transferred to a

PC via an IEEE-488 interface. Monitoring the fragment yield as a function of the IR OPO/OPA wavelength generates an IR spectrum of the parent ion.

Density functional theory (DFT) was used to study the small $Nb^+(N_2)$ complexes. Structures and energetics for the $Nb^+(N_2)_{1-6}$ complexes were calculated using the B3LYP functional available on the Gaussian O3W package.[43] The DGDZVP basis set was employed for Nb^+ while the 6-311+G* basis set was used to describe nitrogen. All calculations allowed for symmetry breaking and for each initial geometry, multiple spin states were considered. The calculated frequencies were scaled by 0.96 which is the recommended scaling factor for the 6-311+G* basis set.[44,45]

Results and Discussion

The mass spectrum of $Nb^+(N_2)_n$ is shown in Figure 5.1 and is similar to the spectrum presented for $V^+(N_2)_n$ in our previous work.[37a] $Nb^+(N_2)_n$ up to n=15 are produced by laser vaporization of a niobium rod in a pure nitrogen expansion. The mass spectrum shows that these complexes are produced by the addition of intact N_2 molecules around Nb^+ with no evidence for ligand fragmentation. The mass spectrum also shows evidence for complexes of the form $Nb^+(N_2)_n(H_2O)_m$ that are produced from water that is added to the cluster to enhance cluster growth. As each N_2 occupies a binding site around the metal cation, additional N_2 molecules will begin to attach to these "core" ligands. To explore the vibrational spectroscopy of these complexes as a function of size, we excite the N-N stretch of free N_2 near 2330 cm^{-1} and measure resonance enhanced photodissociation.[52]

IR excitation near the N-N stretch of free N_2 in $Nb^+(N_2)_n$ for n=1-3 produced little or no dissociation. Although these cluster sizes are produced in high abundance, their

Figure 5.1 The mass spectrum of $Nb^+(N_2)_n$ complexes generated in our experiment.

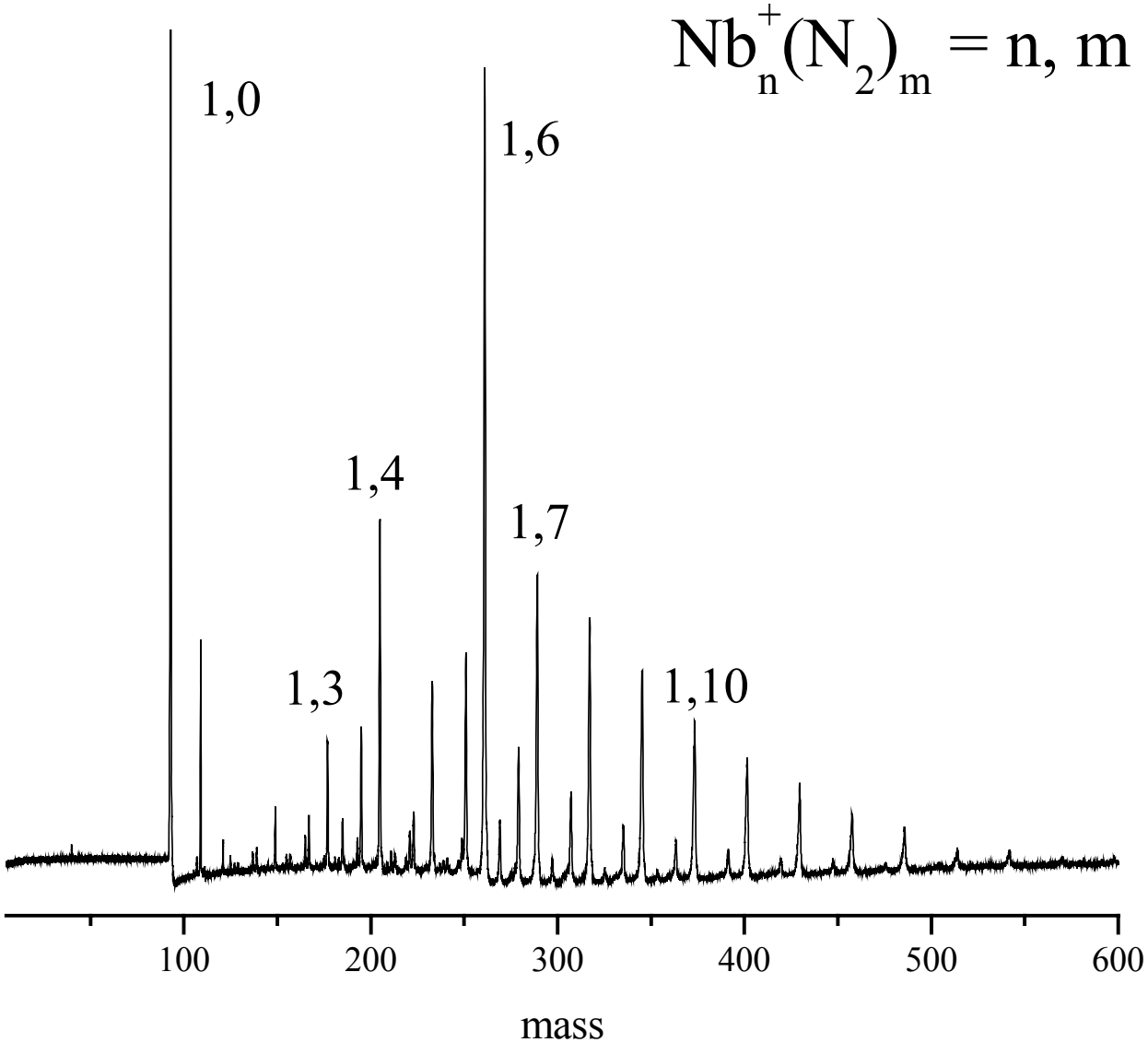
$Nb_n^+(N_2)_m$ = n, m
1,0
1,6
1,4
1,7
1,3
1,10
100
200
300
400
500
600
mass

photofragmentation yields are quite low. Starting with the n=4 and up to the larger complexes, the fragmentation yield does increase enabling us to measure an IR photodissociation spectrum in the 2100-2200 cm^{-1} region. We have observed a similar trend in other TM-ligand systems where no dissociation is observed for the small complexes.[37-41] The small complexes are difficult to dissociate because the IR photons do not possess sufficient energy to break the weakest bond in the complex, i.e. the TM^+-ligand bond. As the cluster size increases, the bonding capacity of the TM cation is distributed to the additional ligands thereby reducing the per-bond dissociation energy. Eventually, the IR photons are sufficiently energetic to dissociate the TM^+-ligand complex. Binding energies for the $Nb^+(N_2)_n$ complexes are not available and so we employed DFT to calculate them. The essential results of the calculations are presented in Table 5.1 while a full description of the results is given in the Appendix B. Although the B3LYP method tends to misjudge dissociation energies, the errors are usually within 6 kcal/mol of the corresponding experimental and CCSD(T) values.[46] The B3LYP results show that the dissociation energy for the small $Nb^+(N_2)$ complexes is over 17 kcal/mol (~6000 cm^{-1}). Excitation near the free N_2 stretch (2330 cm^{-1}) would not fragment these complexes unless a multiphoton process occurs and such processes are inefficient given our OPO pulse energies. Therefore, the observed low photodissociation yields for the small complexes is consistent with the predicted energetics of this system.

Figure 5.2 shows the fragmentation mass spectra for the n=6-9 complexes acquired by tuning the IR OPO to a wavelength of 2215 cm^{-1}. These spectra are obtained by first mass selecting the parent ion of interest and recording a mass spectrum with the IR laser off. The IR laser is then turned on and a second mass spectrum is recorded. Subtracting the first spectrum from the second results in the fragmentation spectrum for the size selected ion where the

Table 5.1 The results of theory for the quintet and triplet electronic states of $Nb^+(N_2)_n$ complexes. Relative energies, binding energies [relative to separated Nb^+ (^5D and ^3P respectively) and nN_2], dissociation energies (D_e) for the process $Nb^+(N_2)_n \rightarrow Nb^+(N_2)_{n-1}$, predicted frequencies and IR oscillator strengths for the calculated structures shown in Figure 5.5 (using B3LYP/6-311+G*). Frequencies were scaled 0.96. All energies are in kcal/mol.

n	Structure	Rel. Energy	B.E.	D_e	IR Freq. (cm^{-1}) (Osc. Str., km/mol)
1	L($^5\Sigma$) ($\sigma\pi^2\sigma$)	0.0	17.0	17.0	2265(58)
	T($^5B_1$) ($a_1b_2a_2a_1$)	+14.1	2.9	2.9	2212(95)
	L($^3\Sigma$) ($\sigma^2\pi^2$)	+43.7	3.4	3.4	2191(164)
	T($^3A_2$) ($a_2b_2^2a_2$)	+22.7	24.3	24.3	1795(169)
2	L($^5\Sigma_g$) ($\pi_g^2\delta_g^2$)	0.0	42.4	25.4	2244(383)
	M($^5A_1$) ($b_2b_1a_2a_1$)	+13.7	28.7	25.8, 11.7[a]	2216(221), 2247(101)
	T(^5A_g) ($b_{3g}b_{2g}b_{1g}a_g$)	+28.8	13.6	10.7	2221(252)
	L($^3\Sigma_g$) ($\sigma_g^2\pi_g^2$)	+18.0	54.4	51.1	2188(732)
	M($^3B_1$) ($a_1b_1b_2^2$)	+28.1	44.5	20.2, 41.2[a]	2033(505), 2220(205)
	T($^3B_2$) ($a_2^2b_2a_1$)	+36.7	35.7	11.3	1992(848), 2044(3)
3	L($^5A_1$) ($b_2a_2b_1a_1$)	0.0	61.1	18.7	2226(165), 2251(317)
	L($^3B_2$) ($b_1a_2b_2^2$)	+11.5	79.6	25.1	2171(310), 2197(661)
4	L($^5B_{2g}$) ($b_{2g}e_g^2a_{1g}$)	0.0	79.5	18.4	2251(336), 2251(336)
	L($^3A_{1g}$) ($e_g^2b_{2g}^2$)	+8.4	101.1	21.5	2209(605), 2209(605)

5	L($^5B_1$) ($b_1e^2a_1$)	+10.8	81.7	2.2	2235(400), 2235(400) 2257(15), 2321(4)
	L(^3A) (a^2aa)	0.0	122.5	21.4	2203(158), 2208(609) 2210(148), 2217(536)
6	L(^3B_g) ($a_g{}^2b_ga_g$)	0.0	140.8	18.5	2225(472), 2225(459) 2227(539)

[a]for removal of the T-configured ligand.

Figure 5.2 The mass fragmentation spectra for $Nb^{+}(N_2)_{6-9}$ complexes. The complexes fragment by the loss of intact N_2 molecules and the larger complexes terminate at n=6.

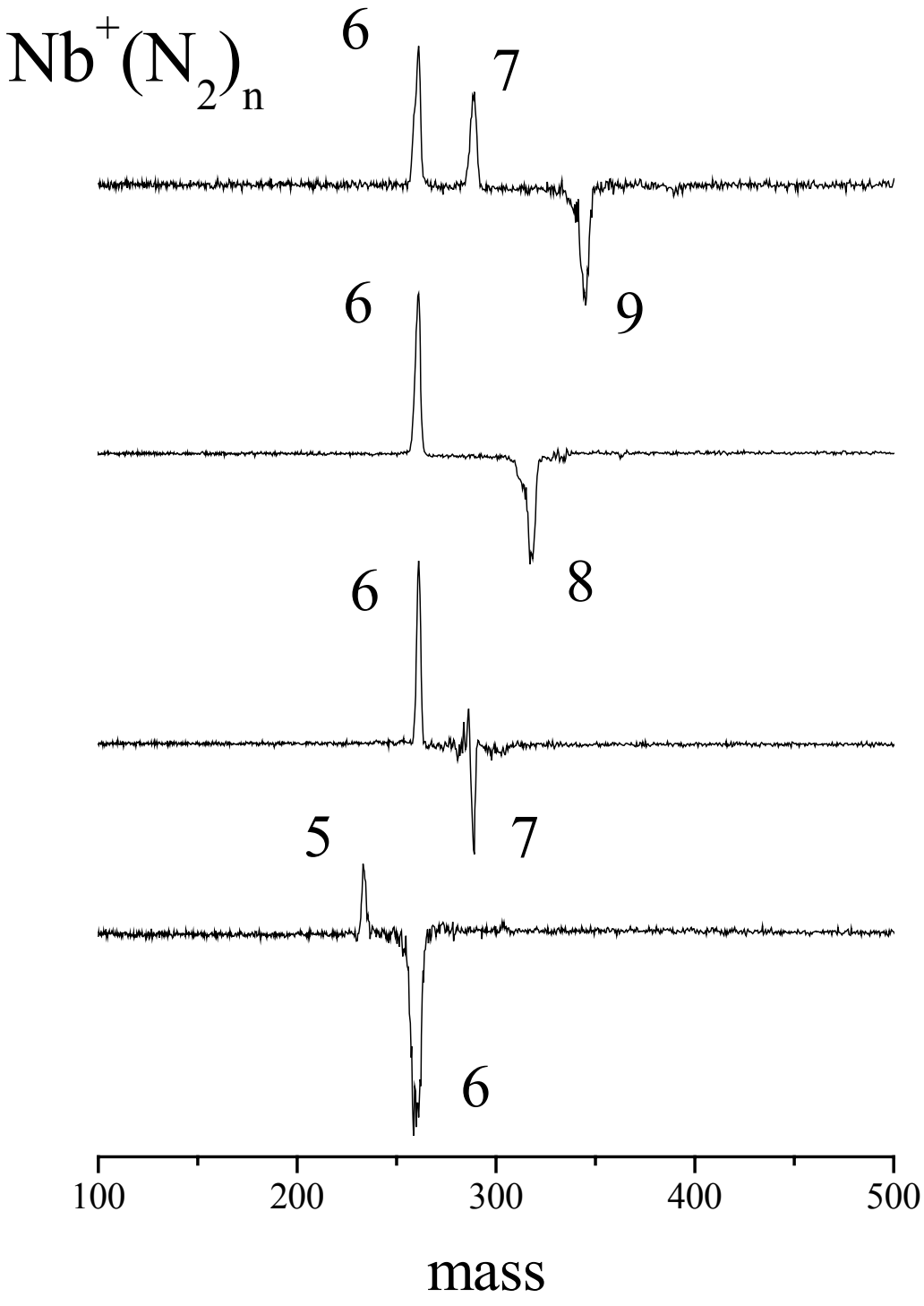
Nb+(N2)n
6
7
6
9
6
8
5
7
6
100
200
300
400
500
mass

negative peaks correspond to the parent ion and the positive peaks to the photofragments. The fragmentation spectra show that photodissociation results in the elimination of intact N_2 molecules. The absence of any nitride fragments in the spectra indicates that the N-N bond does not dissociate despite the metal bonding and photochemistry. In data not shown, the complexes smaller than n=6 all fragment by the loss of a single N_2 molecule. Likewise the n=6 complex also dissociates by losing one N_2 molecule. Beginning with the n=7 complex and extending out to n=9 (and beyond) the complexes eliminate single or multiple N_2 molecules to terminate at the cluster size of n=6. Such a common termination point for other TM^+-ligand complexes has been observed previously and indicates the preferred coordination number of the TM cation.[37-41] Ligands attached directly to the TM cation that form the "core" are strongly bonded as compared to the external ones and survive the photodissociation process. In the case of Nb^+ the fragmentation spectra indicates a coordination of six nitrogen molecules, which is the cation's favored coordination in the condensed phase as well.[9]

The IR photodissociation spectra for $Nb^+(N_2)_n$ n=3-7 are shown in Figure 5.3. The spectra are acquired by monitoring the dissociation yield of the parent ion as a function of the IR wavelength. If the parent ion has multiple fragments, each fragment channel is monitored to see if the spectra are different. In this case, all channels for a particular parent signal produced similar spectra differing only in the signal/noise (S/N) ratio. The spectra presented in Figure 5.3 for each cluster size is therefore the one that carries the highest S/N ratio. The dashed line in Figure 5.3 indicates the frequency of free N_2 at 2330 cm^{-1}. As discussed above, the complexes for n=1-3 have low fragmentation yields producing a IR spectrum with low S/N ratio. The n=3 complex has a barely discernable resonance around 2250 cm^{-1}. The spectra for n=4-7 complexes have a single feature between 2200-2300 cm^{-1} which corresponds to a red shift of ~70-120 cm^{-1}

Figure 5.3 The IRPD spectra for $Nb^+(N_2)_n$ n=3-7 acquired by monitoring the loss of N_2 as a function of OPO wavelength. The dashed vertical line indicates the frequency of the N-N stretch in free N_2.

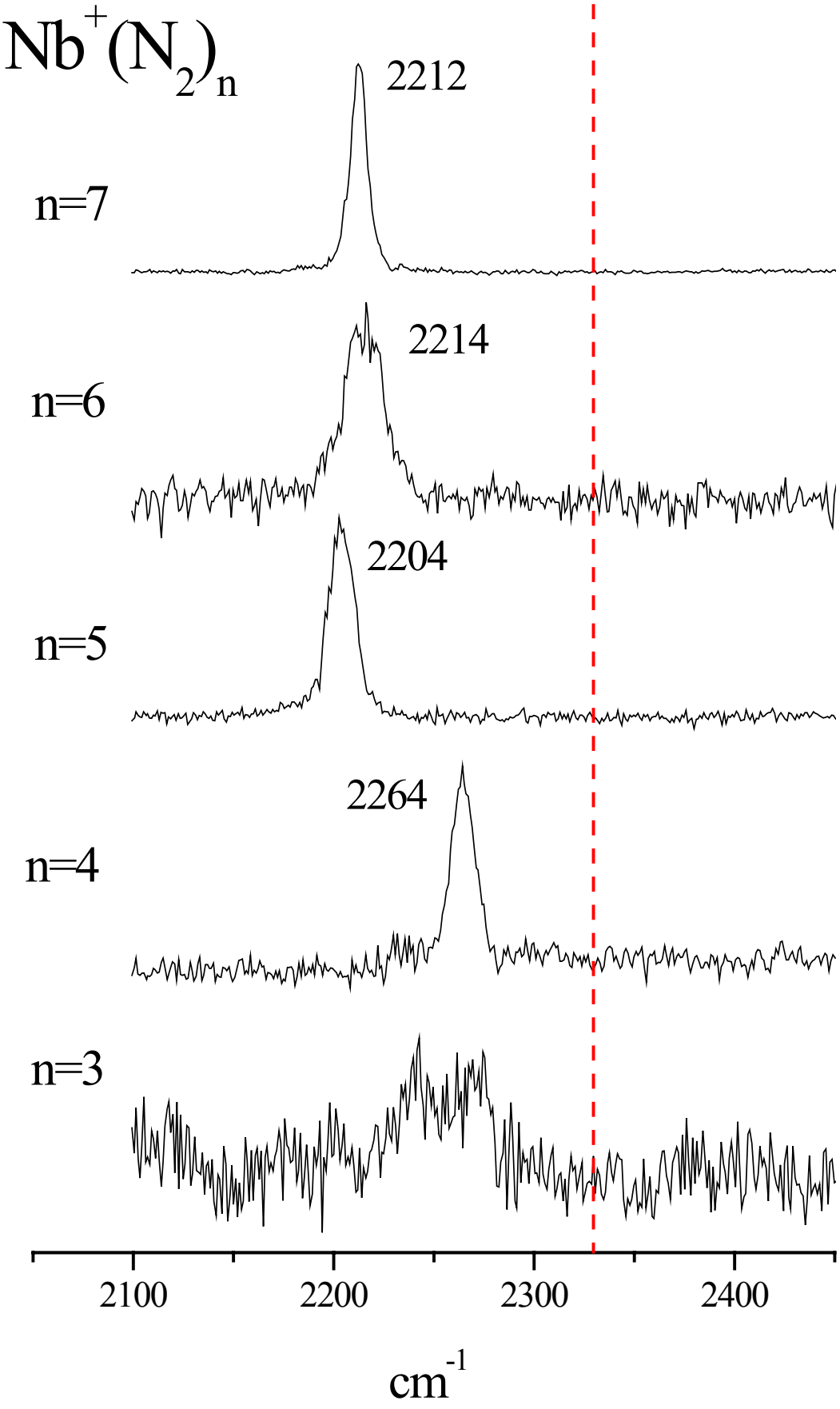
Nb+(N2)n
2212
n=7
2214
n=6
2204
n=5
2264
n=4
n=3
2100
2200
2300
2400
cm-1

from free N_2. The larger complexes up to n=16 essentially have identical spectra with resonances red-shifted by approximately ~70-120 cm^{-1}. As seen previously, binding to a TM cation does activate the IR forbidden stretch of free nitrogen.[37] The significant red-shifts seen for all the complexes agree qualitatively with the predictions of the Dewar-Chatt-Duncanson (DCD) model.[47,48] The model considers the TM-ligand bond as a synergistic mix of σ-type donation of electron density from the ligands into the TM d-orbitals and π-type back-donation from the TM orbitals into the antibonding orbitals of the ligand. Such a bonding mechanism weakens the bonding in nitrogen, lowering its vibrational frequency.[22]

The $Nb^+(N_2)_n$ for n=1-3 have such low dissociation yields that their photodissociation spectra barely show a resonance. Beginning with $Nb^+(N_2)_4$, the dissociation yields are higher and we obtain an IR spectrum that has a band at 2265 cm^{-1}. This is a red-shift of 65 cm^{-1} with respect to the free N_2 vibration. The spectrum for the n=5 complex also has a single peak which is centered at 2204 cm^{-1}. This is a shift of 61 cm^{-1} to the red from the n=4 resonance and a 126 cm^{-1} shift from free nitrogen. The spectra for the n=6 and 7 complex also exhibit a single band, which is slightly *blue-shifted* from the peak in n=5 spectrum. $Nb^+(N_2)_6$ has a single feature at 2214 cm^{-1} which represents a *blue-shift* of 10 cm^{-1} from the $Nb^+(N_2)_5$ band, a red-shift of 51 cm^{-1} from the $Nb^+(N_2)_4$ band and a red-shift of 116 cm^{-1} from free N_2. The single peak for $Nb^+(N_2)_7$ falls at 2212 cm^{-1} which is a red-shift of only 2 cm^{-1} from the $Nb^+(N_2)_6$ band. In Table 5.2 we list all the band positions for all complexes from n=1-16. We have not shown the IRPD spectra for complexes larger than n=7 because they all have a single peak at essentially the same position as the n=7 complex with identical S/N ratio. It is interesting to note that the spectrum for $Nb^+(N_2)_6$ has a lower S/N ratio and a broader peak width as compared to the other complexes in the n=4-7 range. Based on our results from the fragmentation mass spectra and studies in the

Table 5.2 Vibrational band positions measured for the $Nb^+(N_2)_n$ complexes for n=1-16.

n	Frequency (cm^{-1})	n	Frequency
1	-	9	2212
2	-	10	2212
3	2240, 2270	11	2210, 2338
4	2264	12	2210, 2338
5	2204	13	2210
6	2214	14	2209
7	2212	15	2209, 2338
8	2212	16	2208

condensed phase, we have shown that Nb^+ prefers a coordination of six. If this is the case, the n=6 complex should be energetically favored compared to the n=5 and 7 complexes and therefore harder to dissociate. Consistent with this, the dissociation yields for $Nb^+(N_2)_6$ are lower than the other complexes in n=4-7 range, thereby producing a spectrum with low signal level and broader linewidth.

Based on the discussion above, there is strong evidence that beginning with the n=7 complex, the last N_2 molecule binds to a "core" N_2 ligand rather than to the metal ion. This interaction should have properties very similar to those of $(N_2)_2$ dimer. The nitrogen dimer has been investigated theoretically and spectroscopically.[49-51] It is T-shaped, bound by van der Waals forces with an IR frequency at 2329 and 2339 cm^{-1}. However, these modes are expected to be only weakly IR active since the van der Waals interaction causes only a minor perturbation of the N-N bond. Consistent with this, there is hardly any resonance near 2330 cm^{-1} that might result from the presence of an external N_2 for $Nb^+(N_2)_7$. However, our scans of the larger complexes (n=11, 12, 15) do detect such a resonance. Figure 5.4 shows the spectra of the n=11 and 12 complexes where a weak band corresponding to external N_2 at 2338 cm^{-1} is present.

DFT calculations were performed on the n=1-6 complexes to acquire additional insight into these spectra. Studies were only done for n=1-6 complexes because calculations for the larger complexes failed due to convergence difficulties. Figure 5.5 shows the optimized lowest energy structures for each cluster size while the predicted IR active frequencies, oscillator strengths, electronic states, binding energies and dissociation energy (D_e) for the addition of the last ligand are listed in Table 5.1. The ground state of Nb^+ is $(4d^4)\ ^5D$ and its first excited state associated with a spin change is $(4d^4)\ ^3P$, which lies about 16 kcal/mol higher in energy. However, the B3LYP functional exaggerates this atomic spacing, calculating it to be 30

Figure 5.4 The IRPD spectra for $Nb^+(N_2)_{11}$ and $Nb^+(N_2)_{12}$ showing the weak band at 2338 cm^{-1} due to external N_2 molecules bound to core N_2 ligands.

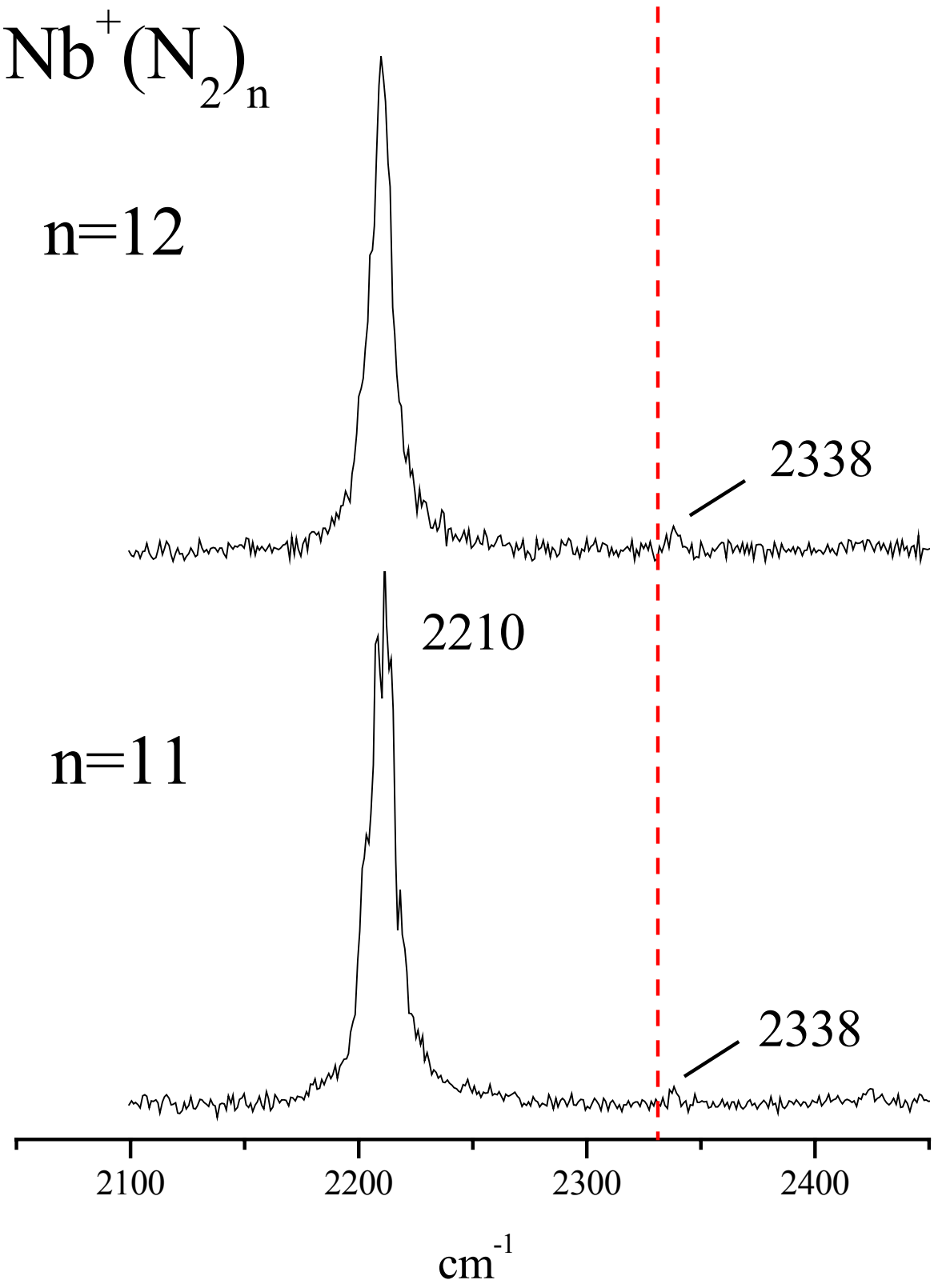
Nb+(N2)n
n=12
2338
2210
n=11
2338
2100
2200
2300
2400
cm-1

Figure 5.5 Lowest energy calculated structures for $Nb^{+}(N_2)_n$ n=1-5 using the B3LYP functional.

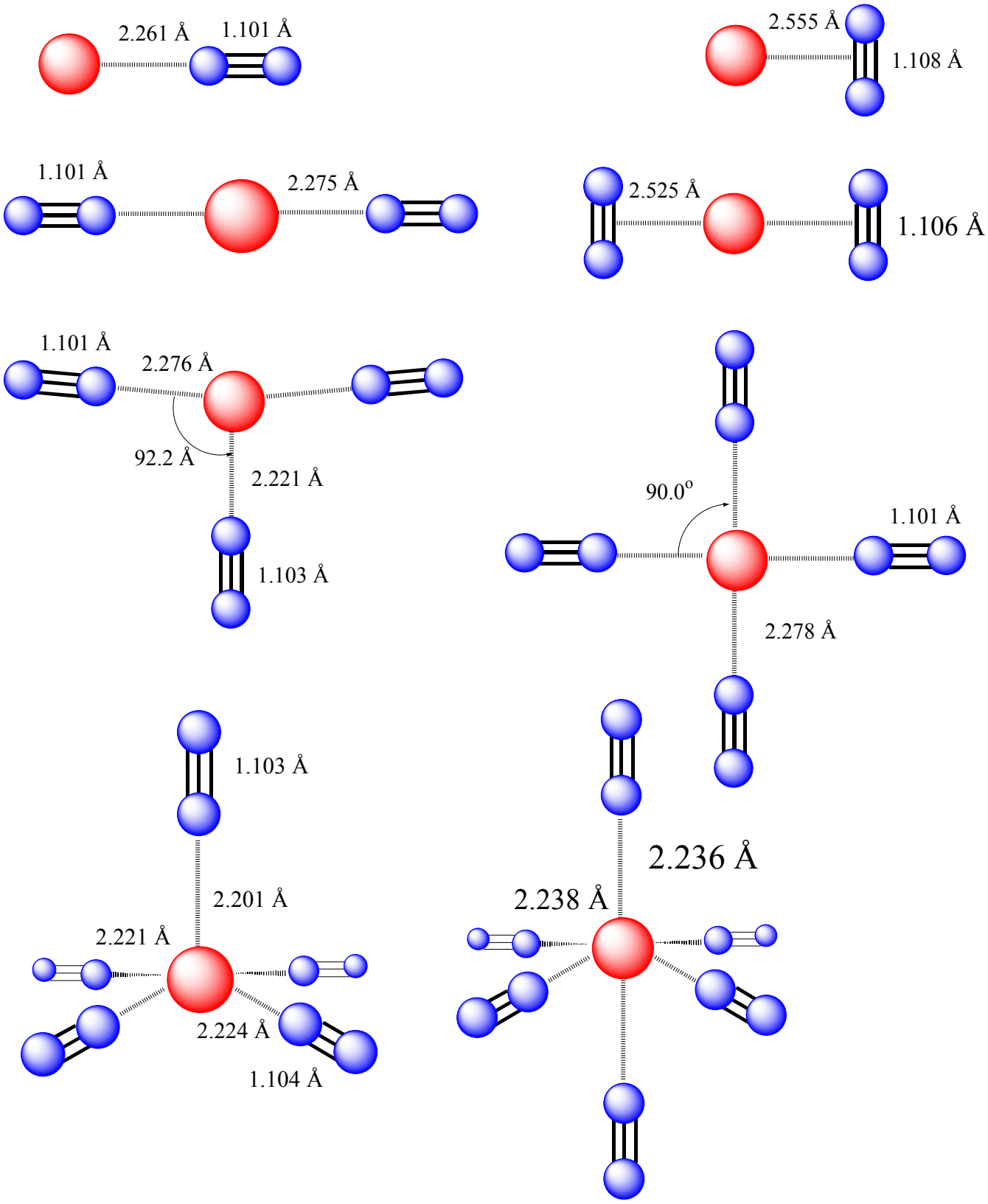
2.261 Å
1.101 Å
2.555 Å
1.108 Å
1.101 Å
2.275 Å
2.525 Å
1.106 Å
1.101 Å
2.276 Å
92.2 Å
2.221 Å
1.103 Å
90.0°
1.101 Å
2.278 Å
1.103 Å
2.201 Å
2.221 Å
2.224 Å
1.104 Å
2.236 Å
2.238 Å

kcal/mol. Nevertheless, this discrepancy is excepted to be reduced in the calculations of the molecular species because DFT is known to be problematic for isolated metal ions but performs well for ligated complexes.[46] It is well known that second row transition metals possess low lying excited states that may bind stronger to a ligand[22,25] and therefore in each complex and geometry we explored both the quintet and triplet states of Nb^+. The D_e's listed here are relative to the respective electronic state of the isolated metal ion. Figure 5.6 shows a schematic of the dissociation energetics of the complex relative to the ^5D metal asymptote (D_e'') and that relative to the ^3P metal asymptote (D_e'). Also indicated is the quintet to triplet energy difference which we define as Δ_{qt}.

Two minima exist for the n=1 complex for each spin state and correspond to "end-on" and "side-on" binding configurations of the N_2 molecule to Nb^+. The linear structure (L-complex, end-on binding) for the quintet state lies lowest in energy overall and is more strongly bound by 14 kcal/mol than the T-shaped (T-complex, side-on binding) quintet complex. For the triplet state, the T-shaped complex is more strongly bonded by about 20 kcal/mol than the corresponding linear complex. Regardless of the electronic state or N_2 binding configuration, DFT predicts a lower N-N vibration with respect to free N_2 for all the complexes in accordance with the DCD model. In the quintet state, the linear and T-shaped complexes are predicted to red-shift by 65 cm^{-1} and 118 cm^{-1} respectively. The triplet state predicted red-shifts are 139 cm^{-1} and 535 cm^{-1} for the linear and T-shaped complexes respectively. To determine the overall lowest energy structure irrespective of N_2 binding configuration or Nb^+ spin state we look to the Δ_{qt} values. Comparing the quintet and triplet linear complexes, we find a Δ_{qt} value of 43.7 kcal/mol with the quintet lower in energy. However, this is not a fair comparison. We compare the lowest energy quintet (linear) with the lowest energy triplet (T-shaped) and obtain a Δ_{qt} value

Figure 5.6 Schematic diagram showing the bonding energetics of Nb^+ in its ground state (^5D) versus its excited state (^3P). D_e'' is the binding in the quintet state and D_e' is the binding in the triplet state. Δ_{qt} is the energy difference between quintet complexes and triplet complexes.

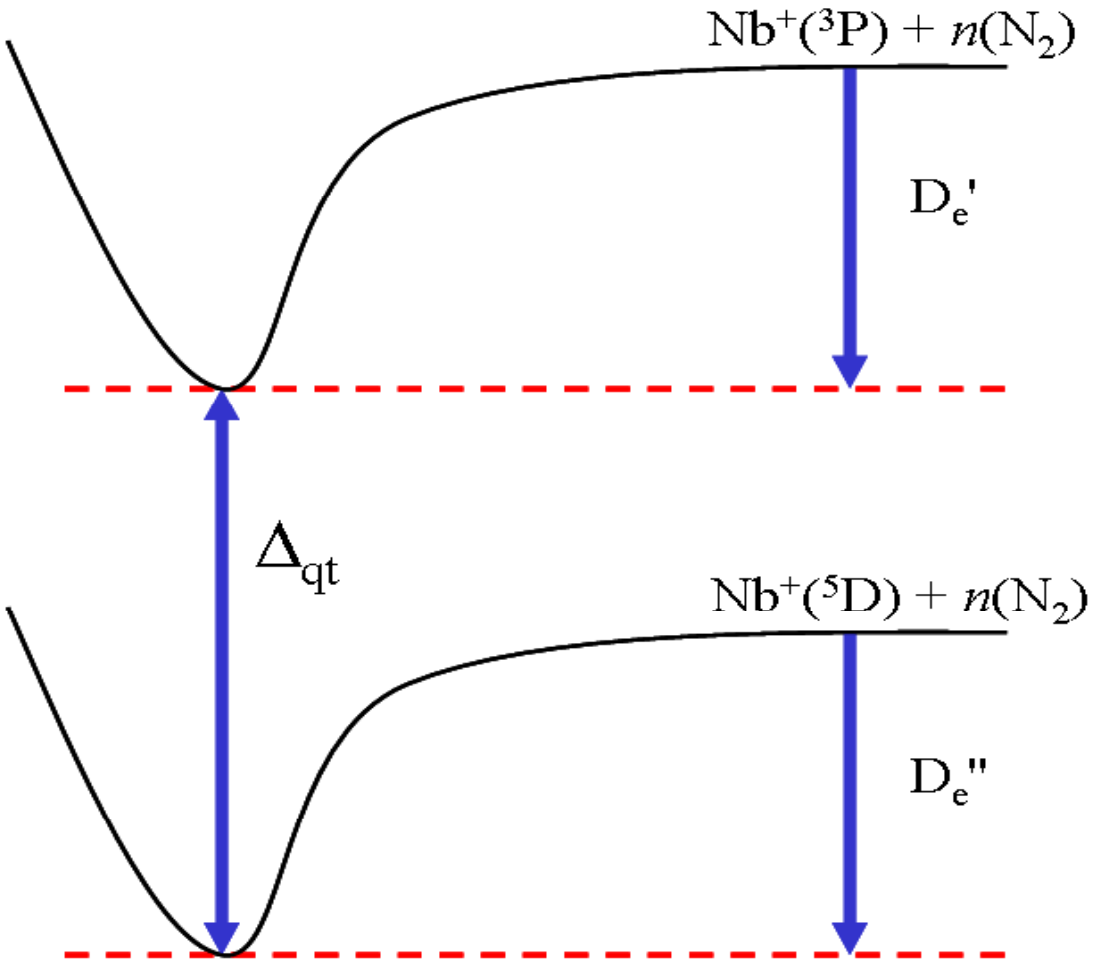
Nb+(3P) + n(N2)
De'
Δqt
Nb+(5D) + n(N2)
De''

of 22.7 kcal/mol favoring the quintet as the overall ground state. Two trends emerge from the predicted frequencies. For a given electronic state, the T-shaped complex results in a greater red-shift than the corresponding linear complex since the TM^+ binds directly to the N_2 π-bond, perturbing the N-N bond to a greater extent. Secondly, for a given N_2 binding configuration, the triplet state of Nb^+ red-shifts the N_2 frequency more than the quintet state. Previous studies on first and second row TM indicate that a TM-ligand bond formed via a low spin state (on the TM) usually possesses larger covalent character than one formed by a high spin asymptote.[22,25] As a result, the lower spin state causes a greater perturbation of the ligand, as clearly seen from our DFT results.

For the n=2 complex, a thorough search of the potential energy surface (PES) for each spin state was performed. Table 5.1 and Figure 5.5 only list the pertinent results but Appendix B contains an extensive list of all the results. For each spin state, minimum energy geometries were located for both N_2 binding end-on (2L-complex), one end-on and one side-on (L-T complex) and both side-on (2T-complex). For the quintet state, the 2L-complex has a higher binding energy than the L-T complex which has a higher binding energy than the 2T-complex. The 2L-complex has a calculated D_e of 25.4 kcal/mol with a frequency of 2244 cm^{-1}. The D_e for the 2T-complex is predicted to be 10.7 kcal/mol with an IR active mode at 2221 cm^{-1}. The L-T species has two D_e values and two vibrations and these values are near the corresponding values of the 2L and 2T complexes. A similar trend is observed for the n=2 complexes in the triplet state. The 2L-complex is more strongly bound than the L-T complex which in turn is more strongly bound than the 2T-complex. The 2L and 2T complexes have D_e's of 51.1 and 11.3 kcal/mol and frequencies of 2188 cm^{-1} and 1992 cm^{-1} respectively. The L-T complex again has two values for D_e and frequencies that correspond to the L and T complexes. However, here the

larger D_e(41.2) corresponds to the loss of the "side-on" N_2 since the T-shaped n=1 isomer is more strongly bound linear isomer in the triplet state. The frequency trends observed for the n=1 complex are repeated for the n=2 complexes where the T-shaped and triplet state species have the furthest red-shift. The lowest energy structure for the n=2 complex is the quintet 2L complex. The Δ_{qt} between this and the lowest triplet (which is also 2L) is 18.0 kcal/mol. For the n=1 complex, this value was 22.7 kcal/mol. Beginning here, we observe a trend where successive addition of N_2 ligands reduces Δ_{qt} because the triplet state possesses greater bonding capacity than the quintet state.

Beginning with n=3, the number of possible L-T isomers increases significantly but as shown for the n=2 species, such complexes would have at least two distinct IR frequencies easily resolvable by our experiment. However, in our spectra we observe only a single band for all the complexes, suggesting that all the N_2 molecules bind in equivalent orientations. Therefore, for complexes larger than n=2, we have not performed an exhaustive search of the PES. The quintet linear complexes are the most strongly bound for the n=1 and 2 complexes. For n=3 the lowest energy structure has all three N_2 molecules binding end-on to Nb^+ but distorted from a trigonal planar structure. The quintet state lies lower in energy than the triplet state with Δ_{qt} = 11.6 kcal/mol, a D_e of 18.7 kcal/mol and two IR frequencies of 2226 and 2251 cm^{-1}. The triplet state leads to further red-shifted frequencies at 2171 and 2197 cm^{-1}. Varying the rotational orientation of the axial nitrogen resulted in stationary points much higher in energy. No minimum exists for all three N_2 molecules in a "side-on" orientation for either spin state. The IRPD spectrum of the n=3 complex does have a broad unresolved band centered at 2250 cm^{-1} but due to the low S/N ratio it is difficult to make any comparisons between our theoretical conclusions and the experiment.

The spectrum of $Nb^+(N_2)_4$ with its single peak at 2265 cm^{-1} is indicative of a highly symmetric structure formed by equivalently binding N_2 molecules. The only structures that fit these criteria are square planar or tetrahedral and we explored them with DFT. The tetrahedral structure does not converge to a stationary point while the square planar structure shown in Figure 5.5 is found to be minimum for both spin states, with the quintet state lower in energy by about 9 kcal/mol. Though Δ_{qt} has decreased further for the n=4 complex, the quintet is still predicted to be lowest in energy. Figure 5.7 depicts the calculated spectra for both spins along with experimental spectra. The predicted IR spectrum in the 2000-2400 cm^{-1} has only a single peak centered at 2251 cm^{-1} which is only 14 cm^{-1} off from the experimental measured band. The corresponding triplet state structure is predicted have a band at 2209 cm^{-1}. We can therefore conclude that the spectroscopic data and theoretical predictions support the presence of end-on bonded N_2 molecules in a square planar arrangement about a quintet spin state Nb^+ for the n=4 complex. It is interesting to note that Nb^+ favors such symmetries in the condensed phase.[9]

The spectrum of $Nb^+(N_2)_5$ reveals a single band at 2204 cm^{-1} which represents a red-shift of about 61 cm^{-1} from the peak in the $Nb^+(N_2)_4$ spectrum and 126 cm^{-1} from the free N_2 stretch. Such an additional red-shift in the major band in going from n=4 to larger complexes was observed in our study of $V^+(N_2)_n$.[37a] In order to understand such an additional red-shift in the larger complexes we consider three possibilities. Firstly it is possible that an *intracluster* reaction has occurred, brought about by solvation effects and/or photochemistry. An intracluster reaction induced by solvation is an intriguing possibility and has been detected in our lab previously with $M^+(CO_2)_n$ (M= Ni, V, Si) complexes.[38] In $Nb^+(N_2)_n$, an intracluster reaction would lead to TM^+-nitride complexes, which seems unlikely for the following reasons. There is no evidence in the mass spectrum or fragmentation spectra for the formation of niobium-nitride or elimination of

Figure 5.7 Comparison of the IRPD spectrum for $Nb^+(N_2)_4$ to the theoretical spectra for quintet and triplet spin states.

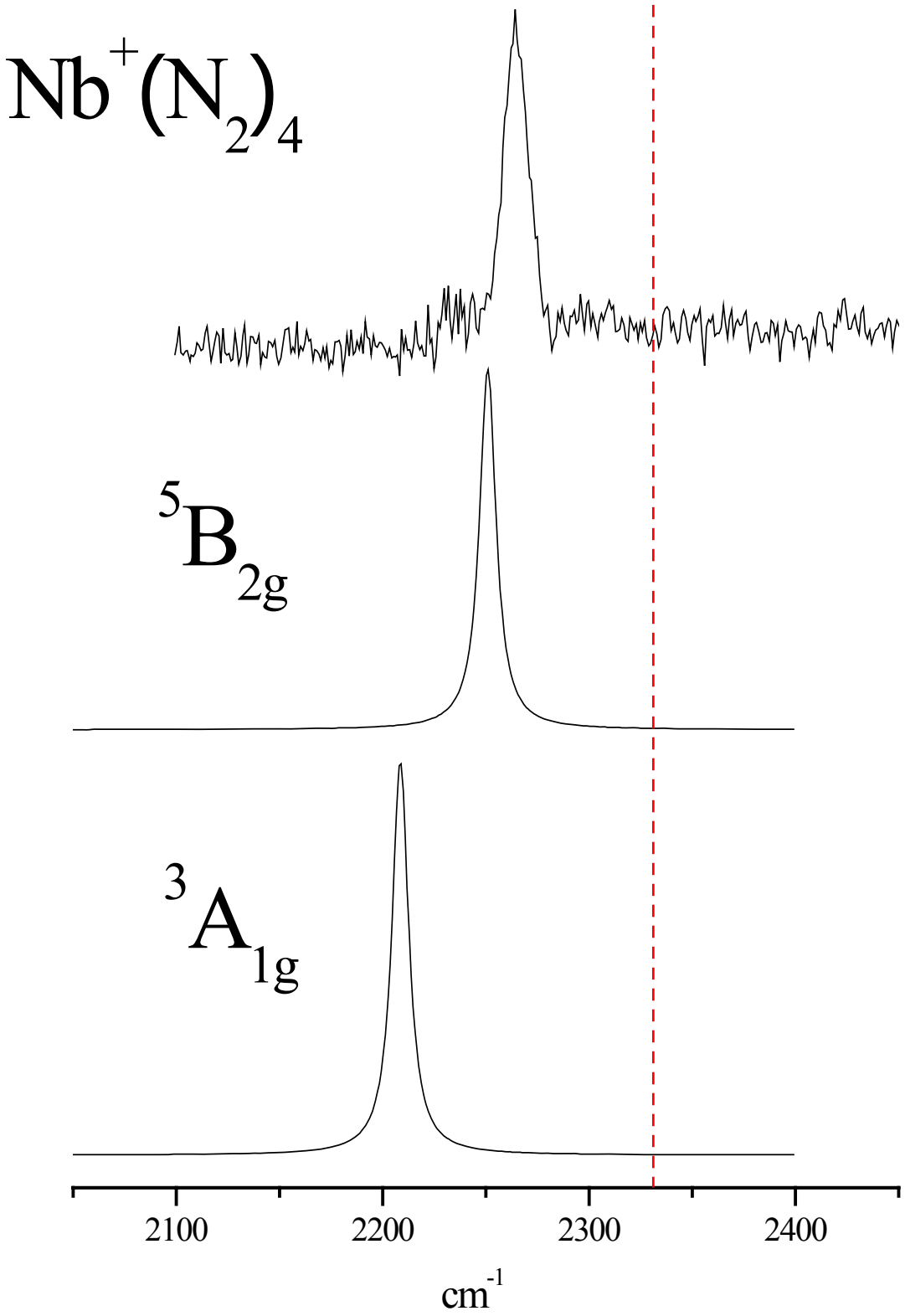
$Nb^+(N_2)_4$
$^5B_{2g}$
$^3A_{1g}$
2100
2200
2300
2400
cm^{-1}

niobium-nitride complexes. The activation energy required to break the N-N triple bond is extremely high and it is unlikely that metal solvation alone can provide this energy.[31-35] Also, in all previous instances when we observed an intracluster reaction, only a small subset of the complexes in our experiment underwent a reaction. Thus the spectra had multiple bands corresponding to the reacted and unreacted isomers. The single peak spectrum of $Nb^+(N_2)_5$ indicates the presence of only a single structure with high symmetry similar to n=4 complex. This eliminates the possibility of some N_2 binding in the side-on configuration to form combinations of L-T isomers. It is also unlikely that all the N_2 molecules bind side-on for the n=5 complex when it is clear that the n=4 complex has all end-on bonded nitrogens and also since DFT calculations consistently favor end-on over side-on binding.

The final alternative to consider is the possibility of a spin change on Nb^+ due to progressive ligand binding. The calculated structure for $Nb^+(N_2)_5$ with all end-on bound nitrogens is a near square pyramidal structure shown in Figure 5.5. In Figure 5.8, the DFT predicted spectra for both the triplet and quintet state are shown along with the experimental spectra. For the quintet state, the structure has C_{4v} symmetry with IR active frequencies at 2235, 2257, and 2321 cm^{-1}. However, the frequency at 2235 cm^{-1} is a doubly degenerate and about 50 times more intense than the other bands. As a result, the IR spectrum would only carry the single band. The triplet state complex too has a similar structure but its overall symmetry is C_1 and attempts to constrain it to C_{4v} failed. The predicted frequencies are 2203, 2208, 2210 and 2217 cm^{-1} but only the 2208 and 2217 cm^{-1} vibrations have sufficient oscillator strength and when plotted at our experimental linewidth, the IR spectrum is a single band centered at 2209 cm^{-1}. As shown in Figure 5.8, this is only 5 cm^{-1} off from the experimentally observed band. Also, addition of the fifth ligand has induced a change in the ordering of the states where now the

Figure 5.8 Comparison of the IRPD spectrum for $Nb^+(N_2)_5$ to the theoretical spectra for quintet and triplet spin states.

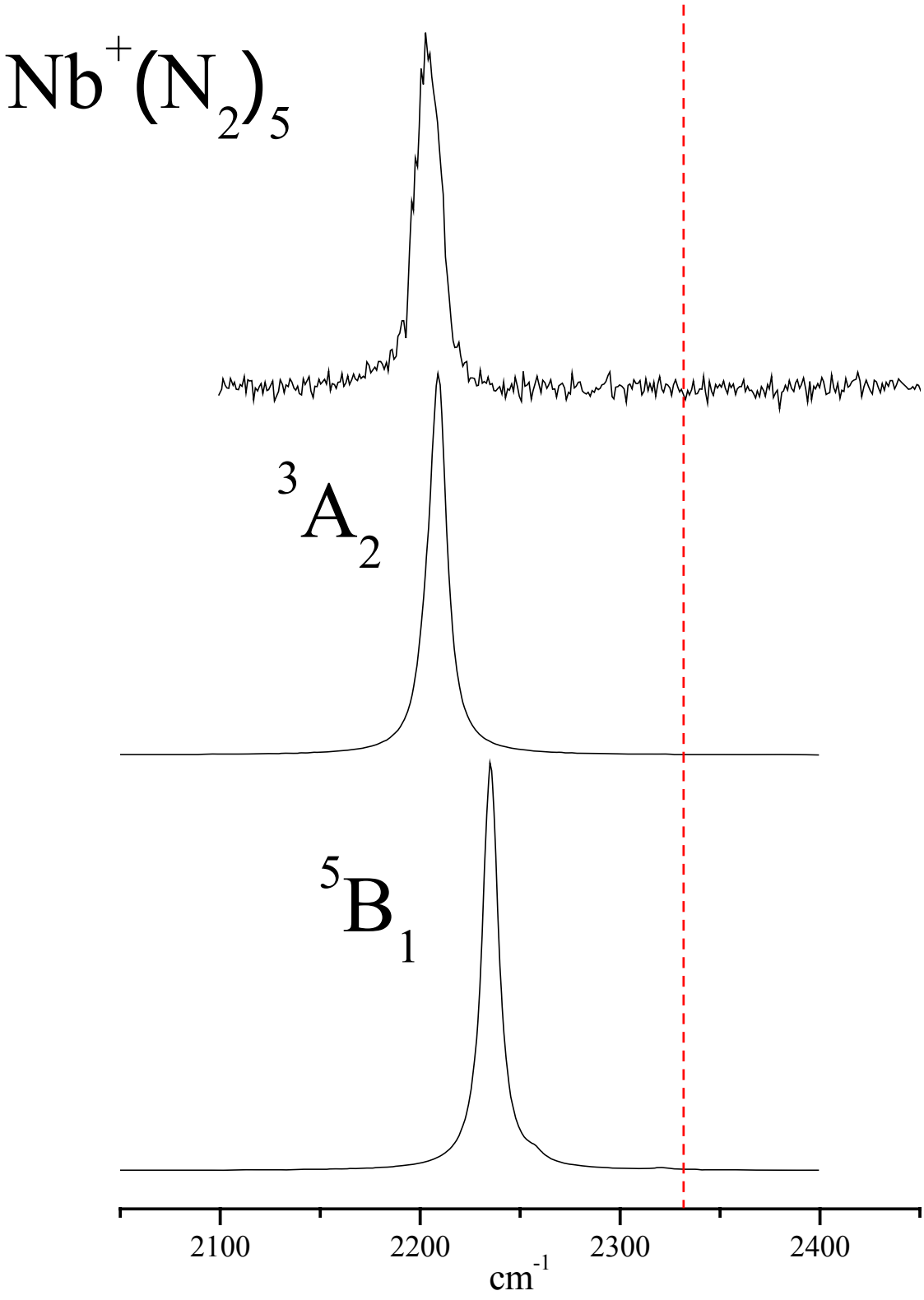
Nb+(N2)5
3A2
5B1
2100
2200
2300
2400
cm-1

triplet has a lower binding energy (i.e. Δ_{qt} = -10.7 kcal/mol) than the corresponding quintet state. Although DFT is known to misjudge the absolute energy values between electronic states, it often predicts the right trends.[46] This fact coupled with the excellent correlation between the theoretical and experimental frequencies leads us to conclude that the additional red-shift seen for the n=5 and larger complexes is due to a spin change induced in the Nb^+. A spin state change of the metal ion induced by progressive ligand binding has been suggested for many transition metals.[25] However, we believe this is the first *spectroscopic* evidence of such an effect in an isolated metal ion complex.

The peak in the spectrum for the n=6 complex falls at 2214 cm^{-1} which 10 cm^{-1} *blue* of the peak in the n=5 spectrum and 50 cm^{-1} red of the band in the n=4 spectrum. This most likely indicates that the Nb^+ spin state in $Nb^+(N_2)_6$ is a triplet. Consistent with this, theory finds a triplet state minimum with frequencies of 2225 and 2227 cm^{-1}. Plotted at our experimental linewidths, the spectrum appears as a single band centered at 2226 cm^{-1}, which is shown in Figure 5.9. The structure is near-octahedral and is shown in Figure 5.5. No minimum energy structure is present in the quintet electronic state indicating that successive ligand binding has induced a complete reversal of the energetics between the two spin states. The blue shift with respect to the n=5 band is possibly due to the metal ion charge being distributed to six ligands (rather than five) and therefore the per-ligand perturbation decreases causing the N-N stretch to shift back toward the value of free N_2. Given that the n=4 and 5 complexes are square planar and square pyramidal, it is reasonable to assume the n=6 has octahedral symmetry. ESR spectra of neutral $Nb(N_2)_6$ provided evidence for a reduced symmetry D_{4h} complex due to Jahn-Teller distortion.[21] It is certainly possible that our cations have similar structures to their neutral

Figure 5.9 Comparison of the IRPD spectrum for $Nb^+(N_2)_6$ to the theoretical spectra for triplet state. No minimum was found for the quintet state.

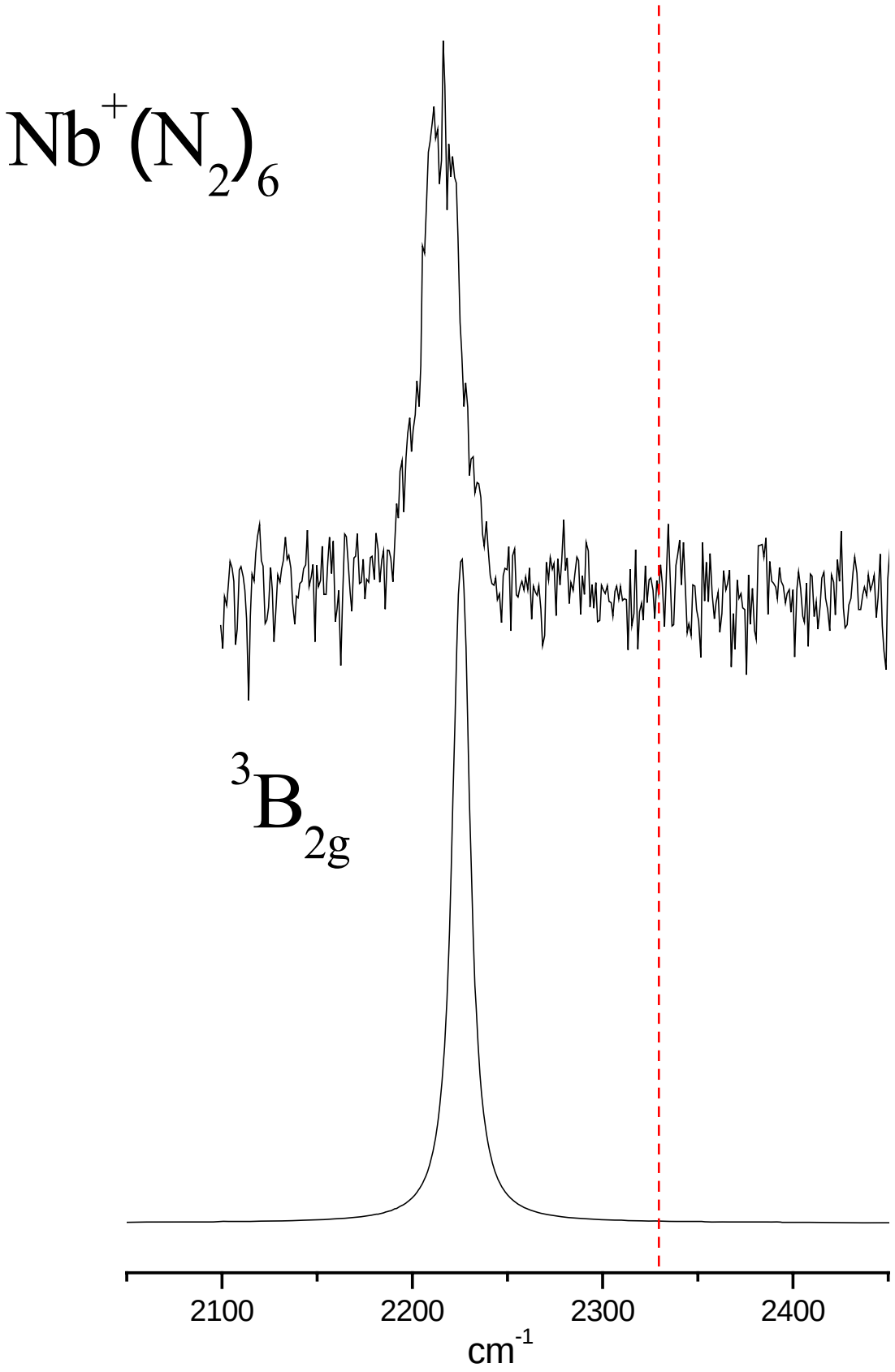
$Nb^+(N_2)_6$
$^3B_{2g}$
2100
2200
2300
2400
cm^{-1}

counterparts. It is interesting to note that niobium forms such geometries in the condensed phase with other ligands such NH_3 and oxides as well.[9]

The spectrum of $Nb^+(N_2)_7$ is basically the same as the n=6 complex except that is has a much higher S/N. As discussed above, our spectra indicate Nb^+ has a coordination of six N_2 ligands with additional N_2's binding to this central "core". The binding energy for the external ligands is significantly less than TM^+-N_2 bond energy and hence these additional ligands should fragment readily and cause very little perturbation of the n=6 spectrum. The n=7 with its near identical band position to the n=6 band but with a higher S/N ratio is consistent with this analysis.

As a final point, it is interesting to compare the relative red-shifts of $V^+(N_2)_n$[37] versus $Nb^+(N_2)_n$. For each corresponding cluster size, the red-shifts in the N-N stretch in $Nb^+(N_2)_n$ are greater than $V^+(N_2)_n$ by about 60-80 cm^{-1}. Since ligands such as N_2 and CO are π-acceptors, all theoretical studies agree that in the TM-N_2 bond, π-back donation from the TM is more important than ligand σ-donation.[22] The 4d-5s orbitals of the second row TMs are more diffuse than the 3d-4s orbitals of the first row TM and hence metals such as Nb can back-donate electron density more effectively than their first row counterparts.[22] As a result, Nb^+ can perturb the N_2 ligand to larger degree than V^+. This qualitative prediction of the DCD model certainly agrees well with the shifts in IRPD spectra of these $TM^+(N_2)_n$ complexes.

Conclusion

Niobium-nitrogen complexes of the form $Nb^+(N_2)_n$ n=3-16 have been studied using infrared photodissociation spectroscopy in the gas phase. The structure, energetics and vibrational frequencies of the n=1-6 complexes were investigated with density functional theory.

The photodissociation studies show that $Nb^+(N_2)_n$ complexes dissociate upon irradiation of IR light, losing intact nitrogen molecules. The fragmentation mass spectra terminate at the n=6 complex indicating a coordination number of six for Nb^+. The infrared spectra show strong resonances near 2200-2300 cm^{-1} region, corresponding to the N-N stretch in the complexes. The binding of N_2 to Nb^+ provides the ligand with infrared activity. The N-N vibrations are red-shifted with respect to free N_2 and are consistent with the predictions of Dewar-Chatt-Duncanson model of transition metal-ligand bonding. The experimental spectra are compared to DFT calculations and show that in all the complexes, N_2 binds in the end-on configuration. The n=4 complex is calculated to have a quintet electronic ground state and a square-planar structure with all end-on nitrogens. Its predicted and experimental spectrum match nicely. DFT also predicts end-on binding in the n=5 complex, with the nitrogens arranged in a near-square pyramidal geometry. The sequential addition of N_2 ligands eventually leads to spin state change of the metal ion and results in a large red-shift of the peak in the n=5 as compared to the n=4 spectrum. The n=6 spectrum has a single resonance near the n=5 band and is suggested to have a near-octahedral structure. The n=7-16 complexes all have a single band which lies essentially at the same position as that for the n=5 and 6 complex. The larger complexes contain N_2 molecules bound to the core n=6 complex. To our knowledge, this study represents the first spectroscopic evidence of a metal ion spin change induced by successive ligation.

References

(1) Seigbahn, P. E. M.; Blomberg, M. R. A. *Chem. Rev*. **2000**, *100*, 421.

(2) Burgess, B. K.; Lowe, D. K. *Chem. Rev*. **1996**, *96*, 2983.

(3) Rincon, L.; Ruette, F.; Hernandez, A. *J. Mol. Spectrosc*. **1992**, *254*, 395.

(4) a) Fryzuk, M. D. *Chem. Record*. **2003**, *3***,** 2. b) Fryzuk, M. D.; Kozak, C. M.; Patrick, B. O. *Inorg. Chim. Acta*. **2003**, *345*, 53.

(5) a) Chatt, J.; Melville, D. P.; Richards, R. L. *J. Chem. Soc (A)*. **1969**, *18*, 2841. b) Chatt, J.; Dilworth, J. R.; Richards, R. L. *Chem. Rev*. **1978**, 78, 589. c) Richards, R. L. *Coord. Chem. Rev*. **1996**, *153*, 83.

(6) Somorjai, G.A. *Introduction to Surface Chemistry and Catalysis*, John Wiley & Sons, **1994**.

(7) Rao, C. N. R.; Rao, G. R. *Surf. Sci. Rep.* **1991**, 13, 221.

(8) Arabczyk, W.; Jasinska, I.; Lubkowski, K. React. *Kinet. Catal. Lett*. **2004**, *83*, 385.

(9) Cotton, F. A.; Wilkinson, G.; Murillo, C. A.; Bochmann, M. *Advanced Inorganic Chemistry*, 6th ed. John Wiley, New York, **1999**.

(10) Zhou, M.; Andrews, L.; Bauschlicher, C. W. Jr. *Chem. Rev*. **2001**, 101, 1931.

(11) Ervin, K. M. *Int. Rev. Phys. Chem*. **2001**, *20*, 127.

(12) a) Chatt, J. *Pure and App. Chem*. **1970**, *24*, 425. b) Chatt, J. *J. Organomet. Chem*. **1975**, *100*, 17. c) Chatt, J.; Richards, R. L. *J. Organomet. Chem*. **1982**, *239*, 65.

(13) Bauschlicher, C. W., Jr.; Petterson, L. M.; Siegbahn, P. E. M. *J. Chem. Phys*. **1987**, 87, 2129.

(14) Zacarias, A.; Torrens, H.; Castro, M.; *Intl. J. Quant. Chem.* **1997**, 61, 467.

(15) Duarte, A. D.; Salahub, D. R.; Haslett, T.; Moskovits, M. *Inorganic Chemistry*. **1999**, 38, 3895.

(16) a) Khan, F. A.; Steele, D. L.; Armentrout, P. B. *J. Phys. Chem*. **1995**, 99,7819. b) Tjelta, B. L.; Armentrout, P. B. *J. Phys. Chem*. **1997**, 101, 2064. c) Tjelta, B. L.; Walter, D.; Armentrout, P. B. *Intl. J. Mass. Spec.* **2001**, 204, 7.

(17) Lever, A. B. P.; Ozin, G. A. *Inorg. Chem.* **1997**, *16*, 2012.

(18) Asher, R. L.; Buthelezi, B.; Brucat, P. J. *J. Phys. Chem*. **1995**, *99*, 1068.

(19) Heinemann, C.; Schwarz, J.; Schwarz, H. *J. Phys. Chem*. **1996**, *100*, 6088.

(20) Andrews, L.; Bare, W. D.; Chertihin, G. V. *J. Phys. Chem. A*. **1997**, *101*, 8417.

(21) Parrish, S. H.; Van Zee, R. J.; Weltner, W., Jr. *J. Phys. Chem. A.* **1999**, *103*, 1025.

(22) Frenking, G.; Frohlich, N. *Chem. Rev*. **2000**, *100*, 717.

(23) Siegbahn, P. E. M.; Blomberg, M. R. A. *Ann. Rev. Phys. Chem*. **1999**, *50*, 221.

(24) Armentrout, P. B. *Intl. J. Mass. Spect*. **2003**, *227*, 289.

(25) a) Langhoff, S. R.; Petterson, L. G. M.; Bauschlicher, C. W. Jr.; Partridge, H. *J. Chem. Phys*. **1987**, *86(1)*, 268. b) Bauschlicher, C. W., Jr.; Langhoff, S. R.; Partridge, H.; Barnes, L. A. *J. Chem. Phys*. **1989**, *91(4)*, 2399. c) Barnes, L. A.; Rosi, M.; Bauschlicher, C. W., Jr. *J. Chem. Phys*. **1990**, *93(1)*, 609. d) Sodupe, M.; Bauschlicher, C. W., Jr. *J. Phys. Chem*. **1991**, *95*, 8640. e) Bauschlicher, C. W., Jr.; Partridge, H.; Sheehy, J. A.; Langhoff, S. R.; Rosi, M. *J. Phys. Chem*. **1992**, *96*, 6969.

(26) a) Carroll, J. J.; Haug, K. L.; Weisshaar, J. C. *J. Am. Chem. Soc*. **1993**, *115*, 6962. b) Carroll, J. J.; Haug, K. L.; Weisshaar, J. C.; Blomberg, M. R. A.; Siegbahn, P. E. M.; Svensson, M. *J. Phys. Chem*. **1995**, *99*, 13955.

(27) a) Eller, K.; Schwarz, H. *Chem. Rev*. **1991**, *91*, 1121. b) Schwarz, H. *Intl. J. Mass. Spect*. **2004**, *237*, 75.

(28) Sievers, M. R.; Chen, Y. M.; Haynes, C. L.; Armentrout, P. B. *Intl. J. Mass. Spect*. **2000**, *195/196*, 149.

(29) Green, D. W.; Hodges, R. V.; Gruen, D. M. *Inorg. Chem*. **1976**, *15*, 970.

(30) Zhou, M.; Andrews. L. *J. Phys. Chem. A*. **1998**, *102*, 9061.

(31) a) Kim. Y. D.; Gantefor, G. *Chem. Phys. Lett*. **2003**, *382*, 644. b) Kim, Y. D.; Gantefor, G. *J. Mol. Struct*. **2004**, *692*, 139.

(32) Mwakapumba, J.; Ervin, K. M. *Intl. J. Mass. Spect. & Ion. Proc*. **1997**, *161*, 161.

(33) Berces, A.; Hackett, P. A.; Lian, L.; Mitchell, S. A.; Rayner, D. M. *J. Chem. Phys*. **1998**, *108*, 5476.

(34) Wu, Q.; Yang, S. *Intl. J. Mass. Spect*. **1999**, *184*, 57.

(35) Sellers, H. *J. Phys. Chem*. **1990**, *94*, 1338.

(36) Berces, A.; Mitchell, S. A.; Zgierski, M. Z. *J. Phys. Chem. A*. **1998**, *102*, 6340.

(37) a) Pillai, E. D.; Jaeger, T. D.; Duncan, M. A. *J. Phys. Chem. A*. **2005**, *109*, 3521. b) Pillai, E. D.; Jaeger, T. D.; Duncan, M. A. *J. Am. Chem. Soc*. **2007.** in press

(38) a) Gregoire, G.; Duncan, M. A. *J. Chem. Phys.* **2002**, *117*, 2120. b) Jaeger, J.; Jaeger, T.; Duncan, M. A. *Intl. J. Mass. Spect.* **2003**, *228*, 285. c) Walker, N. R.; Walters, R. S.; Grieves, G. A.; Duncan, M. A. *J. Chem. Phys*. **2004**, *121*, 10498. d) Walker, N. R.; Walters, R. S.; Duncan, M. A. *J. Chem. Phys*. **2004**, *120*, 10037.

(39) a) Walters, R. S.; Jaeger, T. D.; Duncan, M. A. *J. Phys. Chem. A*. **2002**, *106*, 10482. b) Walters, R. S.; Schleyer, P. v. R, Duncan, M. A. *J. Am. Chem. Soc*. **2005**, *127*, 1100. c)

Walters, R. S.; Pillai, E. D.; Schleyer, P. v. R, Duncan, M. A. *J. Am. Chem. Soc*. **2005**, *127*, 17030.

(40) a) Walker, N. R.; Walters, E. D.; Pillai, E. D.; Duncan, M. A. *J. Chem. Phys.* **2003**, *119*, 10471. b) Walters, R. S.; Duncan, M. A. *Austr. J. Chem*. **2004**, *57*, 1145. c) Walker, N. R.; Walters, R. S.; Jordan, K. D.; Duncan, M. A. *J. Phys. Chem. A*. **2005**, *109*, 7057.

(41) a) Jaeger, T. D.; Pillai, E. D.; Duncan, M. A. *J. Phys. Chem. A*. **2004**, *108*, 6605. b) Jaeger, T. D.; Duncan, M. A. *J. Phys. Chem. A*. **2005**, *109*, 7057.

(42) a) Duncan, M. A.; *Annu. Rev. Phys. Chem*.**1997**, *48*, 69. b) Duncan, M. A. *Intl. Rev. Phys. Chem.* **2003**, *22*, 407.

(43) Frisch, M. J.; Trucks, G. W.; . Schlegel, H. B.; Scuseria, G. E.; Robb, M. A.; Cheeseman, J. R.; Montgomery, J. A., Jr.; Vreven, T.; Kudin, K. N.; Burant, J. C.; Millam, J. M.; Iyengar, S. S.; Tomasi, J.; Barone, V.; Mennucci, B.; Cossi, M.; Scalmani, G.; Rega, N.; Petersson, G. A.; Nakatsuji, H.' Hada, M.; Ehara, M.; Toyata, K.; Fukuda, R.; Hasegawa, J.; Ishida, M.; Nakajima, T.; Honda, Y.; Kitao, O.; Nakai, H.; Klene, M.; Li, X.; Knox, J. E.; Hratchian, H. P.; Cross, J. B.; Adamo, C.; Jaramillo, J.; Gomperts, R.; Stratmann, R. E.; Yazyev, O.; Austin, A. J.; Cammi, R.; Pomelli, C.; Ochterski, J. W.; Ayala, P. Y.; Morokuma, K.; Voth, G. A.; Salvador, P.; Dannenberg, J. J.; Zakrzewski, V. G.; Dapprich, S.; Daniels, A. D.; Strain, M. C.; Farkas, O.; Malick, D. K.; Rabuck, A. D.; Raghavachari, K.; Foresman, J. B.; Ortiz, J. V.; Cui, Q.; Baboul, A. G.; Clifford, S.; Cioslowski, J.; Stefanov, B. B.; Liu, G.; Liashenko, A.; Piskorz, P.; Komaromi, I.; Martin, R. L.; Fox, D. J.; Keith, T.; Al-Laham, M. A.; Peng, C. Y.; Nanayakkara, A.; Challacombe, M.; Gill, P. M. W.; Johnson, B.; Chen. W.; Wong, M. W.; Gonzalez, C.; Pople, J. A. *Gaussian 03 (Revision B.02)*; Gaussian, Inc.: Pittsburgh, PA, 2003.

(44) Scott, A. P.; Radom, L. *J. Phys. Chem*. **1996**, *100*, 16502.

(45) Anderson, M. P.; Uvdal, P. *J. Phys. Chem. A*. **2005**, *109*, 2937.

(46) Klippenstein, S. J.; Yang, C. N. *Intl. J. Mass. Spect*. **2000**, *201*, 253.

(47) Chatt, J.; Rowe, G. A.; Williams, A. A. *Proc. Chem. Soc*. **1957**, 208.

(48) Chatt, J.; Duncanson, L.,A.; Guy, R. G. *J. Chem. Soc*. **1961**, 827.

(49) Long, C. A.; Henderson, G.; Ewing, G. E. *Chem. Phys*. **1973**, *2*, 485.

(50) Couronne, O.; Ellinger, Y. *Chem. Phys. Lett*. **2000**, *306*, 71.

(51) Aquilanti, V.; Bartolomei, M.; Cappelletti, D.; Carmona-Novillo, E.; Pirani, F. *J. Chem. Phys*. **2002**, *117*, 615.

(52) Huber, K. P.; Herzberg, G. Molecular Spectra and Molecular Structure IV. Constants of Diatomic Molecules, Van Nostrand Reinhold Co. **1979**.

CHAPTER 6

CONCLUSIONS

The bonding mechanism of transition metal cation - nitrogen complexes was investigated here by infrared photodissociation (IRPD) spectroscopy and density functional theory (DFT). The vibrational spectroscopy presented in this dissertation is the first IRPD study to probe the N-N stretch of isolated gas phase metal cation - nitrogen (N_2) complexes. The work has relevance to nitrogen activation in biological systems and catalysis. IRPD spectroscopy is used to monitor the effects of progressive ligand binding to transition metal cations. The spectroscopy reveals some interesting factors in the bonding nature of transition metals and has considerable significance to coordination chemistry and transition metal chemistry. These isolated gas phase species are free of solvent and solid interactions present in the condensed phase and hence are tractable models for theoretical investigations. DFT computations are used to predict structural parameters, energetics and electronic states of the metal cation - nitrogen complexes. The theoretical predictions are compared to IRPD spectra to understand the bonding process in these metal-ligand systems.

Analysis of the binding mechanism of first row transition metal cations from Sc^+ to Zn^+ to a single nitrogen molecule (N_2) is carried out by DFT methodology. The calculations show that the lowest energy structures have linear geometries primarily due to the directional properties of the N_2 quadrupole moment. The dissociation energies of the complexes range from about 8 to 30 kcal/mol and depend on the magnitude of the 3d-4s orbital hybridization of the

transition metal cations. All the metals except Fe^+ bond via the ground electronic state of the isolated cation. Fe^+ possesses a low-lying excited state that forms the ground state in $Fe^+(N_2)$. The N-N frequency of free N_2 is predicted to red-shift upon complexation in all the complexes. The magnitude of the red-shift is dependent on the bonding capacity of the metal ion. The early transition metal cations cause a larger red-shift than the late row metals because of the diffuse character of their valence orbitals. Comparison to available experimental data shows that DFT provides accurate estimates of bond energies, geometries and vibrational frequencies for complexes that are bound by electrostatic and covalent forces. However, for purely electrostatic systems, DFT overestimates the energetics and this is ascribed to the absence of dispersion parameters in DFT functionals.

$V^+(N_2)_n$ and $Nb^+(N_2)_n$ complexes are produced in a laser vaporization cluster source and studied by IRPD spectroscopy. The fragmentation mass spectra for both species reveal that they dissociate by the loss of intact N_2 molecules. The large complexes fragment down to the n=6 complex indicating that six is the preferred coordination number for both of these metal ions. Interestingly, this is the preferred coordination number for these metals in the condensed phase as well. The N-N stretch of free nitrogen does not have IR activity but upon binding to the metal cation, the vibration becomes IR active. The IRPD spectra for both complexes have intense resonances that are red-shifted with respect to the N-N stretch of isolated N_2. The predictions of the Dewar-Chatt-Duncanson model that describes transition metal-molecular bonding are consistent with the red-shifts observed. All the spectra of the $Nb^+(N_2)_n$ complexes have a single band with some of the large complexes exhibiting a second weak band which is attributed to N_2 molecules binding to the "core". For $V^+(N_2)_n$, the small complexes have a single band in the IRPD spectra that eventually splits into two intense bands for the large complexes.

DFT calculations were performed for $V^+(N_2)_{1-4}$ and $Nb^+(N_2)_{1-6}$ complexes to understand the geometric and electronic structure of the complexes. Comparison of the computed energetics and vibrational frequencies to the IRPD spectra indicates that N_2 binds in the end-on configuration to both metal ions. The structure of $V^+(N_2)_4$ and $Nb^+(N_2)_4$ is square planar with end-on bonded nitrogens. The ground electronic state of the small complexes is formed from the quintet ground state of isolated V^+ and Nb^+. However, in $Nb^+(N_2)_n$, progressive ligand addition leads to a change in the spin state of the metal cation and is exhibited in the IRPD spectrum of the n=5 complex with a single band that is red-shifted much further to the red than the n=4 complex. In this case, the calculated energetics and vibrational frequencies for the different spin states are in nice agreement with the measured spectra.

DFT calculations were performed up to the n=4 complex in $V^+(N_2)_n$ and suggest that the quintet state is the ground state in the complexes. Various possibilities such as intracluster reactions are considered for the appearance of a second intense band in the IRPD spectra of the large complexes. Here again, a change in the spin state of the metal cation induced by successive ligand binding is seen as the best possibility. Unlike the $Nb^+(N_2)_n$ system, where a change in the spin state occurs for all the complexes, in $V^+(N_2)_n$ a fraction of the molecules do not undergo a spin change. The reasons for this are speculative at this point but require further theoretical work to understand the discrepancies. Since DFT has difficulties with transition metal complexes, other methodologies such CCSD(T) and MP2 are needed to address these puzzling issues in the metal-ligand systems.

There are numerous possible directions to proceed with IRPD spectroscopy in the future and some of these are currently underway in our research. It will be interesting to study the binding of N_2 to other transition metal cations to investigate bonding trends. We have acquired

preliminary scans in the 2100 - 2500 cm^{-1} region for $Fe^{+}(N_2)_n$ and $Co^{+}(N_2)_n$ complexes. So far our group has applied IRPD spectroscopy to only cationic metal-ligand complexes and it would be interesting to extend our studies to the corresponding anionic species as well. It would also be interesting to study mixed metal-ligand complexes of the form $M^{+}(L1)_n(L2)_m$ where L1 and L2 are different ligands. IRPD studies of such complexes would show how the chemistry of the metal ion is influenced by the different ligands. Such studies would make better comparisons to condensed phase data because metals are usually bonded to different ligands in the solid and liquid phases. Finally, it would be appealing to investigate multiple metal - single ligand complexes of the form $(M_n)^{+}L$ because of their relevance to surface science. In surface catalysis, a molecule interacts with a group of metal atoms on a surface rather than a single atom. Therefore complexes of the form $(M_n)^{+}L$ would be a more accurate representation of the chemical interactions on surfaces. IRPD studies of such metal-ligand systems in conjunction with theoretical methods will continue to develop and refine our understanding of metal-molecular chemistry.

APPENDIX A

THEORETICAL STRUCTURES, ENERGETICS, FREQUENCIES AND IR INTENSITIES OF $V^+(N_2)_n$ COMPLEXES USING B3LYP/6-311+G*

$V^+(N_2)$

State	D_e[a]	B.E.[b]	Frequencies (Int.)[c]	M^+-N (Å)	N≡N (Å)
$^5\Sigma(C_{\infty v})$	33.8	33.8	215(3), 215(3), 280(0), 2282(54)	2.105	1.099

[a]Dissociation energy in kcal/mol for the elimination of the outermost ligand.

[b]Total binding energy in the complex relative to V^+ (^5D or ^3F for the quintet and triplet complexes respectively) and separated ligands.

[c]Harmonic frequencies scaled by 0.96. Intensities are in km/mol.

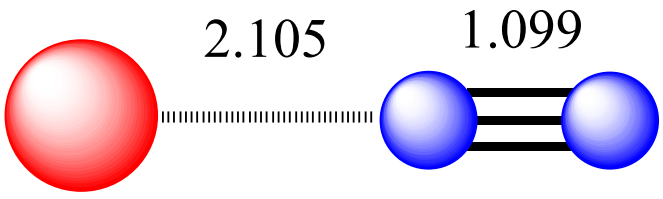

$V^+(N_2)$

State	D_e	B.E.	Frequencies (Int.)	M^+-N (Å)	N≡N (Å)
$^5B_1(C_{2v})$	18.6	18.6	180(2), 209(0), 2162(167)	2.261	1.112

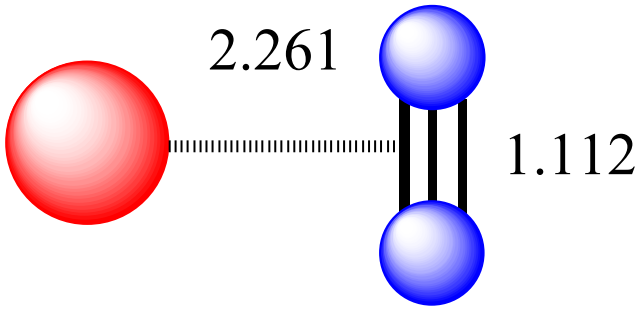

$V^+(N_2)$

State	D_e	B.E.	Frequencies (Int.)	M^+-N (Å)	N≡N (Å)
$^3\Sigma(C_{\infty v})$	25.1	28.8	257(4), 271(6), 368(7), 21545(299)	1.981	1.112

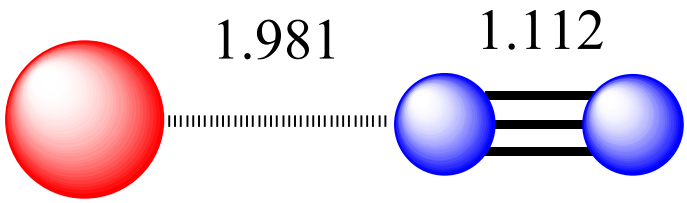

$V^+(N_2)$

State	D_e	B.E.	Frequencies (Int.)	M^+-N (Å)	N≡N (Å)
$^3A_2(C_{2v})$	22.1	16.7	361(1), 419(2), 1858(171)	1.922	1.156

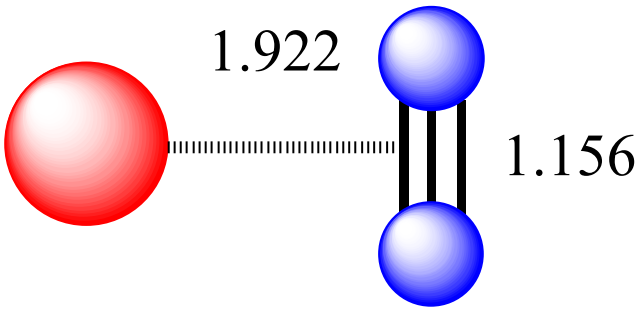

$V^+(N_2)_2$

State	D_e	B.E.	Frequencies (Int.)	M^+-N (Å)	N≡N (Å)
$^5\Sigma_g$	19.7	53.1	51(3), 51(3), 218(0), 218(0), 229(0), 287(27), 305(2), 305(2), 2262(354), 2272(0)	2.135	1.101

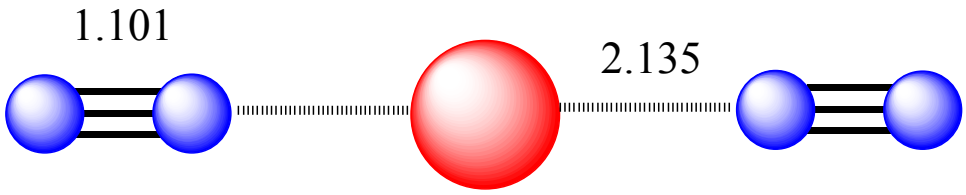

$V^+(N_2)_2$

State	D_e	B.E.	Frequencies (Int.)	M^+-N (Å)	N≡N (Å)
$^5A(C_2)$	8.5	27	52(5), 55(5), 61(0), 117(1), 120(1), 146(0), 171(34), 2176(544), 2199(0)	2.354	1.109

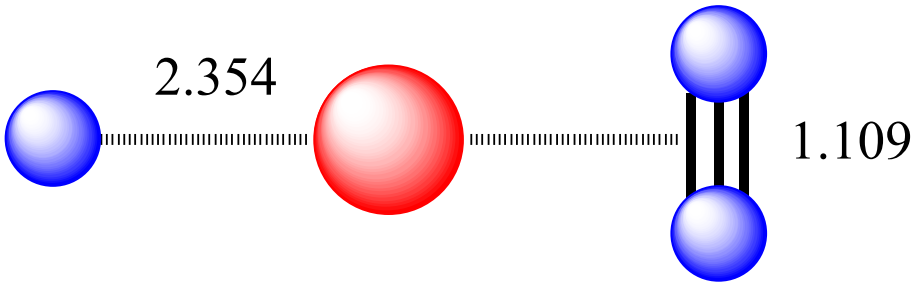

$V^+(N_2)_2$

State	D_e	B.E.	Frequencies (Int.)	M^+-N (Å)	N≡N (Å)
$^3\Sigma_g$ ($C_{\infty v}$)	25.3	23.2	70(5), 79(3), 243(0), 252(0), 290(0), 333(3), 353(76), 455(0), 2178(965), 2217(0)	2.039	1.107

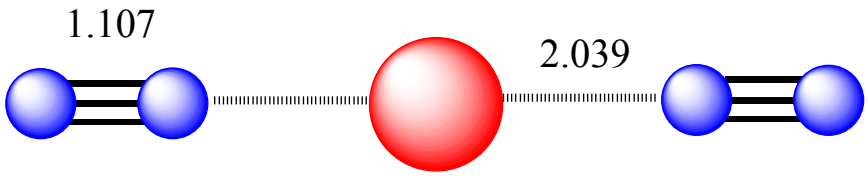

$V^+(N_2)_2$

State	D_e	B.E.	Frequencies (Int.)	M^+-N (Å)	N≡N (Å)
$^3A(C_1)$	11.6	33.7	27(13), 124(5), 206(0), 220(124), 258(0), 306(0), 495(0), 2017(856), 2073(0)	2.070	1.128

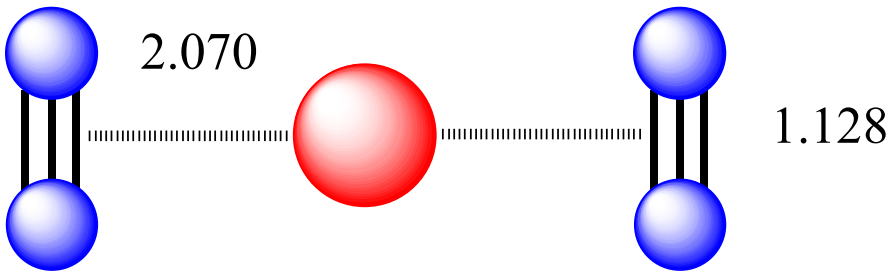

$V^+(N_2)_3$

State	D_e	B.E.	Frequencies (Int.)	M^+-N (Å)	N≡N (Å)
$^5A_1(C_{2v})$	18.9	71.7	50(3), 61(1), 61(1), 216(0), 218(0), 221(2), 223(0), 256(4), 258(15), 285(3), 306(0)	2.139 2.110	1.020 1.100

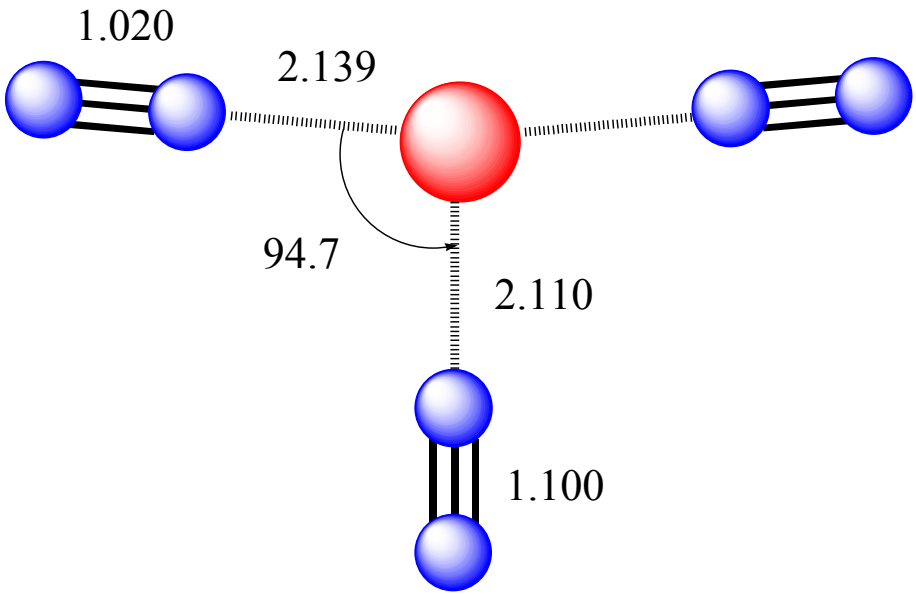

$V^+(N_2)_3$

State	D_e	B.E.	Frequencies (Int.)	M^+-N (Å)	N≡N (Å)
$^3B_2(C_{2v})$	22.8	73.2	71(5), 74(1), 77(1), 236(0), 238(1), 269(1), 272(4), 318(7), 320(56), 322(4), 409(4),	2.057 2.025	1.106 1.106

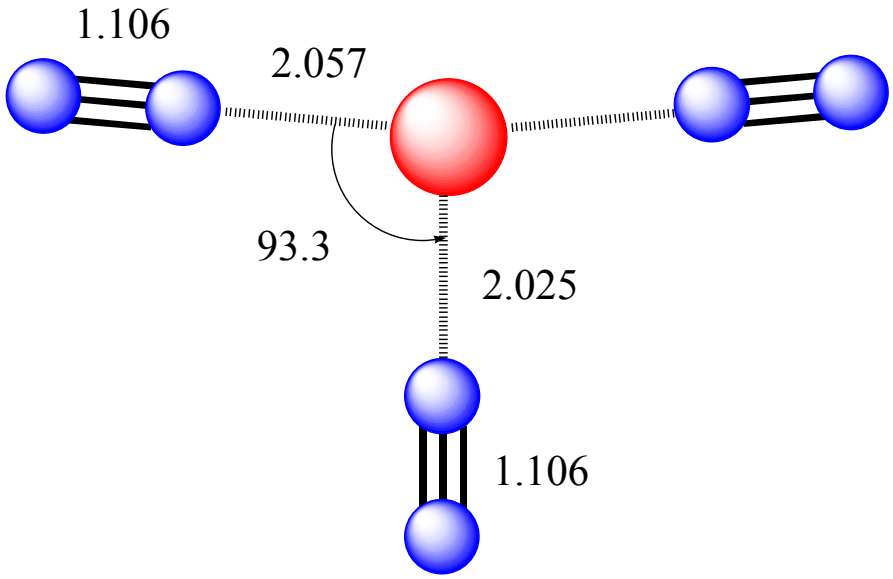

$V^+(N_2)_4$

State	D_e	B.E.	Frequencies (Int.)	M^+-N (Å)	N≡N (Å)
$^5B_{2g}(D_{4h})$	33.8	88.3	30(0), 67(2), 68(2), 70(0), 70(0), 211(0), 216(0), 216(0), 216(0), 222(0), 260(16), 267(0), 286(0), 307(3), 320(5), 320(5), 2269(0), 2270(246)	2.147	1.100

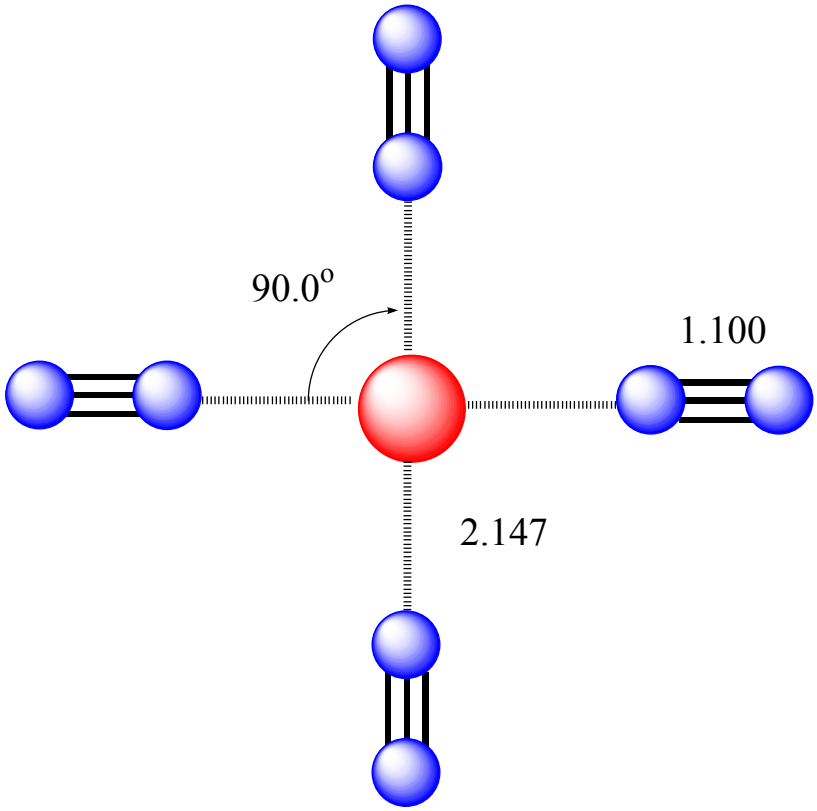

$V^+(N_2)_4$

State	D_e	B.E.	Frequencies (Int.)	M^+-N (Å)	N≡N (Å)
$^3A_{1g}(D_{4h})$	20.5	93.7	47(0), 77(0), 84(1), 84(1), 86(4), 235(0), 235(0), 249(0), 269(0), 270(0), 296(0), 312(36), 312(36), 346(2), 373(0), 445(20), 445(20), 2211(0), 2217(590)	2.074	1.104

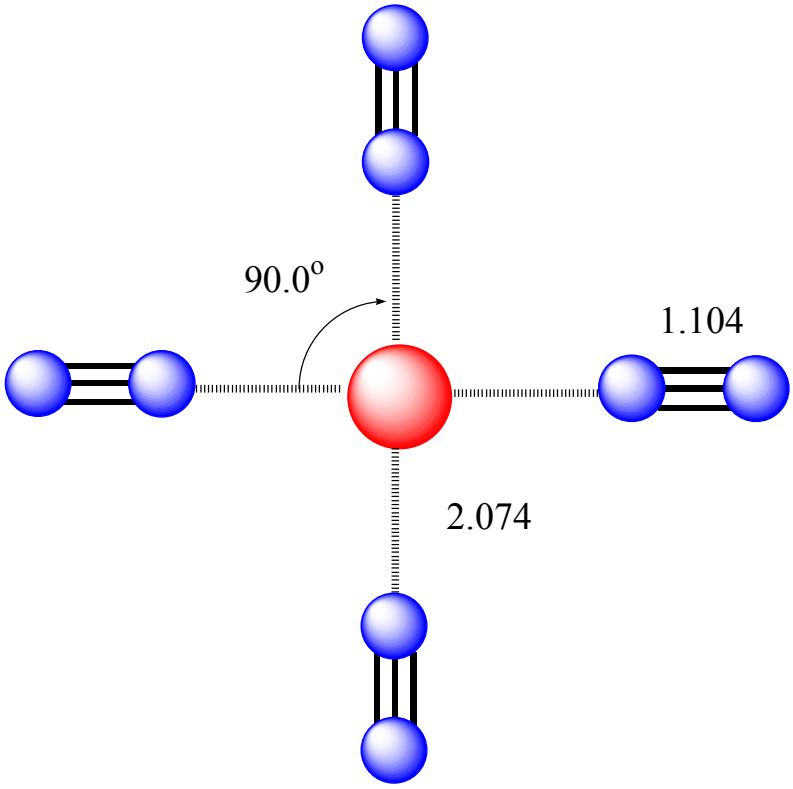

APPENDIX B

THEORETICAL STRUCTURES, ENERGETICS, FREQUENCIES AND IR INTENSITIES OF $Nb^+(N_2)_n$ COMPLEXES USING B3LYP/(DGDZVP/6-311+G*)

$Nb^+(N_2)$

State	D_e[a]	B.E.[b]	Frequencies (Int.)[c]	M^+-N (Å)	N≡N (Å)
$^5\Sigma(C_{\infty v})$	17.0	17.0	195(2), 195(2), 230(1), 2265(58)	2.261	1.101

[a]Dissociation energy in kcal/mol for the elimination of the outermost ligand.

[b]Total binding energy in the complex relative to Nb^+ (^5D or ^3P for the quintet and triplet complexes respectively) and separated ligands.

[c]Harmonic frequencies scaled by 0.96. Intensities are in km/mol.

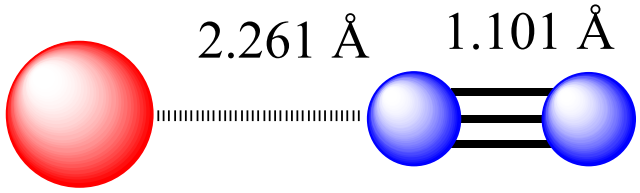

$Nb^+(N_2)$

State	D_e	B.E.	Frequencies (Int.)	M^+-N (Å)	N≡N (Å)
$^5B_1(C_{2v})$	2.9	2.9	23(0), 118(0), 2212(95)	2.555	1.108

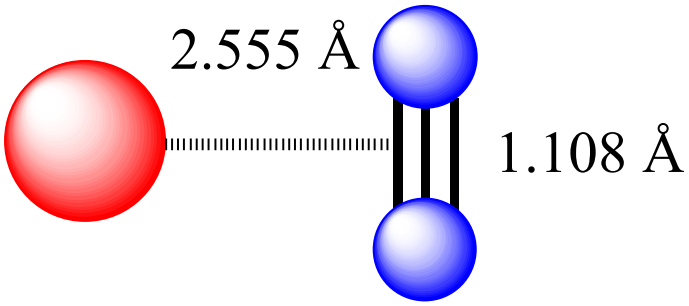

$Nb^+(N_2)$

State	D_e	B.E.	Frequencies (Int.)	M^+-N (Å)	N≡N (Å)
$^3\Sigma(C_{\infty v})$	3.4	3.4	194(6), 235(2), 327(4), 2191(164)	2.124	1.108

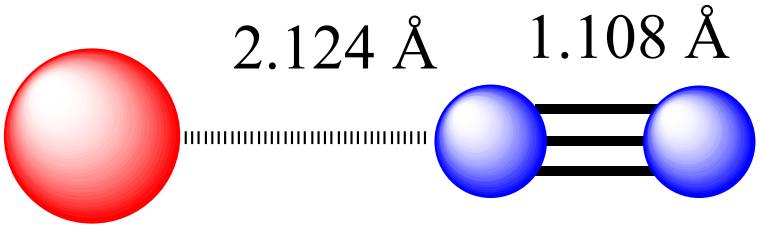

$Nb^+(N_2)$

State	D_e	B.E.	Frequencies (Int.)	M^+-N (Å)	N≡N (Å)
$^3A_2(C_{2v})$	24.3	24.3	299(6), 478(2), 1795(169)	2.059	1.164

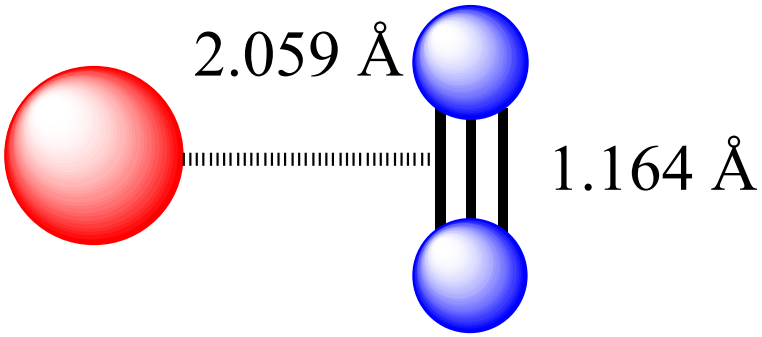

$Nb^+(N_2)_2$

State	D_e	B.E.	Frequencies (Int.)	M^+-N (Å)	N≡N (Å)
$^5\Sigma_g(D_{\infty h})$	25.4	42.4	45(1), 45(1), 219(0), 219(0), 230(0), 231(23), 249(0), 249(0), 2244(383), 2260(0)	2.275	1.101

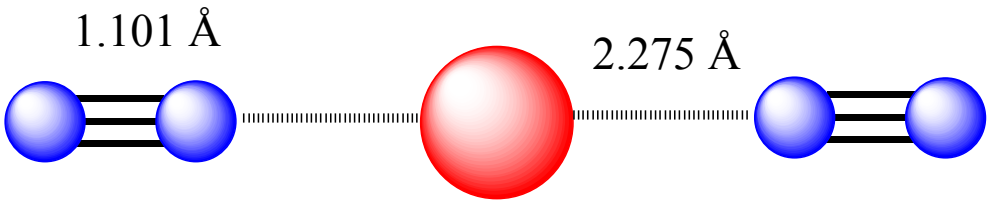

$Nb^+(N_2)_2$

State	D_e	B.E.	Frequencies (Int.)	M^+-N (Å)	N≡N (Å)
$^5A_1(C_{2v})$	11.7(T) 25.8(L)	28.7	39(1), 51(1), 126(0), 155(4), 242(10), 250(1), 265(0), 2216(221), 2247(101)	2.253 2.512	1.102 1.107

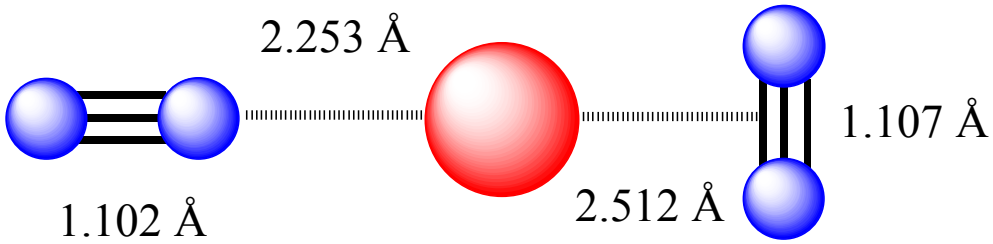

$Nb^+(N_2)_2$

State	D_e	B.E.	Frequencies (Int.)	M^+-N (Å)	N≡N (Å)
$^3\Sigma_g(D_{\infty h})$	51.1	54.4	61(2), 74(1), 245(0), 264(0), 279(48), 282(0), 286(1), 401(0), 2188(732), 2214(0)	2.188	1.107

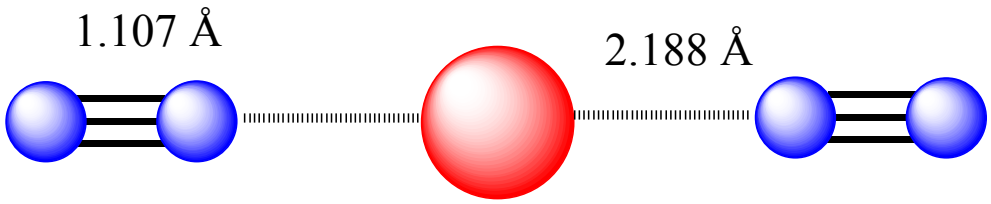

$Nb^+(N_2)_2$

State	D_e	B.E.	Frequencies (Int.)	M^+-N (Å)	N≡N (Å)
$^3B_1(C_{2v})$	41.2(T) 20.2(L)	44.5	73(3), 96(1), 244(26), 273(20), 285(1), 298(0), 438(1), 2033(504), 2220(205)	2.198 2.413	1.105 1.129

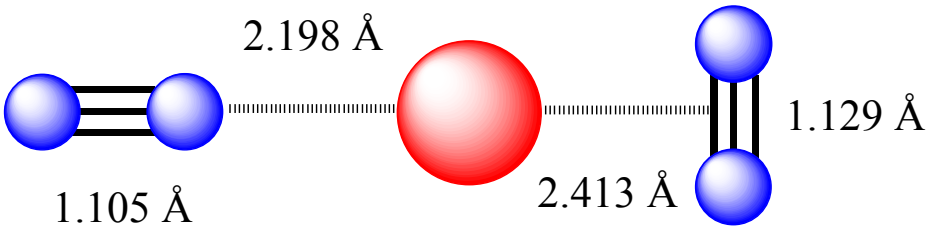

$Nb^{+}(N_2)_2$

State	D_e	B.E.	Frequencies (Int.)	M^{+}-N (Å)	N≡N (Å)
$^5A_g(D_{2h})$	10.7	13.6	-69(0), -35(0), 12(1), 58(1), 112(0), 149(8),153(0), 2221(252), 2236(0)	2.525	1.106

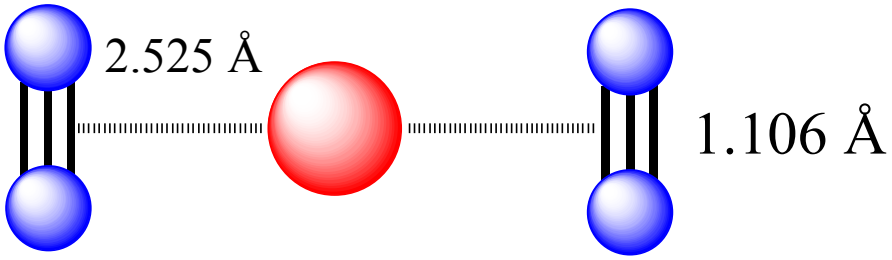

$Nb^+(N_2)_2$

State	D_e	B.E.	Frequencies (Int.)	M^+-N (Å)	N≡N (Å)
$^5B_1(D_{2d})$	7.2	10.0	-105(0), -105(0), 40(2), 40(2), 78(0), 134(0),181(1), 2236(0), 2244(88)	2.541	1.105

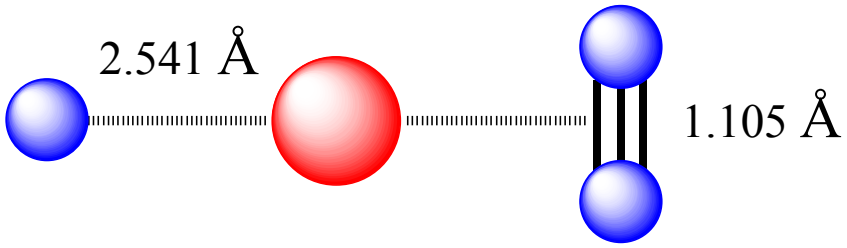

$Nb^+(N_2)_2$

State	D_e	B.E.	Frequencies (Int.)	M^+-N (Å)	N≡N (Å)
$^3B_2(C_{2v})$	11.3	35.7	40(6), 134(1), 172(96), 204(0), 245(0), 353(0), 475(0), 1992(848), 2044(3)	2.235	1.131

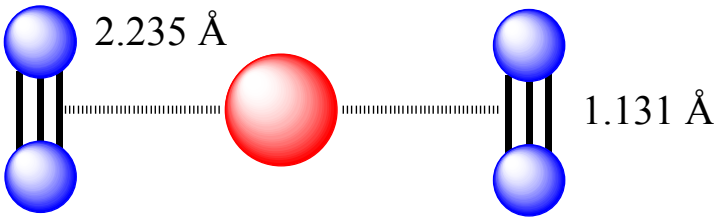

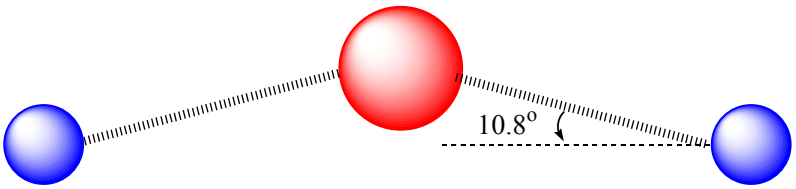

$Nb^{+}(N_2)_2$

State	D_e	B.E.	Frequencies (Int.)	M^{+}-N (Å)	N≡N (Å)
$^3B_3(D_2)$	11.2	35.5	-45(6), 121(1), 165(90), 208(0), 242(0),348(0), 486(1), 1998(814), 2046(0)	2.234	1.131

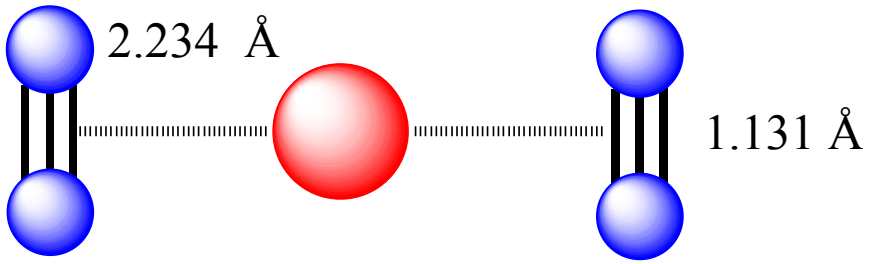

$Nb^{+}(N_2)_3$

State	D_e	B.E.	Frequencies (Int.)	M^{+}-N (Å)	N≡N (Å)
$^5A_1(C_{2v})$	18.7	61.1	43(1), 54(0), 54(0), 224(0), 226(0), 228(20), 229(0), 230(1), 241(2), 253(5), 291(0), 292(0), 2226(165), 2251(317)	2.276 2.221	1.101 1.103

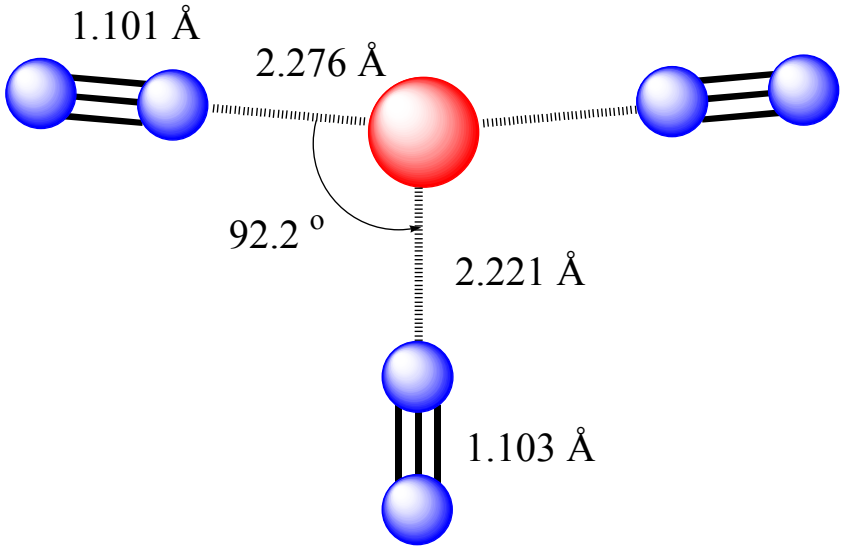

$Nb^+(N_2)_3$

State	D_e	B.E.	Frequencies (Int.)	M^+-N (Å)	N≡N (Å)
$^3B_2(C_{2v})$	25.1	79.6	63(2), 71(1), 74(0), 236(0), 261(1), 268(39), 273(4), 281(3), 289(1), 310(9), 404(3), 407(0), 2171(310), 2197(661), 2225(0)	2.199 2.139	1.106 1.108

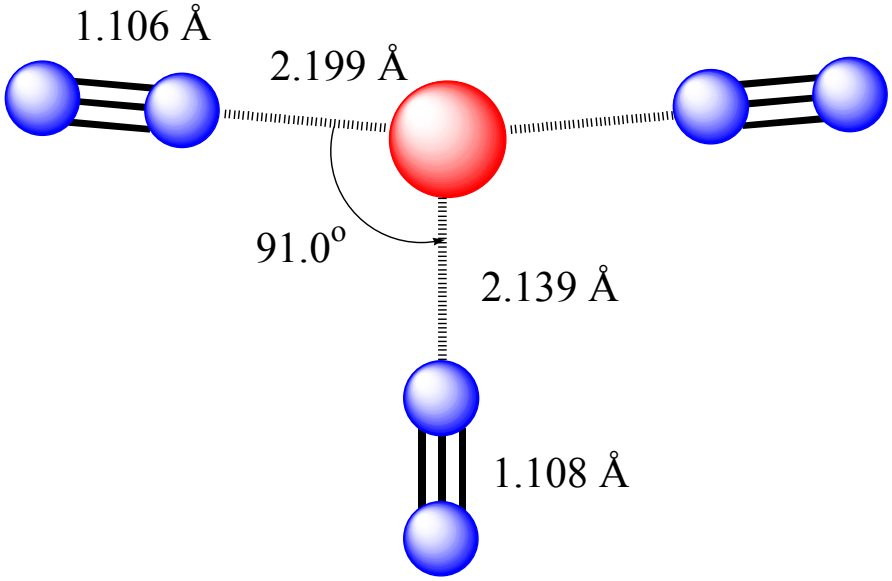

$Nb^+(N_2)_3$

State	D_e	B.E.	Frequencies (Int.)	M^+-N (Å)	N≡N (Å)
$^5A_1$ (C_{2v})	5.1	47.5	46(1), 54(0), 69(1), 90(0), 119(1), 163(3), 226(0),228(14), 237(4), 244(0), 267(0), 2183(165), 2254(288), 2267(4)	2.279 2.480	1.101 1.110

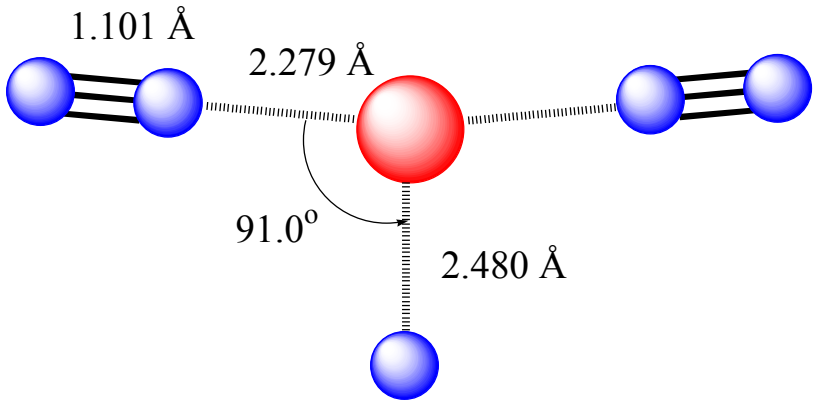

$Nb^+(N_2)_3$

State	D_e	B.E.	Frequencies (Int.)	M^+-N (Å)	N≡N (Å)
$^5A_1$ (C_{2v})	3.0	45.4	-88(0), -55(0), 45(1), 55(0), 64(0), 120(0), 218(0), 227(0), 228(11), 241(0), 243(6), 296(0), 2254(278), 2257(43), 2269(0)	2.282 2.622	1.101 1.103

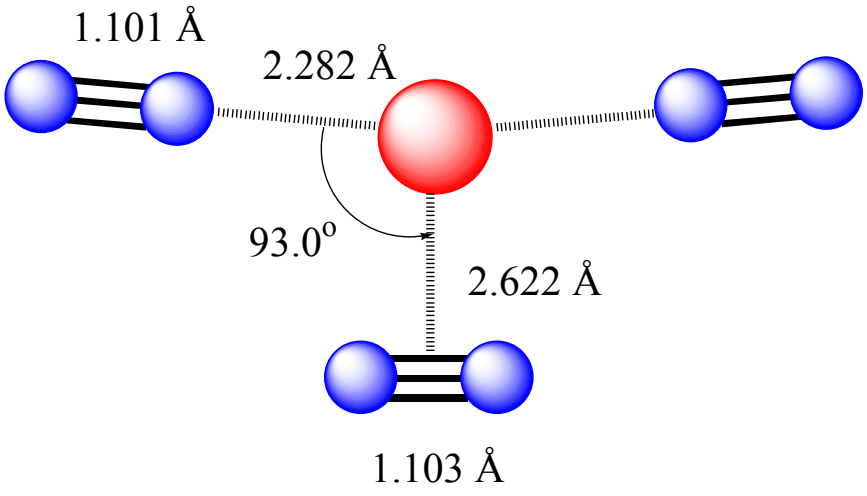

$Nb^+(N_2)_4$

State	D_e	B.E.	Frequencies (Int.)	M^+-N (Å)	N≡N (Å)
$^5B_{2g}(D_{4h})$	18.4	79.5	26(0), 51(1), 55(0), 58(0), 58(0), 198(0), 212(1), 213(0), 213(0), 216(0), 225(0), 225(17), 225(17), 232(0), 260(7), 260(7), 270(0), 2251(336), 2251(336), 2255(0), 2275(0),	2.278	1.101

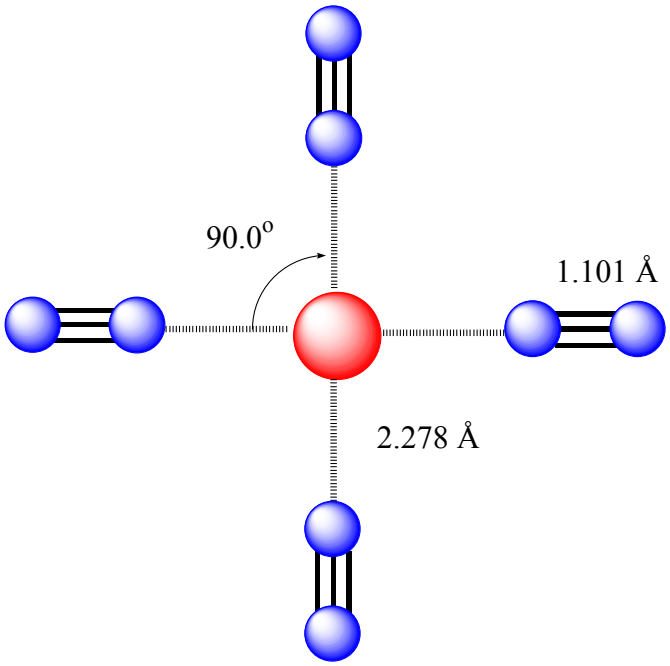

$Nb^+(N_2)_4$

State	D_e	B.E.	Frequencies (Int.)	M^+-N (Å)	N≡N (Å)
$^3A_{1g}(D_{4h})$	21.5	101.1	47(0), 66(0), 71(2), 74(0), 74(0), 226(0), 226(0), 254(0), 257(0), 262(35), 262(35), 267(0), 276(0), 360(0), 385(12), 385(12), 2205(0), 2209(605), 2209(605)	2.210	1.105

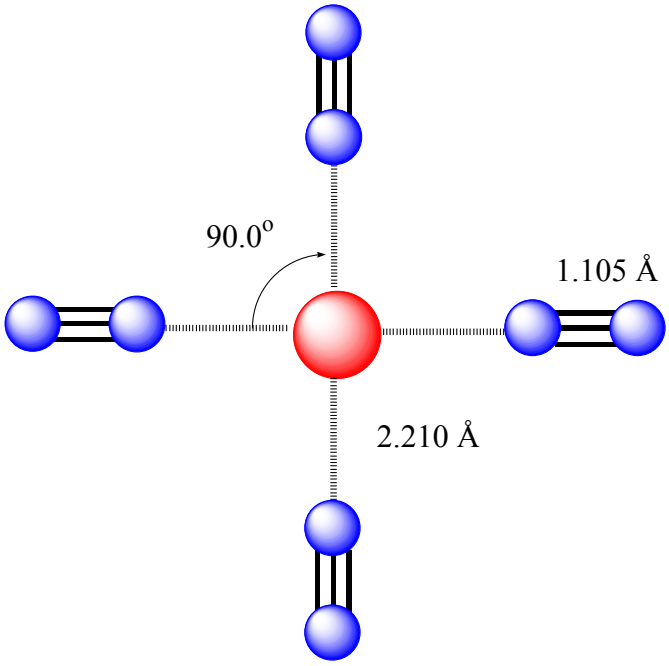

$Nb^+(N_2)_4$

State	D_e	B.E.	Frequencies (Int.)	M^+-N (Å)	N≡N (Å)
$^5B_2(C_{2v})$	13.0	60.6	-190(0), -91(5), 20(1), 40(0), 65(0), 72(0), 114(1), 154(7), 164(8), 196(8), 198(0), 208(0), 212(4), 235(8), 255(4), 273(0), 309(1), 2193(282), 2212(235), 2258(205), 2267(57)	2.391 2.231	1.100 1.104

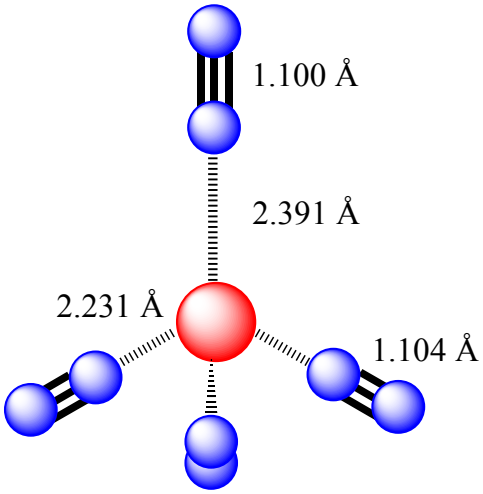

$Nb^+(N_2)_5$

State	D_e	B.E.	Frequencies (Int.)	M^+-N (Å)	N≡N (Å)
$^3A(C_1)$	21.4	122.5	36(0), 48(0), 59(0), 66(0), 72(1), 74(0), 78(1), 234(1), 245(0), 249(1), 250(27), 256(33), 259(8), 264(0), 272(1), 291(2), 299(1), 314(1), 339(3), 345(0), 375(9), 391(10), 2203(158), 2208(609),2210(148), 2217(536), 2252(0)	2.201 2.224 2.212 2.221 2.212	1.103 1.104 1.105 1.104 1.105

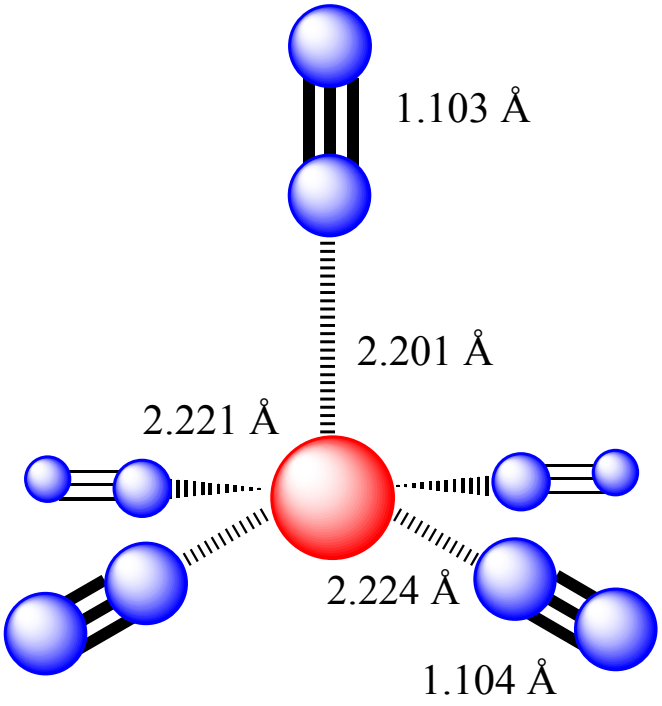

$Nb^+(N_2)_5$

State	D_e	B.E.	Frequencies (Int.)	M^+-N (Å)	N≡N (Å)
$^3A_2(C_{2v})$	21.3	122.4	-103(1), -103(1), 54(0), 69(0), 73(1), 75(0), 75(0), 193(0), 193(0), 246(0), 246(0), 256(5), 257(0), 258(35), 258(35), 268(0), 275(0), 315(0), 344(1), 361(0), 385(10), 385(10), 2203(0), 2207(613), 2207(613), 2224(152), 2251(2)	2.216 2.212 2.211	1.102 1.105 1.105

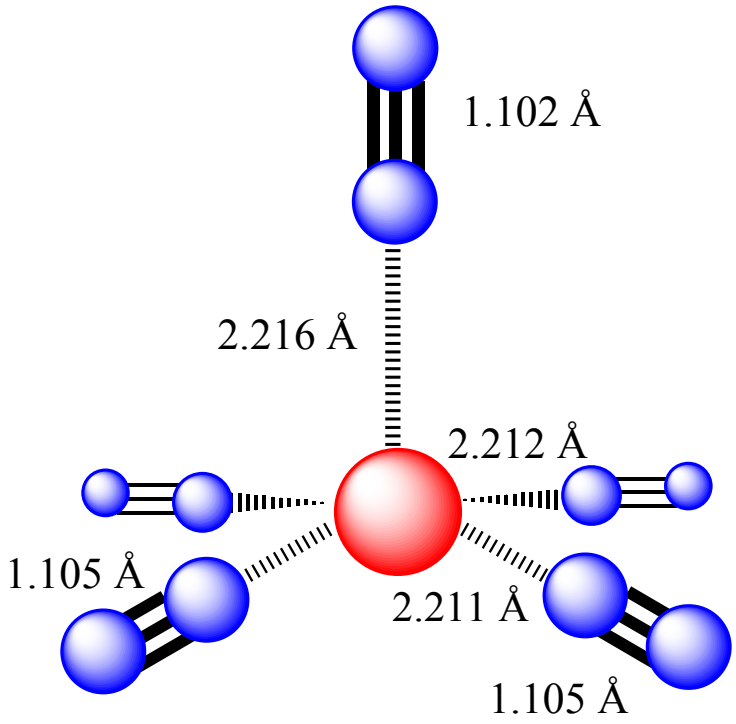

$Nb^+(N_2)_5$

State	D_e	B.E.	Frequencies (Int.)	M^+-N (Å)	N≡N (Å)
$^5B_1(C_{4v})$	2.2	81.7	24(0), 24(0), 30(0), 49(1), 57(0), 59(1), 59(1), 74(3), 74(3), 77(2), 217(0), 223(0), 227(11), 227(11), 234(1), 242(11), 242(11), 261(1), 272(0),292(5), 309(0), 2232(0), 2235(400), 2235(400),2257(15), 2321(4)	2.276 2.635	1.102 1.097

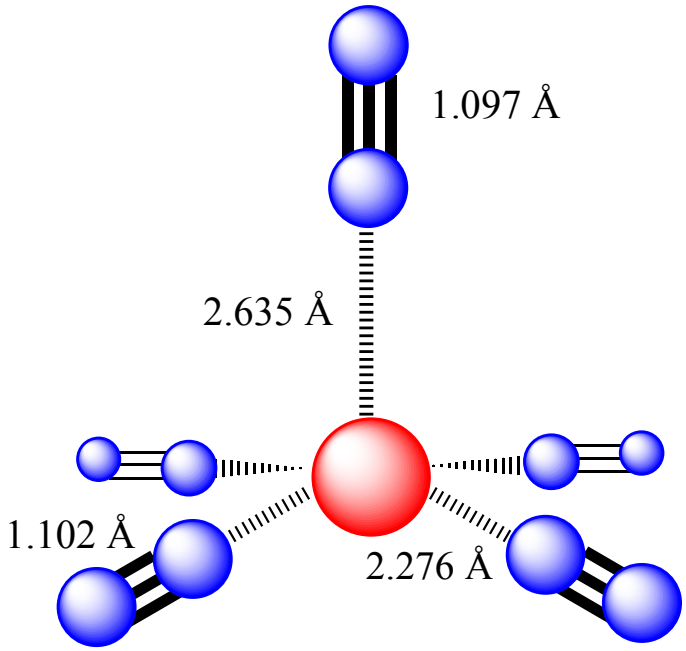

$Nb^+(N_2)_6$

State	D_e	B.E.	Frequencies (Int.)	M^+-N (Å)	N≡N (Å)
$^3B_g(C_{2h})$	18.5	140.8	42(0), 44(0), 48(0), 59(0), 60(0), 64(0), 73(0), 73(0), 79(1), 189(0), 191(0), 228(0), 237(20), 237(19), 238(0), 238(0), 245(27), 247(0), 263(0), 270(7), 271(7), 275(0), 276(0), 323(12), 325(13), 328(0), 347(18), 2197(0), 2198(0), 2225(472), 2225(459), 2227(539), 2266(0)	2.236 2.238	1.103 1.103

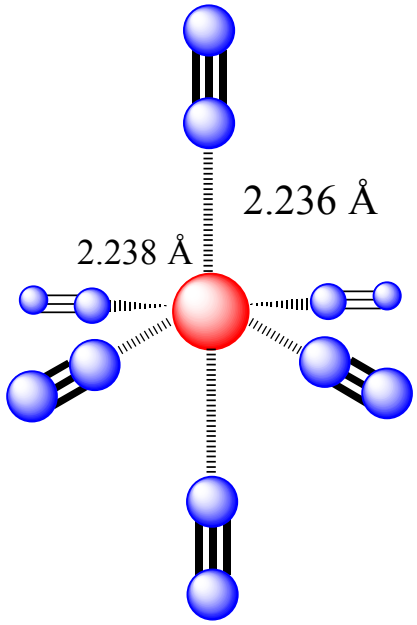

$Nb^+(N_2)_6$

State	D_e	B.E.	Frequencies (Int.)	M^+-N (Å)	N≡N (Å)
$^3A(C_1)$	1.2	123.8	14(0), 22(0), 32(1), 39(0), 52(0), 61(0), 65(0), 65(0), 66(0), 72(1), 74(0), 78(1), 235(9), 245(1), 249(22), 250(4), 256(33), 260(10), 265(0),271(1), 289(2), 305(1), 313(0), 337(3), 346(0),380(9), 399(9), 2203(118), 2208(547), 2211(244), 2217(555), 2253(0), 2348(2)	2.212 2.224 2.222 2.212 2.199 4.357	1.105 1.104 1.104 1.105 1.103 1.095

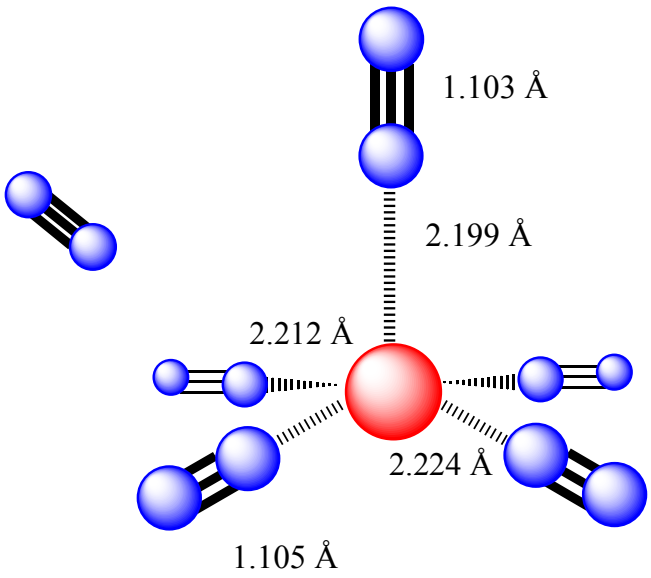

$Nb^{+}(N_2)_6$

State	D_e	B.E.	Frequencies (Int.)	M^{+}-N (Å)	N≡N (Å)
$^5A(C_1)$	1.0	82.7	-8(0), 18(0), 18(0), 22(0), 25(1), 30(0), 44(0), 59(1), 60(0), 44(2), 59(0), 60(1), 61(2), 62(1),64(0), 71(2), 71(2), 75(2), 227(9), 228(8), 234(1),241(7), 243(7), 263(0), 273(0), 295(5), 296(5), 308(0), 2232(72), 2235(414), 2237(334), 2258(15),	2.274 2.275 2.278 2.277 2.647	1.102 1.102 1.102 1.102 1.097